# Caesium-137 in sediments from two Norwegian fjords

# -

# Including dating sediment cores

by

Ingrid Sværen

Master of Science Thesis in Environmental Chemistry


Department of Chemistry

University of Bergen

Norway

May, 2010

INSTITUTE OF MARINE RESEARCH
HAVFORSKNINGSINSTITUTTET

# Caesium-137 in sediments from two Norwegian fjords

# -

# Including dating sediment cores

by

Ingrid Sværen

# Preface

This master thesis has been conducted on part-time, besides my usual work at the Institute of Marine Research in the period August 2007 to May 2010. A master degree which for me has become increasingly interesting as the work has progressed.

Great thanks to my advisor at Institute of Chemistry at the University of Bergen, Professor Leif Sæthre and my other advisors at the Norwegian Radiation Protection Authority (NRPA), Dr. Torbjørn Gäfvert and Professor Elis Holm. I am sincerely grateful for their help in initiating this work, and for helping me throughout the work.

The analysis is conducted at the Chemistry Laboratory of the Institute of Marine Research, which also is my usual place of work. I want to thank my colleagues here and particularly Dr. Hilde Elise Heldal for invaluable help and thorough feedback in the writing process. Further, the director of IMR, Tore Nepstad is thanked for allowing me to make this master in connection to my regular work at the IMR Chemistry Laboratory, and for allowing me to use the laboratory facilities for my measurements.

I further want to acknowledge my colleagues at the IMR: Toril Standal, Jane Strømstad Møgster and Linda Fonnes Lunde for having collected the samples and Kjell Bakkeplass for making the maps. I want to thank Dr. Per Roos at the DTU, Denmark for the Pu-analysis.

I have tried my best when completing this thesis in English, and I am in great debt to Egil for his help with this difficult and strange language!

A particular thanks also to my family and friends who all have enthusiastically supported a grown-up student.

My greatest thanks goes to those who are the rock of my life; my children and my husband Egil, which throughout this work has given me advice, comments and support; I could not have done this without you!

Bergen 30.mai 2010

Ingrid Sværen

# Contents

**List of abbreviations**

| | |
|---|---|
| Bi | Bismuth |
| Bq | Becquerel |
| Ch | Channel |
| CIC | Constant initial concentration |
| Cps | Counts per. Second |
| CRS | Constant rate of supply |
| Cs | Caesium |
| d.w. | Dry weight |
| HPGe | High purity germanium |
| IAEA | International Atomic Energy Agency |
| IMR | Institute of Marine Research |
| KF | Correction factor |
| LORAKON | Lokal radioaktivitets kontroll |
| NKS | the Nordic Committee for Nuclear Safety Research |
| NPL | National Physical Laboratory |
| NRPA | Norwegian Radiation Protection Authority |
| Pb | Lead |
| PBq | Peta Becquerel $10 \cdot 10^{15}$ Bq |
| Pu | Plutonium |
| R/V | Research vessel |
| Ra | Radium |
| RAME | Radioactivity in the Marine Environment |
| Rn | Radon |
| Roi | Region of interest |
| $T_{1/2}$ | Half life |
| TBq | Tera Becquerel; $10 \cdot 10^{12}$ Bq |
| w.w. | Wet weight |

# Summary

The fission product Cs-137 is present in all parts of the Norwegian environment, brought here atmospherically or by ocean currents. The most important sources are fallout from atmospheric nuclear weapons tests, discharges from nuclear fuel repossessing plants and fallout from the Chernobyl accident which have caused the presence of this radionuclide in the marine environment. The environmental presence of this radionuclide is thoroughly monitored, and the content in the Norwegian marine environment is relatively low. Earlier investigations have, however, shown elevated contents of Cs-137 in surface sediments from a few Norwegian fjords compared to the content in surface sediments from open marine areas. The fjords with elevated contents of Cs-137 are all connected to land areas which received relatively high amounts of fallout from the Chernobyl accident in 1986.

In this work the Cs-137 activity concentrations in 14 sediment cores from the outlet and the head of the Laksefjord and the Sognefjord, have been investigated. Using the lead-210 dating method with correction of supported lead-210, each one-centimeter-layer in 11 of the cores has been dated.

The Cs-137 activity concentrations in the upper sediment-layer from all 14 cores show Cs-137 content of three different levels. In the outlet of the Sognefjord the Cs-137 level (approximately 33 Bq/kg (d.w.)) is about 6 times above the level (approximately 5.8 Bq/kg (d.w.)) in the Laksefjord. In the head of the Sognefjord the Cs-137 level (approximately 293 Bq/kg (d.w.)) is about 10 times above the level in the outlet of the Sognefjord. In all cores analyzed, the Cs-137 activity concentrations in the upper layers are highest. This indicates a continuous supply of Cs-137 in the ocean currents or of Cs-137 in run-off from land. There are no specific signals in the dated sediment layers indicating which of the main sources is the dominating. It is likely to believe that the Sognefjord which is much deeper than the areas outside the fjord can accumulate Cs-137 from ocean currents and run-off.

Chernobyl fallout on the land area surrounding the head of the Sognefjord is most likely the source to the elevated contents of Cs-137 there. The Cs-137 can be focused in the head of fjords due to the ratio between the drain-off area and the area receiving the drain-off. There are also elevated contents of Cs-137 in some other Norwegian fjords. These fjords are also located in areas which received a large amount of Chernobyl fallout. Fjords located in areas

which received a relatively moderate amount of Chernobyl fallout does not show these elevated levels.

# 1. Introduction

## 1.1 Radioactivity

Natural occurring and anthropogenic radionuclides exists everywhere both in the terrestrial and in the marine environment. Ionizing radiation from radionuclides can be harmful to humans and environment, and the risk is well documented. To better protect both people and the surrounding environment from harmful effects of radiation, it is important to understand the long-time behavior of radionuclides in nature.

Measurement of anthropogenic radionuclides in marine sediments can provide good estimates of past and present radioactive contamination. The inventory of a certain radionuclide, time and source of deposition can also be determined.

### 1.1.1 Caesium-137

Caesium (Cs) is an alkali metal with atomic number 55. Caesium has physical and chemical properties similar to those of rubidium and potassium. Caesium-137 (Cs-137) is a radionuclide formed mainly as a fission product by nuclear fission. Cs-137 arises from a number of decays after fission: Tellur-137 (3.5 seconds) → Iod-137 (24.2 seconds) → Xenon-137 (3.83 minutes) → Cs-137 (30.17 years) → Barium-137m (2.55 minutes) → stable Barium-137; half life in brackets (Aarkrog, 1994).

Cs-137 did not exist prior to discovery of nuclear fission. But after more than 60 years with nuclear weapons and nuclear industry this nuclide is present almost everywhere on earth, both in marine and terrestrial areas.

Cs-137 has often been chosen as the most significant representative of anthropogenic radionuclides found in the marine environment. It is the most abundant anthropogenic radionuclide, and it is the largest contributor to dose among the anthropogenic radionuclides (Povinec, 2003). The radionuclide can be measured by gamma spectroscopy (Chapter 2.7.1), and there exists several investigations on this radionuclide in Norwegian marine and terrestrial ecosystems.

### 1.1.2 Sources

There are several important sources to the Cs-137 in the Norwegian environment. The domestic source of Cs-137 is limited; most of the nuclide is transported to Norwegian areas

atmospherically or by ocean currents. The most important sources are atmospheric atomic bomb tests conducted mainly in the 1950s and 1960s, i.e. as global fallout, discharges to the marine environment from the repossessing plants at Sellafield and La Hague and fallout from the Chernobyl accident (Povinec, 2003). Table 1.1 shows the amounts of Cs-137 released from the most important sources to Northern European Seas in the period 1952-1998 (Povinec, 2003).

**Table 1.1: Sources of Cs-137 in Northern European Seas (1952-1998), based on IAEA (2001).**

| **Source** | **Cs-137 (TBq)** |
|---|---|
| Global fallout | 12 000 |
| Sellafield | 41 000 |
| La Hague | 1 000 |
| Chernobyl accident | 6 000 |

The Chernobyl accident in 1986 caused large amounts of radioactive fallout throughout Europe; with Norway as one of the most affected countries outside the former USSR. Altogether the accident released several different radionuclides. However, due to the long half life of Cs-137, this is now the main contributor to radioactive contamination of the Norwegian land area (NRPA, 2009a). Run-off from land affected by the Chernobyl accident acts as a secondary domestic source.

Totally, it is estimated that about 85 PBq of Cs-137 was released (UNSCEAR, 2000). Figure 1.1 shows the distribution of Chernobyl fallout onto Norway (NRPA 2009b). Shortly after the fallout, measurements showed very high levels of radioactive fallout cesium in reindeer (150 000Bq/kg), sheep (40 000 Bq/kg,), mushroom (typically 45 000Bq/kg, but levels as high as 1-2 millions Bq/kg was registered) and fresh water fish (30 000 Bq/kg), (Thørring, 2006a); all numbers are activity related to wet weight. Norwegian authorities have established a limit for maximum content of Cs-137 in most foods at 600 Bq/kg (NRPA, 2009c).

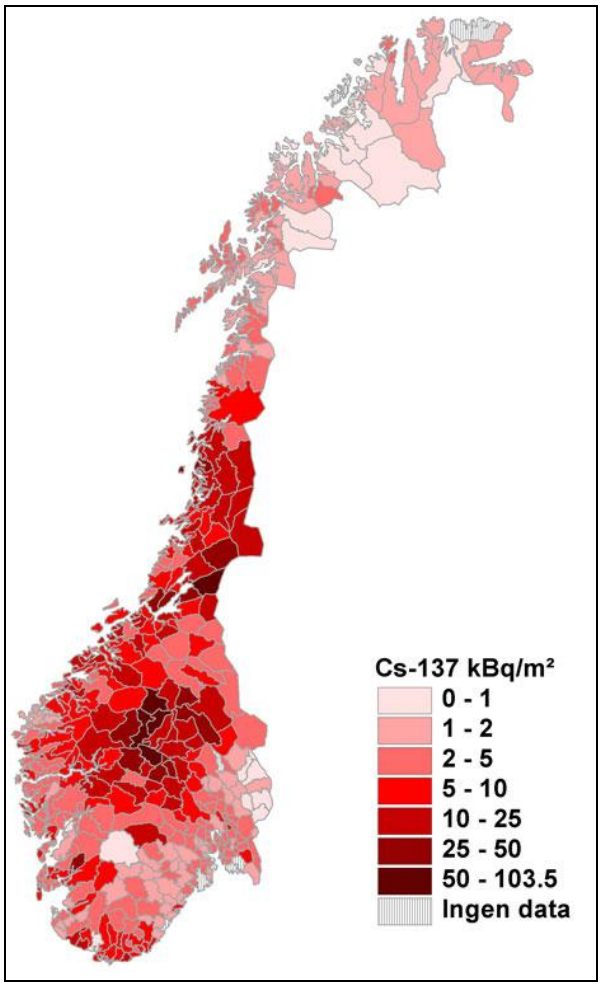


**Figure 1.1: Cs-137 fallout after the Chernobyl accident in 1986 (NRPA, 2009b).**

The Chernobyl accident did also contaminate the Baltic. This was the most affected marine area, totally receiving about 5 PBq of Cs-137 (Evans, 1991). Due to its narrow and shallow entrance; the long exchange time of water; the mean residence time is 25-35 years (Matthäus and Schinke, 1999); the concentration of Cs-137 decreases very slowly in the Baltic. Outflow of contaminated waters from the Baltic, entering the Norwegian Coastal Current, is today one of the most important source to Cs-137 along the entire Norwegian coast (Thørring et.al., 2006b). The outflow from the Baltic to the North Sea was in 2000 approximately 40 TBq/year (Dahlgaard, 2002); reduced to approximately 30 TBq/year in 2006 (Thørring, 2006b); in this work named Chernobyl Baltic.

Earlier deposition of radioactive global fallout from the nuclear weapons test in the 1950s and 1960s onto Norway was also considerable. Globally this is the greatest source to radioactive

pollution of the environment (NRPA, 2009d). The majority of the total atmospheric releases occurred in the two periods 1952-1958 and 1961 -1962 (UNSCEAR, 1993), separated by a test ban treaty in 1959-1960. In 1963, Great Britain, USA and the USSR signed a treaty banning all atmospheric tests, which resulted in a large decrease in the total global fallout (NRPA, 2009d). Calculations show that the total fallout of Cs-137 in Norway from the tests varied between approx. 2 kBq/$m^2$ and approx. 14 kBq/$m^2$ (NRPA, 2009d). Radioactive materials from these tests were transported over large areas in the atmosphere, and the fallout occurred mainly at rainfall; i.e. strongly correlated with rainfall. This caused larger deposition in areas with strong and frequent precipitation. Wet areas along the Norwegian coast were most affected. Figure 1.2 shows annual precipitation in Norway varying from 280 to 4200 mm $year^{-1}$ (Bergan, 2002).

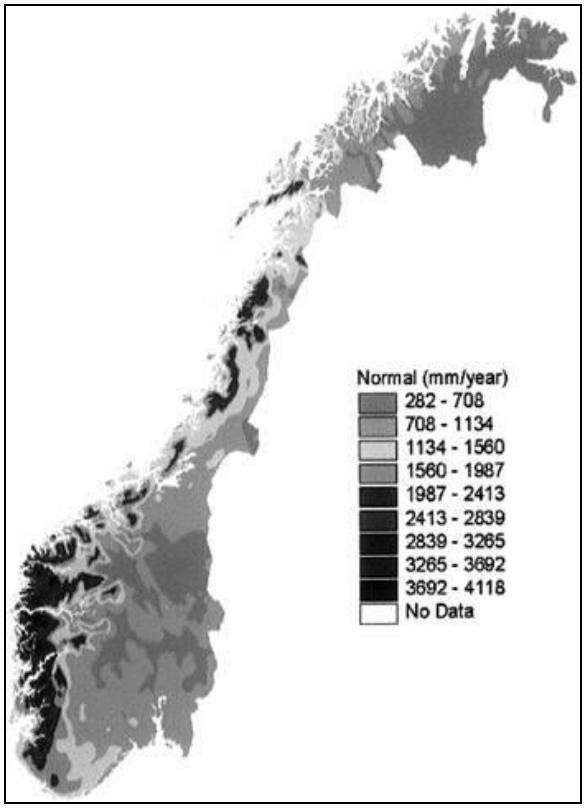


**Figure 1.2: Precipitation map of Norway (Bergan, 2002).**

As seen in table 1.1, controlled liquid discharges from the European nuclear fuel reprocessing plant at Sellafield (UK) is the most important source to radioactivity to Northern European Seas from 1952 to 1998. The discharges of most radionuclides from Sellafield peaked in the mid- to late-seventies. Due to significantly decreasing discharges after 1978, the concentrations of Cs-137 have declined considerably and at present they are only slightly

above the global fallout in North Atlantic surface waters. Remobilization of Cs-137 from the highly contaminated Irish Sea sediment is now a dominant source of water contamination to the North Sea (Povinec, 2003). In Cook et. al. (1997) it is calculated an annual loss of 86 TBq in solution from the North-east Irish Sea. Figure 1.3 indicates how the Chernobyl fallout and Sellafield discharge have dominated the level of Cs-137 in surface water in North European water in one decade each (Povinec, 2003).

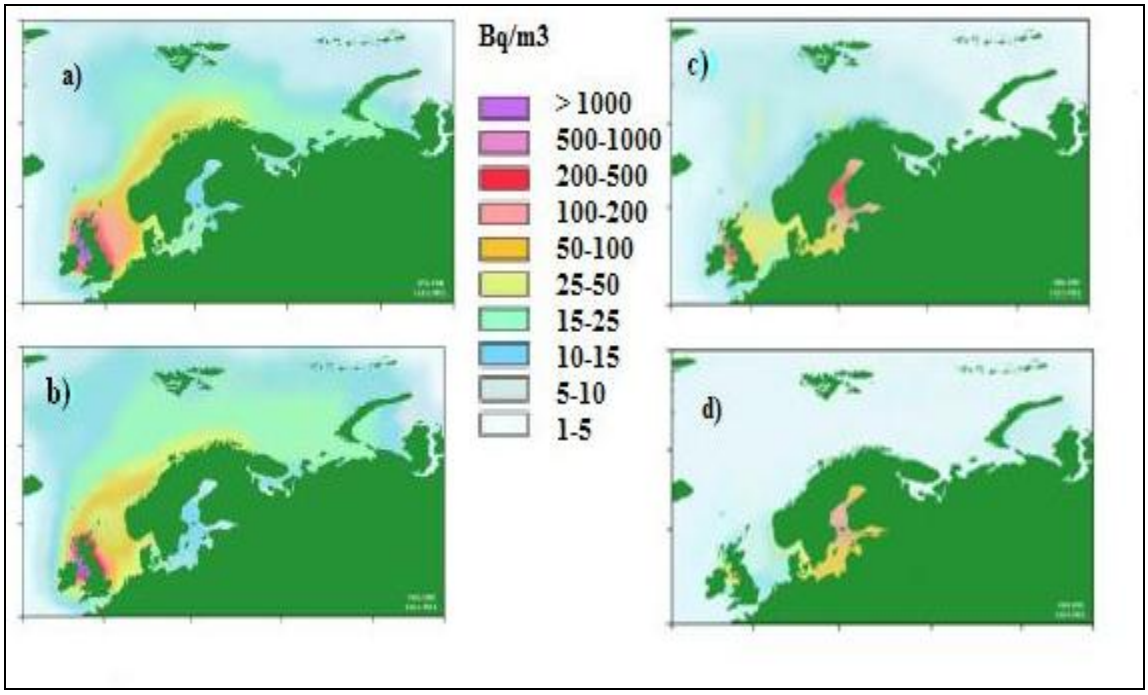


**Figure 1.3: Cs-137 in surface waters (1976–1980) a). Cs-137 in surface waters (1981–1985) b). Cs-137 in surface waters (1986–1990) c). Cs-137 in surface waters (1991–1995) d) (Povinec, 2003)**

### 1.1.3 Source identification

The fallout or discharge from each source has a unique composition and development in time. For most sources this information is available. It is thus possible to identify the source to a radioactive contamination in a location, based on measurements of more than one nuclide, do decay corrections and calculate the ratio between them. This can be exemplified with the ratio between fresh caesium-134 and Cs-137 from the Chernobyl accident which was 0.59 +/- 0.06 (Smith and Beresford, 2005). If measured cesium-contents deviate from this, it would be an indication of one or more additional sources. The ratio between different plutonium-isotopes ($^{238}Pu/^{239,\ 240}Pu$) in a sample can also indicate the source to the radioactive contamination in the sample (Varga, 2007). From weapons test fallout the $^{238}Pu/^{239,\ 240}Pu$ ratio

was 0.033. From Chernobyl the $^{238}Pu/^{239,\ 240}Pu$ ratio was 0.49. Liquid discharges from Sellafield have $^{238}Pu/^{239,\ 240}Pu$ ratio 0.2-0.3 (Becks, 2000).

Sources can also be identified by comparing activity concentration profiles for a specific radionuclide, in dated sediment cores, with age at which the radionuclide was released. A peak in a certain time period indicates the time it was deposited and can thus lead to identification of the actual source.

## 1.2 Norwegian Marine areas

Norway has a very long coastline and is surrounded by Kattegat, Skagerrak, the North Sea, the Norwegian Sea and the Barents Sea. The prevailing ocean current pattern along the Norwegian coast is from south to north. Atlantic water entering the North Sea in the north and an anti clock wise circulation in the North Sea is reaching the outlet from Baltic and continues in the Norwegian coastal current heading north, as shown in Figure 1.4 and Figure 1.5. The Norwegian coastal current are transporting water with its content from the North Sea and up along the coast of Norway.


**Figure 1.4: The North Sea: inflow, outflow, circulation and depth (Gjøsæter, et. al., 2008).**

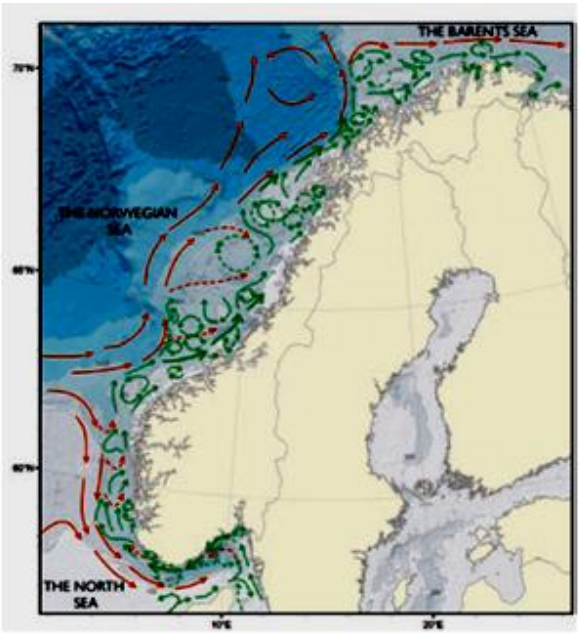


**Figure 1.5: The Norwegian coastal current. Red arrows indicate Atlantic water; green arrows indicate the Norwegian Coastal Current (Dahl et. al., 2007).**

Norwegian fjords are all influenced by the Norwegian coastal current (Figure 1.5) and are all different with respect to length and depth. The presence of a sill or not and sill dept is important for water exchange rate in the fjords. Other factors influencing the water circulation in a fjord and the water content are the amount of river run-off, the drain-off areas and the run-off nature.

### 1.2.1 The Sognefjord

The Sognefjord is the longest and deepest fjord in Norway, located on the west coast. The distance from the sill at the coast to its head in Skjolden is about 178 km. The width is 5 km in the outer part and about 2 km in the Lusterfjord. The fjord has several side arms which are relatively shallow compared to the main fjord. The sill dept is about 165 m. The dept is increasing from the sill to the east with the greatest dept, 1304 m between Ikjefjord and Kyrkjebø. From this point the dept decreases towards the east. The fjord is U-shaped with almost flat bottom and steep slopes on the sides. The bottom is covered with sediments, mainly clay transported to the fjord by the rivers. The area of the fjord is 950 $km^2$. The volume is about 525 $km^3$. Several rivers enter the fjord typically at the head of its arms. The rivers entering the fjord originate from different catchment areas.

Fjord oceanography shows that in the upper 165 m there is free water exchange between the fjord and the coastal water. The basin water is found below the silldept and is the most heavy water in the fjord. In order for this water to be replaced, water with greater density must cross the sill. The brackish water layer (surface) has low salinity, but is dependent of the season. Below the brackish water the salinity is above 32.5 ‰, in the basin water below the sill the salinity is even higher (Svendsen, 2006). In the Sognefjord replacement of the basin water occurs as seldom as every 8th year (Hermansen, 1974). Water mass exchange only occurs at the mouth of the fjord, and the sources of fresh water are rivers at the head of the fjord or head of the side arms.

### 1.2.2 The Laksefjord

The Laksefjord is a fjord in northern Norway in Finnmark County. The length is slightly over 70 km and is in north south direction. There is no sill in the fjord and deepest point; 327 m is in the outlet. Several rivers enter the fjord in the head and along the sides.

In the Laksefjord there is a rapid exchange of water masses between the coastal currents and even the innermost fjords as well as the comparatively small discharge of freshwater from the rivers. The Laksefjord is to a certain degree part of the Norwegian Coastal Current (Wassmann et.al., 1999).

## 1.3 Caesium-137 in Norwegian Marine areas

### 1.3.1 Monitoring marine radioactivity

Radioactivity in Norwegian marine areas, both in coastal areas and in the open sea, is monitored by Institute of Marine Research (IMR) and in the national Radioactivity in the Marine Environment (RAME) Programme funded by the Ministry of the Environment and coordinated by the NRPA. The RAME Programme coordinates sampling and measurements of several radioactive nuclides in sediments, biota and seawater from the Barents Sea, the Norwegian Sea, the North Sea, the Skagerrak, the Kattegat and Norwegian fjords. Cs-137 is one of the radionuclides monitored. The monitoring results from the RAME Programme are presented in annual reports.

### 1.3.2 Biota

Figure 1.6 shows activity concentrations of Cs-137 in cod from different European areas in 2003. The activity concentration ranges from 0.2 Bq/kg (w.w.) to 8.6 Bq/kg (w.w.) (Baltic) (NRPA, 2005). The content of Cs-137 in biota is dependent of salinity in the surrounding seawater (Andersson and Meili, 1994). Biota from Norwegian fjords has also been analyzed on Cs-137 content in the RAME Programme. The content of Cs-137 is generally very low (< 10 Bq/kg w.w.).

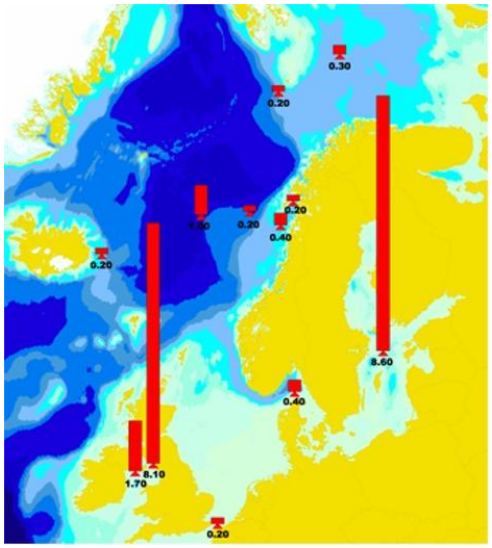


**Figure 1.6: Activity concentrations of Cs-137 in cod, 2003. (NRPA, 2009e)**

### 1.3.3 Water

Activity concentrations of Cs-137 in surface seawater samples collected from the Kattegat, the North Sea, the Norwegian Sea and the Barents Sea in 2006 were between 46.8 Bq/m$^3$ (Kattegat) and 0.6 Bq/m$^3$ (Norwegian Sea) (NRPA, 2008). In Figure 1.7 are shown preliminary results on Cs-137 in surface seawater in Norwegian marine areas in 2008, as analyzed by IMR. The Cs-137 activity concentrations in surface seawater are decreasing when following the ocean current along the Norwegian coast; Figure 1.4 and Figure 1.5.

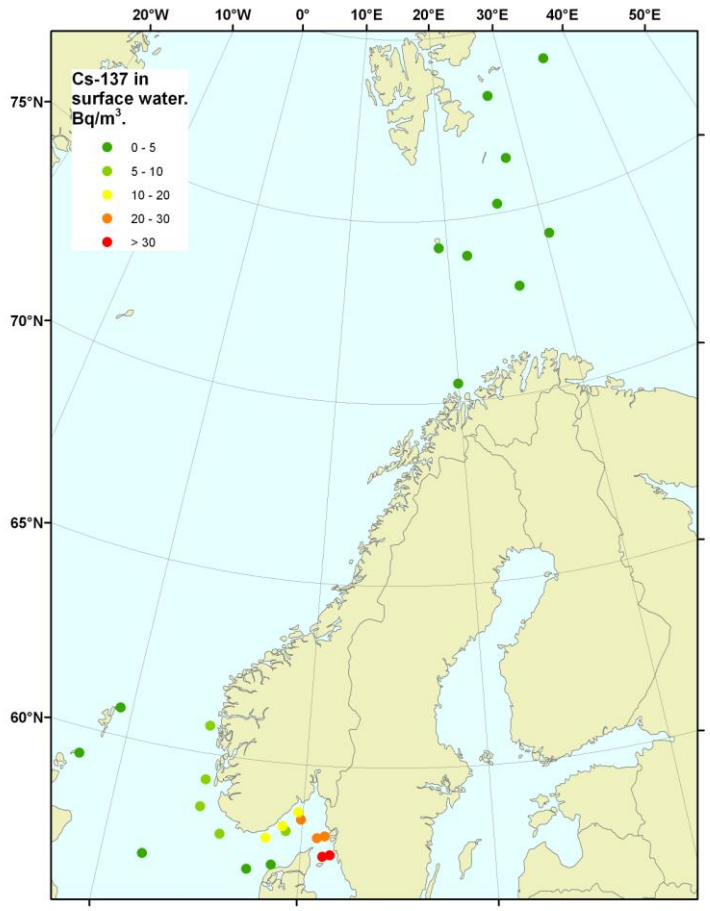


**Figure 1.7: Activity concentrations of Cs-137 in surface water from 2008 (Preliminary results).**

### 1.3.4 Sediments

Activity concentrations of Cs-137 in surface sediments samples collected from the North Sea, the Norwegian Sea and the Barents Sea in 2005 and 2006 were between < 0.9 Bq/kg (d.w.) (Norwegian Sea 2006) and 24.9 Bq/kg (d.w.) (Norwegian Sea 2006) (NRPA, 2007) (NRPA, 2008). Cs-137 in samples of surface sediments from 2008 in the RAME Programme analyzed at the IMR; are presented in Figure 1.8. Surface sediment samples from 2008 indicate a tendency of higher Cs-137 activity concentrations inside the fjords than outside.

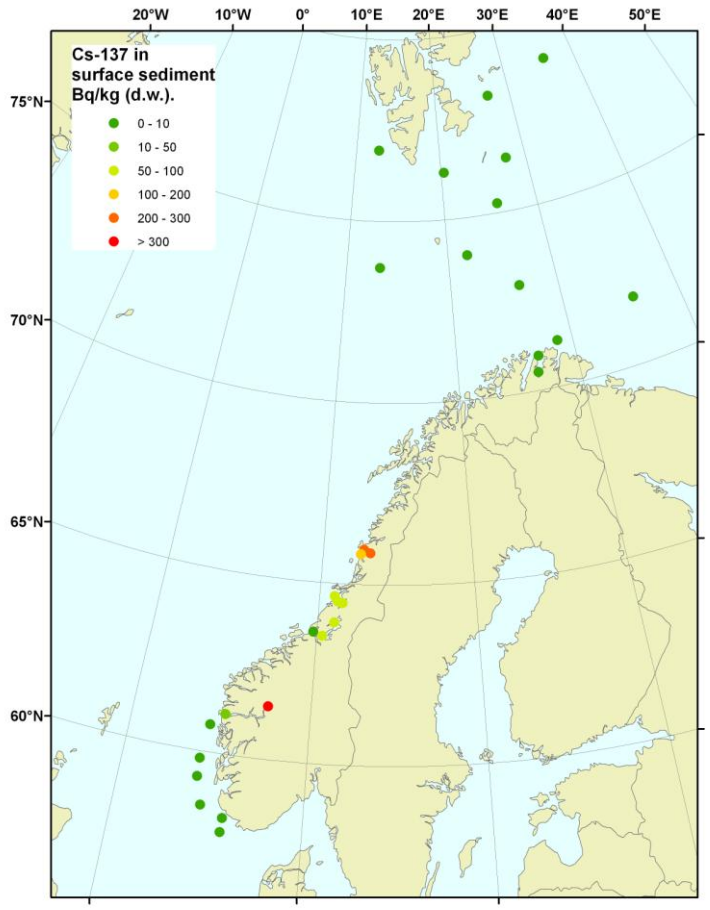


**Figure 1.8: Activity concentrations of Cs-137 in surface sediments from 2008 (preliminary results).**

There are two marine areas in Western Europe which are exceptional with respect to Cs-137 content in surface sediments. These are the Irish Sea and the Baltic. The content of Cs-137 in surface sediments from those areas varies.

The activity concentrations of Cs-137 in Irish Sea surface waters in 2001 is shown in Figure 1.9.The content is decreasing from 100 Bq/m$^3$ near the Sellafield plant to 10 Bq/m$^3$ further away (Department of Food and Rural Affairs, 2003). The activity concentrations of Cs-137 in sediments from the years 1982 and 1999 from the vicinity of Sellafield have a maximum content of 7875 Bq/kg and of 680 Bq/kg Bq/kg respectively in the surface layer (Jones, 2007).

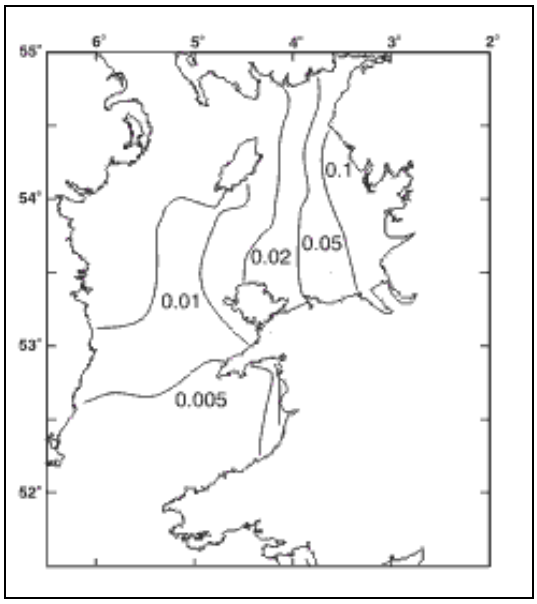


**Figure 1.9: Activity concentrations (Bq /liter) of caesium-137 in filtered surface water from the Irish Sea, September 2001 (Department of Food and Rural Affairs, 2003).**

The activity concentrations of Cs-137 in 2007 in Baltic sediments were about 39 kBq/m$^2$ and 29 kBq/m$^2$ at the sampling stations of the eastern Gulf of Finland and the Bothnian Sea. At the other stations of the Baltic Sea the amounts were clearly smaller: 0.8-5 kBq/m$^2$. In Figure 1.10 are shown the total amounts of Cs-137 in sediments at different sampling stations in the Baltic Sea at the beginning of the 2000's (STUK-B 91, 2008).

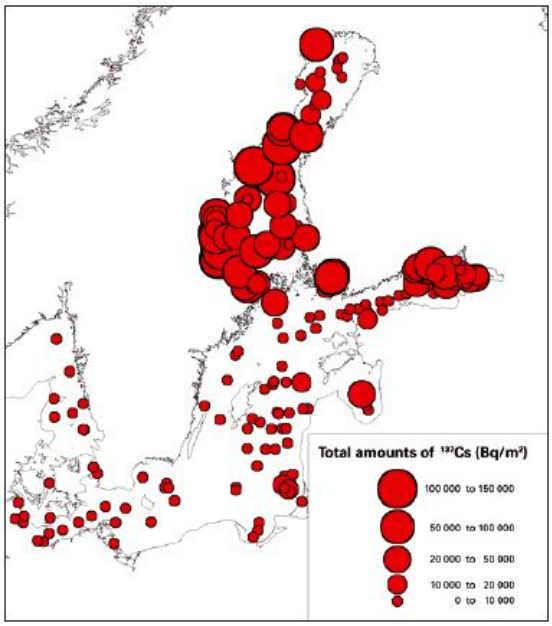


**Figure 1.10: Total amounts of Cs-137 (Bq/m$^2$) in bottom sediments at different sampling stations in the Baltic Sea at the beginning of the 2000's (STUK-B 91, 2008).**

### 1.3.5 Cs-137 in Norwegian fjords

Investigations on surface sediments (0-1, 0-2 cm) from Norwegian fjords and the coast in the period from 1999 to 2008 have been made as a part of the RAME Programme.

As a part of the present study all the results on Cs-137 activity concentrations in surface sediment samples from Norwegian fjords have been collected, Appendix I Table A1 to Table A4. The Cs-137 activity concentrations in Norwegian fjords from 1999 to 2008 are shown in Figure 1.11.

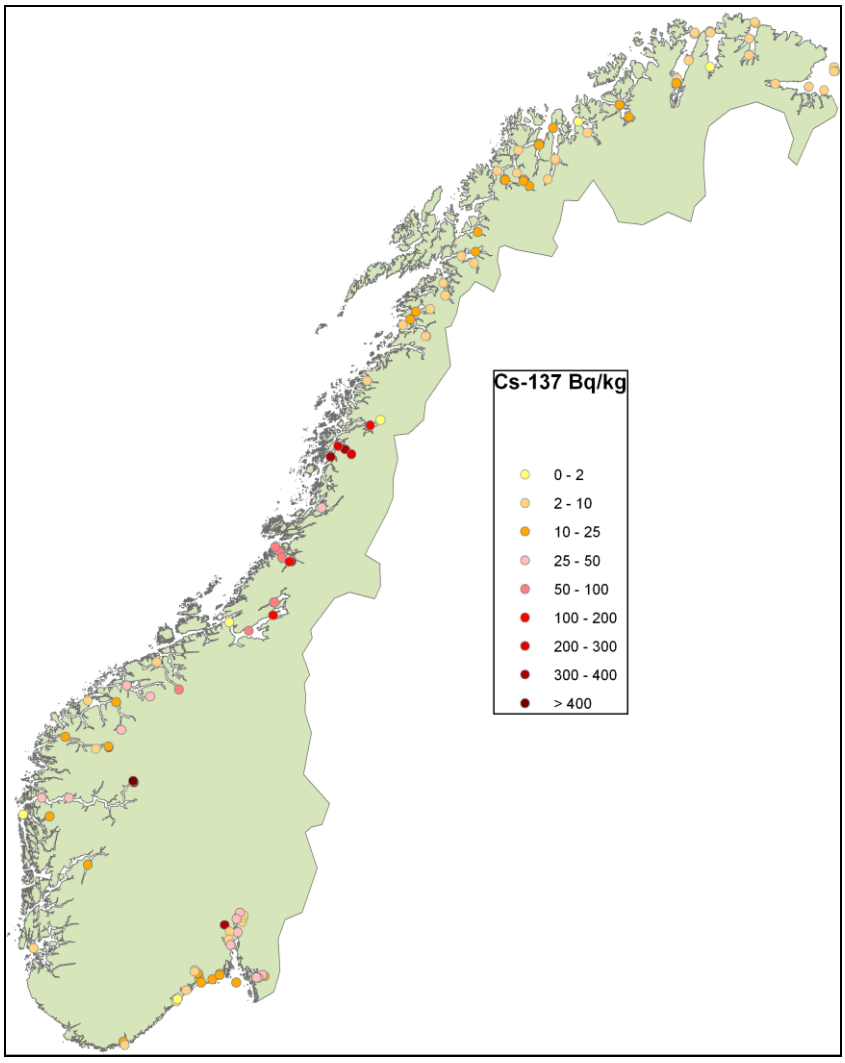


**Figure 1.11: Cs-137 in surface sediments, Bq/kg (d.w.).**

The activity concentrations of Cs-137 in the surface sediments differ considerably along the coast. The activity concentrations (including preliminary results) are in the range from < 0.7 Bq/kg (d.w.) to 415 Bq/kg (d.w.) (NRPA, 2001) (NRPA, 2003) (NRPA, 2004) (NRPA, 2005) (NRPA, 2006) (NRPA, 2007) (NRPA, 2008) (NRPA, 2009f).

The activity concentrations on the Skagerrak coast (totally 34 measurements) ranges from < 0.7 to 40 Bq/kg (d. w.), with the highest values in the eastern part of the Skagerrak coast. One exception is the inner part of the Drammensfjord with a value of 290 Bq/kg (d.w.); Appendix I Table A1.

Samples from the coast from Kristiansand up the west coast of Norway (totally 17 measurements), has in general activity concentrations of Cs-137 from 2 to 41 Bq/kg (d.w.). Important exceptions are 415 and 323 Bq/kg (d.w.) in the Sognefjord, 102 Bq/kg (d.w.) in the Nordfjord and 85 Bq/kg (d.w.) in the Sunndalsfjord; Appendix I Table A2.

In the area from Trøndelag to Lofoten (totally 26 measurements) the activity concentrations are in general in the range from 2 to 48 Bq/kg (d.w.). Exceptions are 67 Bq/kg (d.w.) in the Trondheimsfjord, 102 Bq/kg (d.w.) in the Beistadfjord, 330 Bq/kg (d.w.) in the Namsfjord, 365 Bq/kg (d.w.) in the Velfjord, 317 Bq/kg (d.w.) in the Vefsnfjord and 126 Bq/kg (d.w.) in the Ranafjord; Appendix I Table A3.

From Lofoten to the Russian border (totally 59 measurements) the activity concentrations of Cs-137 are in the range from 1.9 to 20.2 Bq/kg (d.w.). All the measured samples from this coastline are within this range; Appendix I Table A4.

## 1.4 Cs-137 dynamics

Cs-137 behavior in the marine water column is very similar to that of conservative tracers (Povinec, 2003). Conservative tracers are less particle-reactive than others. Complexed cesium in seawater has a weak affinity for sediment particles; cesium remains in solution and are transported by the flow field more or less passively without being affected by other processes. Conservative tracers can travel over a long distance from the point of injection without being deposited on the seabed. In the marine environment, most anions, alkali and alkali earth group elements behave conservatively (Vintro, 2009). In the marine environment conservative radionuclides introduced at the surface will migrate downwards by the process of diffusion and advection (Boven, 1979). Of all Cs-137 transported through the North Sea, only about 2 % is stored in the North Sea sediments, the rest passes through (Becks, 2000).

Cs-137 in run-off from land bound in organic particles is desorbed from suspended particles in the river when salinity increases (Vintro, 2009).

Some clay minerals have a high adsorption capacity for cesium. Coughtrey and Thorne (1983) stated that the degree to which Cs-137 binds to sediments depends primarily on their content of the clay mineral illite, as Cs-137 is expected to bind irreversibly to this mineral. This is also the case for Cs-137 bound to clay particles in river run-off. In small particles the surface area in contact with cesium is relatively larger than for larger particles. Knowledge about the particle size distribution within the sediment is important when evaluating the Cs-137 content.

In open marine areas the Cs-137 is conservative, but when reaching coastal areas with a high content of clay particles it will bind to sediment particles and rapidly be transferred into the sediments.

## 1.5 Sediments

Sediments are the final sink for most particles and organic material present in the seawater. Marine sediments accumulate by sinking of particulate matter, deposition on seabed and buried by subsequent accumulations. Organisms living in surface sediments will cause bioturbation in the top layer, but when sediments are buried and the density of organisms is reduced in the sediments, the sediments are left more or less undisturbed. Bioturbation is the displacement and mixing of sediment particles by benthic fauna. This can also cause transport of oxygen into the sediments changing the chemical form of the elements present and thus change the mobility (SFT, 2010).

Resuspension of sediments occur at the surface of the seabed. On sites with strong current or mechanical disturbance (waves, tidal activity) the degree of resuspension may be high, especially of materials with low volume density. On sites with weak current there will be less resuspension and smaller particles will not be removed. Smaller particles will therefore be concentrated in deep areas with low current velocity near the bottom as in deep fjords. Other factors also influencing sediments are avalanches and landslides. This is highly relevant in fjords with steep slopes like some of the Norwegian fjords.

### 1.5.1 Lead 210 dating with Ra-226 correction

Sediment cores from marine sediments can be sliced into samples representing sediment layers deposited in a certain period of time. When sediments accumulate undisturbed, it is possible to measure the age of these sediment layers and the sedimentation rates. The age (within the last 120 years) of the sediments can be measured based on the content of natural radioactivity; Lead-210 (Pb-210) and radium-226 (Ra-226) (Goldberg, 1963). Fresh Pb-210 ($t_{1/2}$ =22 years) will be deposited on surface sediments together with precipitating material. When buried, the Pb-210 will decay and the Pb-210 concentration in the profile of the core will follow the exponential decline with depth as a result from radioactive decay. The age of a particular layer is found by calculating the amount of Pb-210 which has decayed. Dated sediment layers, therefore enables investigations of sediment layers deposited at a certain time in near history.

### 1.5.2 Cs-137 dating

As described; Chapter 1.1.2; the main sources of Cs-137 to the marine environment are known with respect to time and change of quantity. The single most known incidence is the Chernobyl accident in April 1986, causing a steep change in Cs-137 content in the environment. This can be utilized when examining sediment profiles; at which layer in the sediment core is the Chernobyl peak found? If the sediments have been undisturbed, this is the sediment layer deposited in 1986. It is then possible to calculate the sedimentation rate and thus the age of every layer in the core. This method is frequently used, but is normally followed and verified by Pb-210 dating (Tadjiki and Erten, 1994) (Ritchie and McHenry, 1990). This method is not useful when the sediments consist of sand (Ritchie and McHenry, 1990).

## 1.6 Background for this study

From the regular monitoring of radioactivity in Norwegian marine areas; the surface sediment sample with the maximum Cs-137 activity concentration is 415 Bq/kg (d.w.) in a surface sediment sample from 2005, from the head of The Sognefjord (NRPA, 2007). Several other surface sediment samples from Norwegian fjords have Cs-137 activity concentrations which are considerably higher than samples from open marine areas.

The samples with high contents of Cs-137 are all from fjord bottoms and from fjords which receive drain-off from areas which received considerable amounts of fallout after the Chernobyl accident in 1986; Figure 1.12.

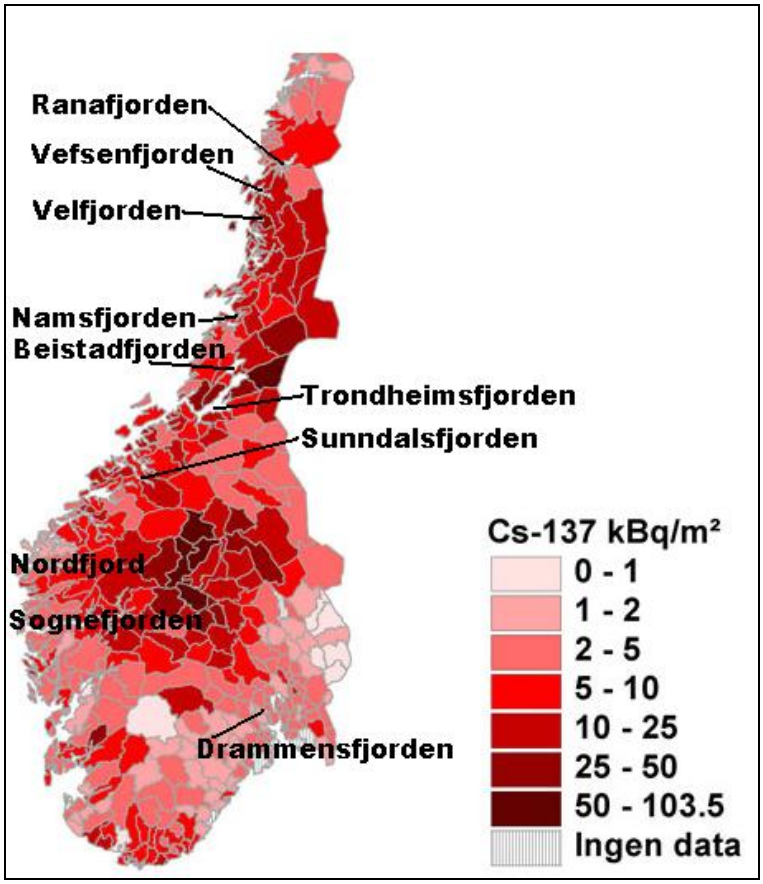


**Figure 1.12: Chernobyl fallout (NRPA, 2009b) and fjords with high contents of Cs-137.**

Some of these areas also overlap with areas receiving considerable amounts of precipitation during weapon test global fallout, Figure 1.2. Chernobyl fallout on land surrounding the inner part of the Sognefjord was high. In some specific catchment area with rivers ending up in the Sognefjord the fallout was 10-25 kBq/m$^2$ Cs-137 (Figure 1.1). The western part of the Sognefjord is also in an area with heavily affected by global fallout, Figure 1.2.

In Northern Norway (Troms and Finnmark) there are no fjords with elevated Cs-137 content. This district received considerable less Chernobyl fallout. This confirms the conclusion from Matishov and Matishov (2005); in Northern Norway (Troms and Finnmark), the origin of Cs-137 in the terrestrial environment is mainly global weapons fallout.

One of the reasons for the elevated levels of Cs-137 in the Sognefjord can be direct fallout from the Chernobyl accident and run-off from nearby areas affected by the Chernobyl

accident. Radionuclides held in the catchment soils are slowly transferred to river water by erosion of soil particles and by desorption from the soil. The Cs-137 is further transported to the sea where it reaches water with a specific salinity, and Cs-137 will be dissolved or deposited in sediments. Cs-137 binds to sediments, but the degree of binding is dependent of the particle and the water in which it exists (Salbu et.al., 1998).

The fate of this Cs-137 in the fjords will depend of many processes influencing the bioavailability and mobility of the nuclide. The water exchange may be very slow in some fjords and run-off from land will continue. This may result in increasing contents of Cs-137 in Norwegian fjords. Contamination in Norwegian terrestrial areas and in open ocean areas will also influence the content of Cs-137 in the Norwegian fjords.

## 1.7 Objective

The main objective with this study is to measure and compare the content of Cs-137 in sediment cores from the head and near mouth of the Sognefjord and head and near mouth of the Laksefjord.

The secondary objective is to examine to in which degree the three known sources; Chernobyl, Sellafield and global weapons test fallout, have affected the content of Cs-137 in the sediments of the two fjords.

In order to meet the second objective, dating the sediments was necessary and was conducted using the Pb-210 dating method with correction of Ra-226 (Goldberg, 1963) (Appelby and Oldfield, 1977), and also introducing this new method at the IMR-laboratory. In addition there have been done investigations on particle size distribution and on the ratio between Pu-isotopes in the sediments.

# 2. Material and Methods

## 2.1 Sample description

Sediment samples were taken in two Norwegian fjords; the Laksefjord in northern Norway and the Sognefjord in southern Norway; Figure 2.1.

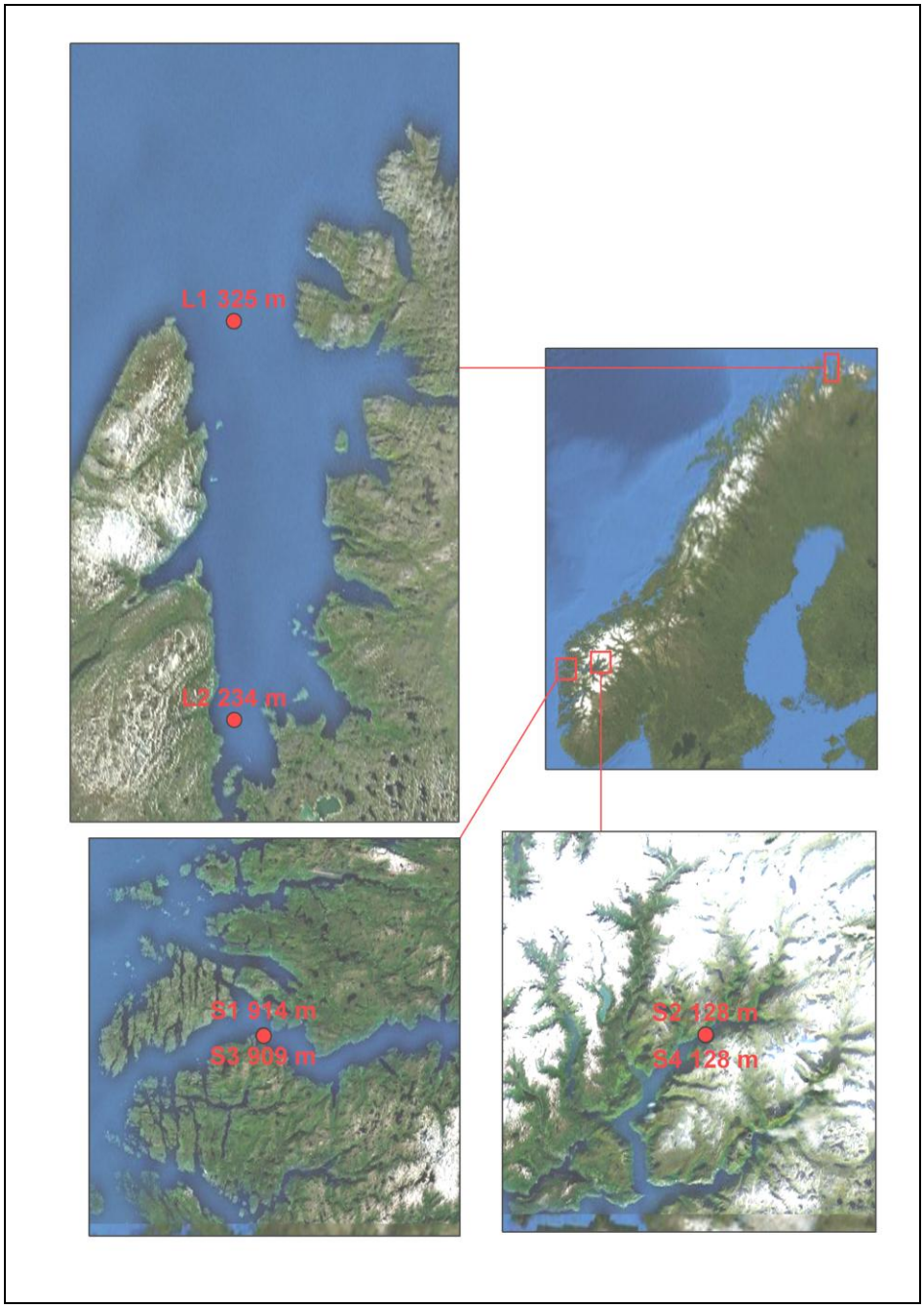


**Figure 2.1: Sampling areas; sites L1 and L2 in the Laksefjord, sites S1 and S3 in the outlet of the Sognefjord and sites S2 and S4 in the head of the Sognefjord.**

The Sognefjord was chosen as investigation area based on earlier knowledge of relatively high Cs-137 content in the surface sediment measured in samples from the inner part of the fjord in 2005 (NRPA, 2007). The Laksefjord was chosen as investigation area as a comparison to the Sognefjord due to its long distance from Sellafield, the Baltic Sea and other areas with relatively high amounts of Chernobyl fallout. The Laksefjord is still a fjord in the Norwegian coastal current, and in vicinity to Russian areas with nuclear industry.
The sampling sites from inner part of the Sognefjord were placed approx. at the same position as the surface sediment sample with extraordinary high Cs-137 content from 2005. The sampling sites from outer part of the Sognefjord were chosen based on knowledge of depth, bottom conditions and the geographical position near the outlet of the fjord, but inside the sill. The sampling sites in the Laksefjord were chosen as a representative for a fjord adjacent to the Norwegian coastal current; and in the inner and outer part of the fjord.

In the Laksefjord there were 2 sampling sites, L1and L2, and in the Sognefjord there were 4 sampling sites; S1 to S4; Figure 2.1. L1 and L2 were taken from R/V "Johan Hjort" in November 2007, S1 and S2 were taken from R/V "Håkon Mosby" in November 2007. S3 and S4 were taken from R/V "Håkon Mosby" in November 2008 in the same position as the sample taken the previous year; Table 2.1.

**Table 2.1: Position, depth and sampling date for all samples**

| Sampling site | Position | Dept | Sampling date | Fjord |
|---|---|---|---|---|
| L1 | N70 º 57'-E26 º 54' | 325 m | 03.11.08 | Laksefjord |
| L2 | N70 º 30'-E26 º 38' | 234 m | 03.11.08 | Laksefjord |
| S1 | N61 º 06'-E05 º 12' | 914 m | 20.11.07 | Sognefjord |
| S2 | N61 º 28'-E07 º 33' | 128 m | 18.11.07 | Sognefjord |
| S3 | N61 º 06'-E05 º 12' | 909 m | 23.11.08 | Sognefjord |
| S4 | N61 º 28'-E07 º33' | 128 m | 22.11.08 | Sognefjord |

## 2.2 Sample collection

The samples were taken with a Smøgen boxcorer; Figure 2.2.

**Figure 2.2: Smøgen boxcorer**

The boxcorer is a grabtype sample device equipped with an inner box in stainless steel with area 30 x 30 cm and height of 40 cm. This device takes a surface undisturbed portion of the seabed, Figure 2.3; in the following called a grab sample.

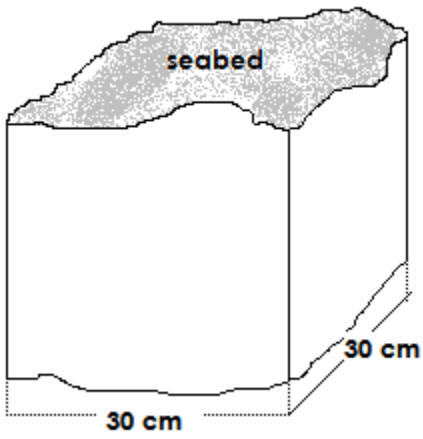


**Figure 2.3: A grab sample of undisturbed seabed taken with a Smøgen boxcorer.**

The boxcorer is supported with lead weights on a supporting frame, and is forced into the seabed by the weights. How far into the sediments the sample device penetrates depends on

the compactness of the seabed. When removing the boxcorer from the seabed a grab is closing the device in the bottom beneath the sediment sample. On top the device is closed by hatches to prevent the top layer from disturbance. The undisturbed surface includes a water layer on top of the sediments.

From the boxcorer grab sample, subsamples were taken with PVC sewage tubes with an inner diameter of 10 cm. The tubes had a length of 40 cm and they where manually pressed into the boxcorer grab sample; Figure 2.4. Excess material was removed. Lids were put in bottom and on top of each core sample, and they were frozen in standing position to –20 ºC and transferred to the laboratory for further preparation and analysis.

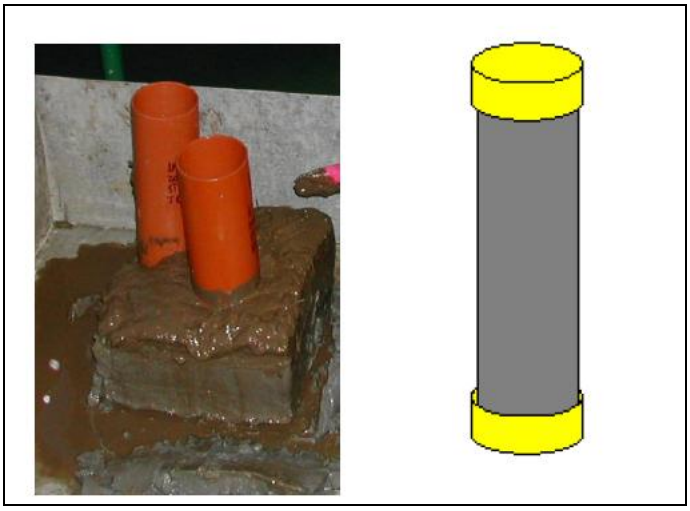

**Figure 2.4: Sub sampling from grab sample; photo: Hilde Elise Heldal.**

The total sampling included two or three cores from each boxcorer grab sample, Table 2.2.

**Table 2.2: Sample identification**

| Sampling site | Number of cores | Core identity |
|---|---|---|
| L1 | 2 | L1-1 and L1-2 |
| L2 | 2 | L2-1 and L2-2 |
| S1 | 3 | S1-1, S1-2 and S1-3 |
| S2 | 3 | S2-1, S2-2 and S2-3 |
| S3 | 2 | S3-1 and S3-2 |
| S4 | 2 | S4-1 and S4-2 |

## 2.3 Sample preparation

Before sample preparation, the tubes with sediments were thawed over night in standing position. The sediment cores were sequentially cut in standing position by using a piston from the bottom of the tube pressing towards the top of the tube; Figure 2.5.

**Figure 2.5: Corer cutting device; photo: Hilde Elise Heldal.**

The cores were gradually pressed upwards and cut in one centimeter slices and transferred to pre weighed aluminum dishes and dried. The water on top of the sediment cores were collected and dried and the material remaining was added to the top slice. All sample-slices were weighed before and after drying, and % dry weight was calculated.

The samples from S1 and S2 were dried in room temperature until complete dryness. Samples from L1, L2, S3 and S4 were freeze-dried until complete dryness. The length of the sediment cores varied between 7 cm and 16 cm. Altogether the sediment cores were sliced into 140 samples, varying from 7 to 16 slices from each core. An overview of the samples and dry weight data are given in Appendix II, Table A5.

After drying, the samples were crushed and homogenized using a mortar. Known amounts of dry sample material were transferred to the specific sample geometry. The geometry used was

a flat 60 ml geometry; 60 ml p.e. box with lid counting container; 60 ml p.e.box: Nolato AB, art.no. 110170 (box) and 112040 (lid).

The samples were wrapped in aluminum foil and taped with aluminum tape to prevent radon-222 (Rn-222) leakage from the sediment and marked, Figure 2.6. Samples were stored at least 4 weeks to allow ingrowth of lead-214 (Pb-214) and bismuth-214 (Bi-214) prior to analysis.

**Figure 2.6: Sample preparation**

A Mettler Toledo PG 5001-S, with weighing range of 2 g to 2 kg and a resolution on 0.1 g was used for sample weighing.

## 2.4 Instrument and facilities

The samples have been measured on the IMR Chemistry Laboratory on an ORTEC gammadetector: GMX Series GAMMA-X HPGE (High Purity Germanium) Coaxial Photon Detector system with PopTop cryostat configuration. Resolution (FWHM) at 1.33 MeV (Co-60) is 1.95 keV. Relative efficiency at 1.33 MeV is 38%. Crystal diameter is 59.0 mm and crystal length is 78.3 mm. The detector is cooled electrically with Ortec X-Cooler; mechanical cooler for HPGe detectors. The cooler is protected by Ortec CryoSecure Compressor Power Controller.

For detector shielding a Mdl Fabcast 04B1, low background shielding is used. This is a circular lead shield from machined stepped lead rings mounted in a frame with 10 cm solid lead with Cu/Cd lining and 25mm lead under shield.

The counting room at IMR is a low background counting room with 195 mm concrete walls including sand with a high content of olivine; giving low background and low quantification limits. The mean count rate from background the last five years in the Cs-137 peak ROI is 0,00411cps for the detector used.

The program used to collect the gammaspectra is ORTEC GammaVision.

Particle size analysis was done on Endekott thread sieves. The particle sizing was carried out at Unifob AS, Seksjon for anvendt miljøforskning (Uni Environment, SAM-Marin).

All the calculations are done in Microsoft Excel.

## 2.5 Particle size analysis

Particle size analyses (Buchanan, 1984) were done on the 0-1 cm slice samples from one of the cores from each sampling site. The samples were sieved in the fractions: $< 63$ μm, $> 63$ μm $< 2$ mm, $> 2$ mm. Results on particle size analysis are given in chapter 3.1.

## 2.6 Pu-analysis

The Pu-analysis has been carried out at the NUK-division at Risø DTU, Denmark. The method used is an internal modified method using ICP-MS based on several previous published methods (pers.comm. DR. Per Roos, DTU, Denmark).

## 2.7 Measurements

### 2.7.1 Gamma spectroscopy

Gamma spectroscopy enables identifying and quantifying gamma ray emitters. Each gamma ray emitter emits radiation with one or more unique energies as given in Schøtzig and Schraeder (1993). The intensity of the radiation is depended of the amount of the radionuclide. When gamma ray emissions from a sample are collected and analyzed with a gamma spectroscopy system, a gamma energy spectrum is produced. A detailed analysis of this spectrum is made in order to determine the identity and quantity of gamma ray emitters present in the sample. A peak in the spectrum at one or more exact energies enables an identification of the radionuclide. The area of the peak is proportional to the activity of the radionuclide. The equipment used in gamma spectroscopy includes an energy-sensitive

radiation detector, a pulse sorter (i.e., multichannel analyzer), and associated amplifiers and data readout devices.

Radionuclides with gamma ray emissions at known energies are used to calibrate the spectrum from channels to keV.

### 2.7.2 Measuring Cs-137

Cs-137 decays by beta decay with a half life of 30.17 years (Schøtzig and Schraeder, 1993), to a metastable nuclear isomer of barium-137 (Ba-137m). Barium-137m has a half life of 2.55 minutes and is responsible for the gamma ray emission at 662 keV (Schøtzig and Schraeder, 1993). This energy is conventionally regarded as the 'Cs-137 gamma' energy. Cs-137 can be measured by gamma spectroscopy using the 662 keV line or by beta counting after radiochemical separation.

An accredited method is used for analyzing dried sediment samples for Cs-137 at IMR (Sværen, 2001), is based on the method described by Anderson et.al. (1992) used within the Lorakon programme (Brungot and Amundsen, 2003).

After washing the detector and lead shielding, the background is measured, normally overnight. In this work this background is called the external background. The background data are used both in Cs-137, Pb-210 and Ra-226 measurements.

A known amount of the sample is transferred to the specific geometry and measured. The detector is calibrated with a known quantity of Cs-137 measured in the same geometry as the sample.

The standard used for calibrating the detector is delivered from Analytics; a 60 ml solid matrix with density 1.15g/cc. The Cs-137 activity is specified to 76.7 Bq, with a total uncertainty of 4.4%. The reference date is 01.10.2002. This standard is made in the specific geometry; 60 ml container equipped from the laboratory.

The detector is controlled weekly with a Cs-137 point source to ensure that the peak of the Cs-137 is not moving and that the efficiency of the detector is as expected; Appendix III, Figure A1.

Every second month a control sample is measured. The control sample is an ordinary sediment surface sample with 2.8 +/- 0.3 Bq/kg Cs-137. The control sample has been measured over several years. The results are shown in Appendix III, Figure A2.

Gamma Vision functions: mark the region of interest, ROI, gross area and live counting time are used. The energy area where the Cs-137 peak is expected is marked; ROI 1, ROI 2 and ROI 3 as shown in Figure 2.7a. ROI 1 is covering the peak with a width of 41 channels. ROI 2 and ROI 3 are each 5 channels out to each side of the peak, both with a width of 10 channels, and representing the internal background. In each measurement the gross area in ROI 1, ROI 2 and ROI 3 with corresponding counting time are manually read.

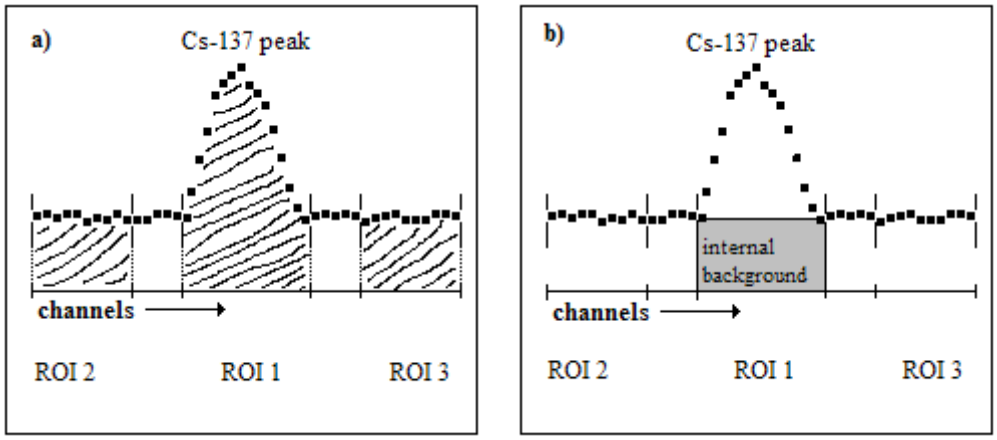


**Figure 2.7: Marking individual ROIs for measuring Cs-137 (a), the internal background (b).**

**Background**

External background is measured and calculated: The Cs-137 background level of the detector is measured once every second month to ensure that the detector is not contaminated; gross area and counting time are read.

$$bk = \frac{B_1 - \left[\left(\frac{B_2 + B_3}{20}\right) \cdot 41\right]}{T} \quad \text{, cps} \qquad (1)$$

$B_1$ = Gross area in ROI 1

$B_2$ = Gross area in ROI 2

$B_3$ = Gross area in ROI 3

T = Counting time, sec.

In all measurements in this work the external background, bk is zero. All data are presented in Appendix III, Table A6.

Internal background is related to each measurement and is exemplified in Figure 2.7b. Gross area and counting time are read and the internal background is calculated:

$$BK = \frac{\left(\frac{N_2 + N_3}{20}\right) \cdot 41}{T} \quad \text{, cps} \qquad (2)$$

$N_2$ and $N_3$ = Gross area in ROI 2 and ROI 3

T = Counting time, sec.

**Calibration**

The detector is calibrated every second month to find the geometry factor (efficiency) for the Cs-137 peak. The detector is calibrated with the Cs-137 standard; measured normally over night. Gross area and counting time are read.

Cs-137 activity in the standard on calibration date is calculated:

$$A_{Cs-137} = A_0 \cdot e^{-\ln\frac{2}{t_{\frac{1}{2}}}t} \quad \text{,Bq} \qquad (3)$$

$A_0$ = Cs-137 activity on reference date, Bq

$t_{½}$ = 11020 days, (Schøtzig and Schraeder, 1993)

t = days since reference date

Internal background connected to standard measurement is calculated (eq. 2) and geometry factor is calculated:

$$G = \frac{A_{Cs-137}}{\frac{N_1}{T} - BK}$$ , Bq/cps (4)

$N_1$ = Gross area in ROI 1

T = counting time, sec.

BK = internal background from eq. (2)

$A_{Cs-137}$= from eq. (3)

These calibrations are repeated every second month. All data are presented in Appendix III, Table A7.

**Measurement**

All samples are measured and gross area and counting time are read. The activity of Cs-137 in the sample is then calculated:

Internal background connected to the sample measurement is calculated from eq. (2), and Cs-137 activity in sample is calculated:

$$a_{Cs-137} = G \cdot (\frac{N_1}{T} - BK)$$ ,Bq (5)

G = Geometry factor from eq. (4)

$N_1$ = Gross area in ROI 1

T = Counting time, sec

BK = internal background from eq. (2)

The results are calculated to activity/ weight:

$A = (a / w) \cdot 1000$, Bq/kg (6)

a = from eq. (5), Bq

w = sample weight, g

The activity A is decay corrected to activity $A_0$, on sampling date according to equation (3). All data on Cs-137 measurements are presented in Appendix IV Table A19 to A32.

**Quantification limit**

The quantification levels are dependent on the background, the counting time and amount of sample. The quantification limit is based on the minimum net counts in the Cs-137 gamma line. L.A. Currie (1968) defines three limiting levels: Lc is the net signal level (instrument response) above which an observed signal may be reliably recognized as "detected". Ld is the "true" net signal level which may be a priori expected to lead to detection. Lq is the level at which the measurement precision will be satisfactory for quantitative determinations. The Lq is the conservative way of calculating the lowest measurable level; this to make sure that low levels of Cs-137 are not false identified and quantified.

$$Lq_m = 50\left[1+\sqrt{1+\frac{B_m}{25}}\right] \quad (7)$$

$Lq_m$ is the minimum number of net counts in ROI 1 necessary to reach the quantification limit. $B_m$ is the number of internal background counts: BK from equation (2) is multiplied with counting time, giving $B_m$. The sum of $B_m$ plus Lq is compared with the number of counts in the ROI 1. When $N1 - B_m > Lq$ the measurement is above the quantification limit. When the measurement is below quantification limit, the result is reported to be less than the quantification limit.

**Measurement uncertainty:**

The uncertainty in all results is found by the principle that every variable in calculating the result has an uncertainty. The uncertainty used is two times the standard deviation. To find the standard deviation the following general equation is used, on the variables x, y, z… (Bjørnes and Hovde, 1978):

$$s(\text{Result}) = \sqrt{\left(\frac{\partial f}{\partial x}\cdot s_x\right)^2+\left(\frac{\partial f}{\partial y}\cdot s_y\right)^2+\left(\frac{\partial f}{\partial z}\cdot s_z\right)^2+.....} \quad (8)$$

The measurement uncertainty includes uncertainty in background, sample measurement, calibration and sample amount. Uncertainty calculations conducted with this method is in good agreement with results from repeated measurement of Cs-137 in a control sample, Appendix Figure A2.

All variables involved in the calculation of Cs-137 activity concentration have an uncertainty, also calculated by the general equation (8). The uncertainty is here specified as s(variable).

Uncertainty in measured internal background:

$$sBK = \frac{sB}{T} \quad \text{,cps} \qquad (9)$$

$$sB = \sqrt{\left[\frac{41 \cdot sN_2}{20}\right]^2 + \left[\frac{41 \cdot sN_3}{20}\right]^2} \quad \text{, counts} \qquad (10)$$

Variables from sample counting:

$sN_2$ = $(N2)^{1/2}$

$N_2$ = Gross area in ROI 2

$sN_3$ = $(N3)^{1/2}$

$N_3$ = Gross area in ROI 3

T = counting time, sec.

Uncertainty in the Geometry factor:

$$sG_{Cs-137} = \sqrt{\left[\frac{T \cdot sA}{N - BK \cdot T}\right]^2 + \left[\frac{A \cdot N \cdot sT}{(N - BK \cdot T)^2}\right]^2 + \left[\frac{A \cdot T^2}{(N - BK \cdot T)^2} \cdot sBK\right]^2 + \left[\frac{-A \cdot T}{(N - BK \cdot T)^2} \cdot sN\right]^2} \text{,Bq/cps} \qquad (11)$$

Variables from standard counting:

T = counting time, sec.

sT = 1 sec.

N = Gross area in ROI 1

sN = $(N)^{1/2}$

BK = BK from eq. (2)

sBK = sBK from eq. (9)

A = $A_{Cs-137}$ from eq. (3)

sA = $sA_{Cs-137}$ from certificate, 4,4%.

Uncertainty in Cs-137 activity in sample, Bq:

$$sa_{Cs-137} = \sqrt{[(\frac{N}{T} - BK) \cdot sG\ ]^2 + [\frac{G}{T} \cdot sN\ ]^2 + [\frac{-G \cdot N}{T^2} \cdot sT\ ]^2 + [-G \cdot sBK\ ]^2} \quad \text{, Bq} \qquad (12)$$

Variables from sample counting:

N = Gross area in ROI 1

sN = $(N)^{1/2}$

T = counting time, sec.

sT = 1sec.

BK = BK from eq. (2)

sBK = sBK from eq. (9)

G = G from eq. (4)

sG = $sG_{Cs-137}$ from eq. (11)

Uncertainty in Cs-137 activity concentration in sample, Bq/kg:

$$sA = \sqrt{[\frac{1000}{P} \cdot sa\ ]^2 + [\frac{-a \cdot 1000 \cdot sP}{P^2}\ ]^2} \quad \text{,Bq/kg} \qquad (13)$$

A = activity in the sample

sa = uncertainty in activity from eq. (12)

P = sample weight, g

The activity concentration of Cs-137 in samples is given as A± 2sA.

All data on uncertainty are presented in Appendix IV Table A19 to A32.

### 2.7.3 Quality assurance in Cs-137 measurements

To ensure the quality of the Cs-137 measurements, a control sample has been measured every second months in several years with satisfactory results; Appendix III Figure A2. In addition IMR participate regularly in intercomparison exercises on sediment and aqueous samples. In the period 1995 to 2009 samples with Cs-137 activity concentrations between 0.3 Bq/kg and 23 700 Bq/kg have been measured; all with acceptable results and within the given uncertainty. The intercomparison exercises have been organized by The Nordic Committee for Nuclear Safety Research (NKS) (1995, 1999, 2001 and 2004), International Atomic Energy Agency (IAEA) (2000 and 2002), IMR and NRPA (2004) and National Physical Laboratory (NPL) (2007, 2008 and 2009).

### 2.7.4 Pb-210 and Ra-226

Uranium-238 is a natural radionuclide existing on earth. U-238 decays in the uranium decay series, Figure 2.8. Pb-210 and Ra-226 are daughters in the uranium decay series. Ra-226 decays by alpha to Rn-222. Rn-222, an inert gas, escapes from earth's surface into atmosphere. Decay daughters of Rn-222, of which Pb-210 has the longest half-life, is removed from the atmosphere via washout, forming a widespread, continuously deposited on the earth's surface. Individual Pb-210 atoms become readily attached to airborne particulate material and are removed both by washout and by dry deposition.

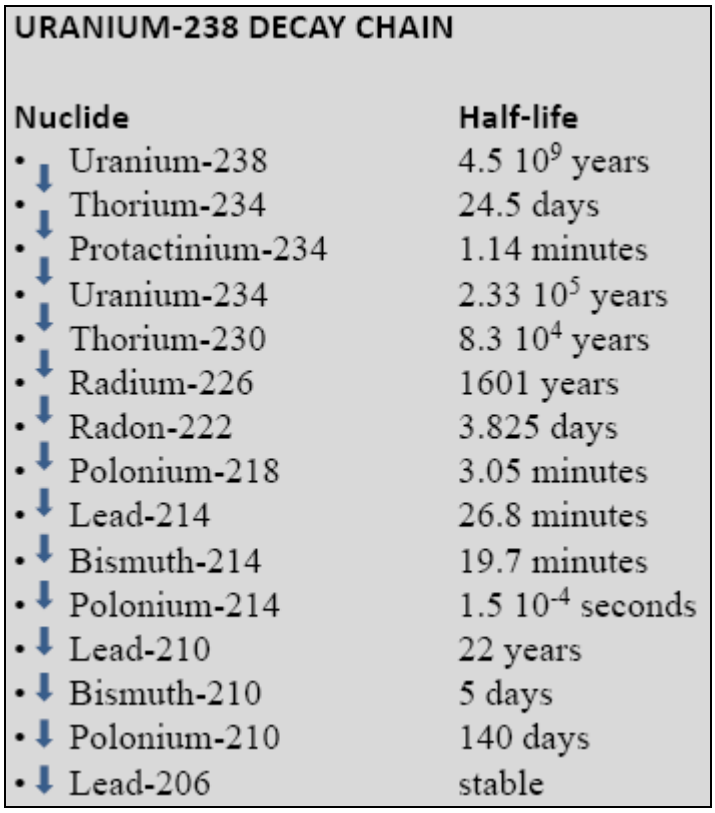


**Figure 2.8: Uranium-238 radioactive decay (Schøtzig and Schraeder, 1993).**

In aquatic systems, Pb-210 is removed from the water column by settling particles and deposited on the sediments. Measurements of Pb-210 and Ra-226 in sediment cores will provide data which enable calculating the age of the sediment.
Pb-210 decays by gamma to Bi-210 with a half life of 22.3 years and is responsible for the gamma ray emission at 46.5 keV (Schøtzig and Schraeder, 1993). Pb-210 is measured by gamma spectroscopy on this energy-line.

A known amount of sample is transferred to the specific geometry and measured with gamma spectroscopy. The detector is calibrated with a standard with a known amount of Pb-210 in the same geometry as the sample.

The standard used for calibrating the detector is delivered from QSA Global GmbH; specified to be 7.46 kBq Pb-210, with a total uncertainty of 4.4%. The reference date is 1 of July 2008 at 12:00 UTC; calibrated at Deutscher Kalibrierdienst, DKD. Density is approx 1.0g/cm3. The standard is made in the specific geometry; 60 ml container equipped from the laboratory.

Gamma rays from Pb-210 at 46.5 keV can be partially absorbed in the sample; self - absorption. This self-absorption depends on sample composition. The problems of self-

absorption, are solved by making a direct transmission measurement on each sample; making a sample specific self-absorption correction factor, KF (Cutshall et. al., 1983). An empty sample container, the Pb-210 standard, and the samples are each measured with a Pb-210 point source placed on top, Figure 2.9.

The point source used is QSA Global GmbH: 255 kBq Pb-210, reference date 1 of July 2008 at 12:00 UTC; calibrated at Deutscher Kalibrierdienst, DKD.

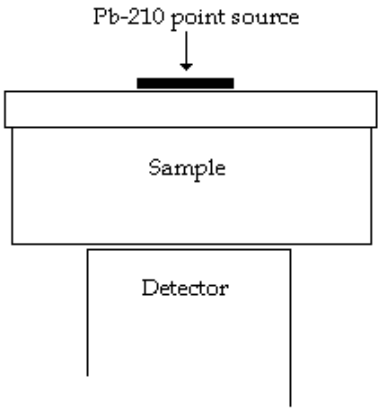


**Figure 2.9: Transmission-measurement on each sample.**

In uranium decay series Ra-226 decays via radon and polonium to Pb-214 and further on to Bi-214. If radon is prevented from escaping, there will be equilibrium between Ra-226, Pb-214 and Bi-214 after 4 weeks. Ra-226 can then be determined by gamma spectroscopy on the Pb-214 gamma lines at 295 keV and 352 keV and by the Bi-214 gamma line at 609 keV (Schøtzig and Schraeder, 1993). Ra-226 content is further calculated from the average of Pb-214 and Bi-214 content (Zaborska et.al., 2008).
The standard used for calibrating the detector is delivered from QSA Global GmbH; specified to be 3.54 kBq Ra-226, with a total uncertainty of 5%. The reference date is 1 of July 2008 at 12:00 UTC; calibrated at Deutscher Kalibrierdienst, DKD. Density approx 1.1 g/cm$^3$. The standard is made in the specific geometry; 60 ml container equipped from the laboratory.

The program Gamma Vision is used when marking the detected peaks, mark peak function; and finding the net area with uncertainty and counting time.

### 2.7.5 Measuring Pb-210

All variables and equations are presented in Table 2.3.

Background: The gamma emission peak at 46.5 keV from the background measurement is manually marked and net area of the peak, uncertainty in net peak area and counting time are read. The background measurements are presented in Appendix III Table A8.

**Calibration:** Detector is calibrated by measuring a standard with a known quantity of Pb-210 in the same geometry as the samples. The standard is normally measured over night. The gamma emission peak at 46.5 keV from the Pb-210 standard is marked and net area of the peak, uncertainty in net peak area and counting time are read. The counting rate $R_{cal}$ is calculated. $R_{cal}$ data are presented in Appendix III table A9.

The standard activity on calibration date is calculated. The activity data are presented in Appendix III table A10.

The geometry factor, $g_{Pb\text{-}210}$, is calculated. The data on $_{gPb\text{-}210}$ are presented in Appendix III Table A11.

Density correction factor (KF) for the Pb-210 standard is found by a 600 second measurement of the standard with the Pb-210 point source placed on top of it, $R_{cal+.}$ The data on $R_{cal+}$ are presented in Appendix III Table A12.

Additionally a 600 second measurement of an empty container of the same type as the standard and sample container with a Pb-210 point source placed on top, $R_s$. The data on $R_s$ are presented in Apendix III Table A13.

The density correction factor KF for the standard is calculated, and the geometry factor is further corrected for density. The data on KF and corrected geometry factor are presented in Appendix III Table A14. The corrected geometry factor is further used to calculate the Pb-210 content in the samples.

**Sample measurement:** At least 4 weeks after filling the measuring container and wrapping it in aluminum foil, the sample was measured overnight and count rate in 46.5 keV was found and corrected for background; R. The sample was then consecutively measured in 600

seconds with the Pb-210 point source placed on top to find the count rate; $R_+$. The density correction factor KF, for each sample was calculated followed by calculation of the Pb-210 activity concentration.

Finally, the activity A is decay-corrected to activity $A_0$ on sampling date according to radioactive decay equation. All data on Pb-210 from sample measurements are presented in Appendix V Table A33 to A43.

**Uncertainty:** All variables used in the calculation of Pb-210 in sediment samples also have an uncertainty. The uncertainty is given as s(variable). All data on uncertainty in Pb-210 measurements are presented in Appendix V Table A33 to A43.

Finally, the activities of Pb-210 in samples are given as $A \pm 2sA$.

The method is further controlled by measuring samples with a known quantity of Pb-210; Table 2.5.

**Table 2.3: Variables and equations in Pb-210 measurements and calculations.**

| Variable | Symbol | **Pb-210 peak at 46.5 keV** Equation | Uncertainty |
|---|---|---|---|
| Background measurement | BK | BK = net area/ counting time, cps | sBK = s(net area) / counting time, cps |
| **Calibration:** | | | |
| Counting rate standard | $R_{cal}$ | $R_{cal}$ = net area/ counting time, cps | $sR_{cal}$ = s(net area) / counting time, cps |
| Activity in standard on reference date | $A_{0Pb-210}$ | $A_0$ = 7,46 kBq | 4,4 % |
| Half life | t½ | t½ = 8145 days | 8 days |
| Days decayed | t | t = days from reference date to measuring date | |
| Activity in standard on calibration date | $A_{Pb-210}$ | $A_{Pb-210} = A_0 \cdot e^{-\ln\frac{2}{t\frac{1}{2}}t}$ , Bq | $sA_{Pb-210}$ = +/- 5 % |
| geometry factor | g | = $A_{Pb-210}$ / $R_{cal}$ , Bq/cps | sg = sA / $R_{cal}$ , Bq/cps |
| Counting rate standard point source on top | $R_{cal+}$ | $R_{cal+}$= net area/ counting time, cps | $sR_{cal+}$ = s(net area) / counting time, cps |
| Counting rate empty container point source on top | $R_s$ | $R_s$= net area/ counting time, cps | $sR_s$ = s(net area) / counting time, cps |
| Density correction factor standard | KF | KF= ln [ ( $R_{cal+}$ - R ) / $R_s$] / [ ( ($R_{cal+}$ - R ) / $R_s$) –1] | sKF is set to 0,01. |
| Geometry factor | G | $G_k$ = g / KF, Bq/cps | $sG = \sqrt{[\frac{sg}{KF}]^2 + [\frac{-g \cdot sKF}{KF^2}]^2}$ , Bq/cps |
| **Sample Measurement:** | | | |
| Count rate sample | R | R=(net area/counting time)–BK, cps | sR = s(net area) / counting time, cps |
| Count rate sample point source on top | $R_+$ | $R_+$ = net area/ counting time, cps | $sR_+$ = s(net area) / counting time, cps |
| Density correction factor for the sample | KF | KF = ln ( $R_+$ - R ) / $R_s$ / ( $R_+$ - R ) / $R_s$ - 1 | sKF is set to 0,01. |
| Activity in sample on measuring date | A | A = $G_k$ · R · KF / V , Bq/kg | $sA = \sqrt{\left(\frac{sG \cdot R \cdot KF}{V}\right)^2 + \left(\frac{sR \cdot G \cdot KF}{V}\right)^2 + \left(\frac{sKF \cdot G \cdot R}{V}\right)^2 + \left(\frac{-G \cdot R \cdot KF}{V^2}\right)^2}$ , Bq/kg |
| Sample weight | V | kg | $1 \cdot 10^{-4}$ kg |
| Activity in sample on sampling date | $A_0$ | $A_0 = \frac{A_{Pb-210}}{e^{-\ln\frac{2}{t\frac{1}{2}}t}}$ , Bq/kg | |

### 2.7.6 Measuring Ra-226

All variables and equations are presented in Table 2.4.

**Background:** The gamma emission peaks at 295keV, 352keV and 609keV from background measurement is marked and net area of the peak and counting time are read. The background measurements are presented in Appendix III Table A15.

**Calibration:** The detector is calibrated by measuring a standard with a known quantity of Ra-226 in the same geometry as the samples. In a similar manner as for previous measurements the gamma emission peaks at 295 keV, 352 keV and 609 keV are marked, and the net area of the peaks and counting time are read; followed by calculation of count rates (cps) in each of the three peaks.

The activity of Ra-226 in standard on calibration date is calculated. The activity data are presented in Appendix III Table A16.

The geometry factors (G) for each peak are calculated and background corrected according to values in Appendix III Table A15.The geometry factors are given in Appendix III Table A17.

**Sample measurement:** The sample is measured overnight and the gamma emission peaks at 295 keV, 352 keV and 609 keV are marked, and the net area of the peaks and counting time are read. The count rate in each peak is calculated.

The background corrected activity of Pb-214 (two peaks) and Bi-214 (one peak) in the sample is calculated. The activity, ARa-226, used in dating calculations is the average of the Pb-214 and Bi-214 measurements.

The Ra-226 activity is not corrected for decay due to its long half-life.

All data on Ra-226 from sample measurements are presented in Appendix VI Table A44 to A54.

**Uncertainty:**

All variables used in the calculation of Ra-226 in sediment samples have an uncertainty. The uncertainty is given as s(variable).

All data on uncertainty in Ra-226 results are presented in Appendix VI Table A44 to A54.

Finally, the activities of Ra-226 in samples are given as A ± 2sA.

**Table 2.4: Variables and equations in Ra-226 measurements.**

| Variable | Sign | **Ra-226 determination** | |
|---|---|---|---|
| | | Equation | Uncertainty |
| Background measurement | $BK_{295keV}$ | BK = net $area_{295keV}$/ counting time, cps | sBK = s(net $area_{295keV}$) / counting time, cps |
| Background measurement | $BK_{352keV}$ | BK = net $area_{352keV}$/ counting time, cps | sBK = s(net $area_{352keV}$) / counting time, cps |
| Background measurement | $BK_{609keV}$ | BK = net $area_{352keV}$/ counting time, cps | sBK = s(net $area_{609keV}$) / counting time, cps |
| **Calibration:** | | | |
| Count rate standard | $cps_{295keV}$ | $cps_{295keV}$ = net $area_{295keV}$/ counting time, cps | s($cps_{295keV}$) = s(net $area_{295keV}$) / counting time, cps |
| Count rate standard | $cps_{352keV}$ | $cps_{352keV}$ = net $area_{352keV}$/ counting time, cps | s($cps_{352keV}$) = s(net $area_{352keV}$) / counting time, cps |
| Count rate standard | $cps_{609keV}$ | $cps_{609keV}$ = net $area_{609keV}$/ counting time, cps | s($cps_{609keV}$) = s(net $area_{609keV}$) / counting time, cps |
| Activity in standard on reference date | $A_{0Ra-226}$ | $A_0$ = 3,54 kBq | 5 % |
| Half life | t½ | t½ = 1601 years (Schøtzig and Schraeder, 1993) | 7 years |
| Days decayed | t | t = days from reference date to measuring date | |
| Activity in standard on calibration date | $A_{Ra-226}$ | $A_{Pb-210} = A_0 \cdot e^{-\ln\frac{2}{t_{\frac{1}{2}}}t}$ , Bq | $sA_{Ra-226}$ = +/- 5 % |
| Geometry factor | $G_{295keV}$ | = $A_{Ra-226}$ / $cps_{295keV}$, Bq/cps | sG = sA / $cps_{295keV}$ , Bq/cps |
| Geometry factor | $G_{352keV}$ | = $A_{Ra-226}$ / $cps_{352keV}$, Bq/cps | sG = sA / $cps_{352keV}$ , Bq/cps |
| Geometry factor | $G_{609keV}$ | = $A_{Ra-226}$ / $cps_{609keV}$, Bq/cps | sG = sA / $cps_{609keV}$ , Bq/cps |
| **Measurement:** | | | |
| Sample measurement | $cps_{295keV}$ | $cps_{295keV}$ = net $area_{295keV}$/ counting time, cps | s($cps_{295keV}$) = s(net $area_{295keV}$) / counting time, cps |
| Sample measurement | $cps_{352keV}$ | $cps_{352keV}$ = net $area_{352keV}$/ counting time, cps | s($cps_{352keV}$) = s(net $area_{352keV}$) / counting time, cps |
| Sample measurement | $cps_{609keV}$ | $cps_{609keV}$ = net $area_{609keV}$/ counting time, cps | s($cps_{609keV}$) = s(net $area_{609keV}$) / counting time, cps |
| Weight of sample | V | | $1 \cdot 10^{-4}$ kg |
| Activity in sample on measuring date | A | A = G · (cps – BK) / V | $sA = \sqrt{\left(\frac{sG(cps-BK)}{V}\right)^2+\left(\frac{G\cdot scps}{V}\right)^2+\left(\frac{G\cdot sBK}{V}\right)^2+\left(\frac{-G(cps-BK)\cdot sV}{V^2}\right)^2}$ , Bq |

### 2.7.7 Quality assurance in Pb-210 and Ra-226 measurements

Implementing a new method in the laboratory will require precautions to secure the accuracy of the results.

To ensure the quality of Pb-210 and Ra-226 measurements, sediment samples with a known content of those nuclides have been analyzed (IMR result) as shown in Table 2.5. All results are within the uncertainty given.

**Table 2.5: Comparison of IMR-results with reference materials on Pb-210 and Ra-226 content.**

| Reference material | Reference value, Bq/kg | | IMR result, Bq/kg | | Reference |
|---|---|---|---|---|---|
| | Pb-210 | Ra-226 | Pb-210 | Ra-226 | |
| IAEA-368 measured 24.04.09 | 23,2 (19,8-27,2) | 21,4 (20,3-22,6) | 23,0 ±3 | 22,9±2,8 | IAEA, 1991 |
| IAEA-368 measured 18.05.09 | 23,2 (19,8-27,2) | 21,4 (20,3-22,6) | 25,3±2 | 23,3±2,5 | IAEA, 1991 |
| IAEA-368 measured 13.01.10 | 23,2 (19,8-27,2) | 21,4 (20,3-22,6) | 21,9±4 | | IAEA, 1991 |
| IAEA-384 | 20,9 (19-21,9) | 2,4 (2-2,9) info.value | | 3,7 +/- 1,6 | IAEA, 2000 |
| IAEA-385 | 35,5 (31,2-38,9) info.value | 22,7 (21,8-24,0) | 42,6±5 | 22,2 +/- 2,9 | IAEA, 2005 |

95% confidence interval in parentheses.

## 2.8 Dating

The Pb-210 dating method (Goldberg, 1963) is based on fractionation of U-238 series nuclides, Figure 2.8, in near surface rocks and soil. The total content of Pb-210 in the sediments has its origin from Ra-226 in the sediments (supported) and from deposit of Rn-daughters (Pb-210) on earth's surface (unsupported). There is equilibrium between the nuclides in the U-238 decay series and the content of Ra-226 in the sediments equals the Pb-210 supported. The excess Pb-210 compared to Ra-226 (Pb-210 supported) represents the amount of Pb-210 in settling particles (unsupported); eq. 14.

At sites where the deposition rate of unsupported Pb-210 has been constant over the past century and disturbance of the sediments has not occurred, the concentration profile in cores

follows the exponential decline with depth which results from radioactive decay (Goldberg, 1963).
The content of excess Pb-210 in each layer can be calculated:

$C_{Pb\text{-}210}$unsupported = $C_{Pb\text{-}210}$total - $C_{Ra\text{-}226}$ Bq/kg **(14)**

C = concentration

Two models can be used when calculating age of sediment layers from cores as described in Appleby and Oldfield (1977).

CIC-model: Age - depth profiles is determined from Pb-210 measurements assuming a constant initial concentration (CIC) of unsupported Pb-210 pr. dry weight sediment.

Age of layer: $$X = \frac{1}{\lambda} \cdot \ln \frac{C_{top}}{C_X}$$ ,Years (15)

λ = decay constant for Pb-210; 0,0315 år-1 (Appleby and Oldfield 1977)
$C_{top}$ = excess Pb-210 in top layer
$C_x$ = excess Pb-210 in layer X

CRS-model: Age - depth profiles is determined from Pb-210 measurements assuming a constant rate of supply (CRS) of unsupported Pb-210 to the sediments per unit time (not per unit dry weight as CIC-model). This method will give better results if sedimentation rates are altering (Appleby and Oldfield 1977).

The content of excess Pb-210 in each layer is calculated.

$C_{Pb\text{-}210unsupported}$ = $C_{Pb\text{-}210unsupported}$ • LW ,Bq (16)

LW = layer weight, kg

The inventory of excess Pb-210, A0, in the entire core can then be calculated:

$$A_0 = \int_0^L C \qquad \text{,Bq} \qquad (17)$$

L= length of core

The inventory of excess Pb-210 in the layers beneath the layer of dept X is calculated:

$$A_X = \int_X^L C \qquad \text{,Bq} \qquad (18)$$

The age of the layer X is calculated:

Age of layer: $$X = \frac{1}{\lambda} \cdot \ln \frac{A_0}{A_X} \qquad \text{,Years} \qquad (19)$$

λ = decay constant for Pb-210

λ = ln 2 / $t_{1/2}$ =0,0315 years-1

**Uncertainty:**

Uncertainty in the dating are not calculated using the principle as described in Chapter 2.7.2, but estimated according to Binford (1989). Ninety-five percent confidence intervals range from 1-2 years at 10 years of age (10-20%), 10-20 (10-20%) years at 100 years and 8-90 (5-60%) at 150 years old.

# 3. Results

The work includes measuring Cs-137 in 14 cores from 6 different sampling sites. 11 of the cores were analyzed for Pb-210 and Ra-226 in order to date each of the 1 cm slices from the cores. In all the 14 cores there were Cs-137 activity concentrations above the quantification level in the upper sediment layers.

## 3.1 Particle analysis

One specific 0-1cm layer from each sampling site was analyzed for particle size, Figure 3.1. At all 6 sites the content of clay and silt was dominating. The content of clay and silt was above 90 % in all 6 samples. The two sampling sites in the outlet of the Sognefjord contained the highest sand content, with 9.7% (S3) and 8.0% (S1) respectively. There was no gravel in any of the samples. The detailed results from particle size analysis are shown in Appendix IV Table A18.

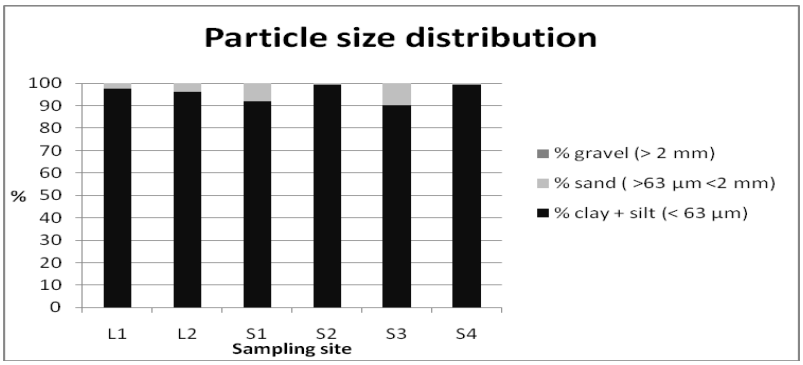


**Figure 3.1: Particle size distribution.**

## 3.2 Results on Pu-analysis

One specific 0-1 cm layer from each sampling site was analyzed for content of Pu-isotopes. The $^{238}Pu/^{239+240}Pu$ ratio was calculated and are shown in Table 3.1. All the $^{238}Pu/^{239+240}Pu$ ratios were in range 0.025 to 0.067.

**Table 3.1: 238Pu/239+240Pu ratio in surface sediment layer from the 6 sampling sites.**

| Sampling site | $^{238}Pu/^{239+240}Pu$ activity ratio |
|---|---|
| L1 | 0.044 |
| L2 | 0.039 |
| S1 | 0.067 |
| S2 | 0.058 |
| S3 | 0.067 |
| S4 | 0.025 |

## 3.3 Cs-137 results

The Cs-137 activity concentrations in sediment cores from the 6 sampling sites differ considerably and are presented in Figures 3.2 to 3.7. The Cs-137 activity concentrations in the upper sediment-layer from all 14 cores show Cs-137 activity concentrations in three activity concentration levels. In the outlet of Sognefjorden the Cs-137 level is about 6 times above the level in Laksefjorden. In the head of Sognefjorden the Cs-137 level is about 10 times above the level in the outlet of Sognefjorden.

In Laksefjorden the Cs-137 activity concentration in 0-1 cm layer is from 5.0 Bq/kg (d.w.) to 6.7 Bq/kg (d.w.) at the two sampling sites L1 and L2. The activity concentrations are decreasing with increasing depth in the sediments, Figure 3.2, 3.3 and Table 3.2. The quantification limits are reached at 4 to 6 cm depth. There seems to be no difference in the concentrations in the outlet of the fjord (L1) and in the head of the fjord (L2).

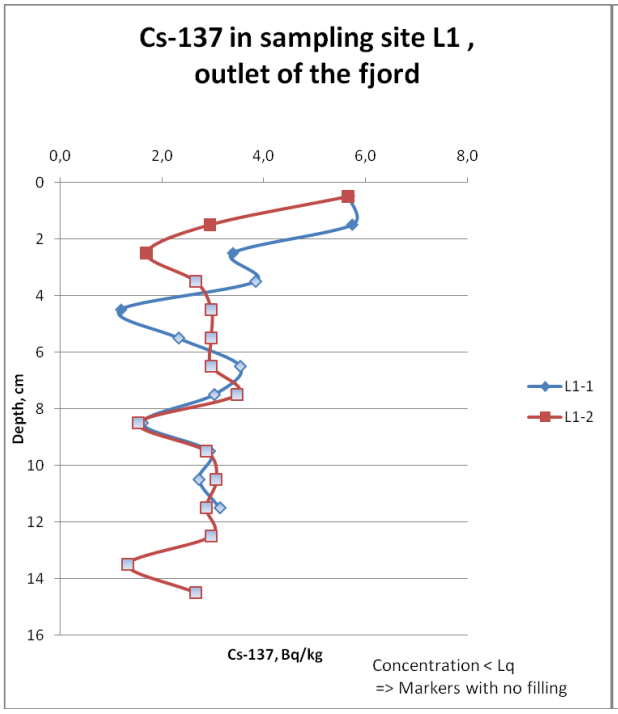


**Figure 3.2: Cs-137 in cores from outlet of Laksefjorden, sampling site L1 (2008).**

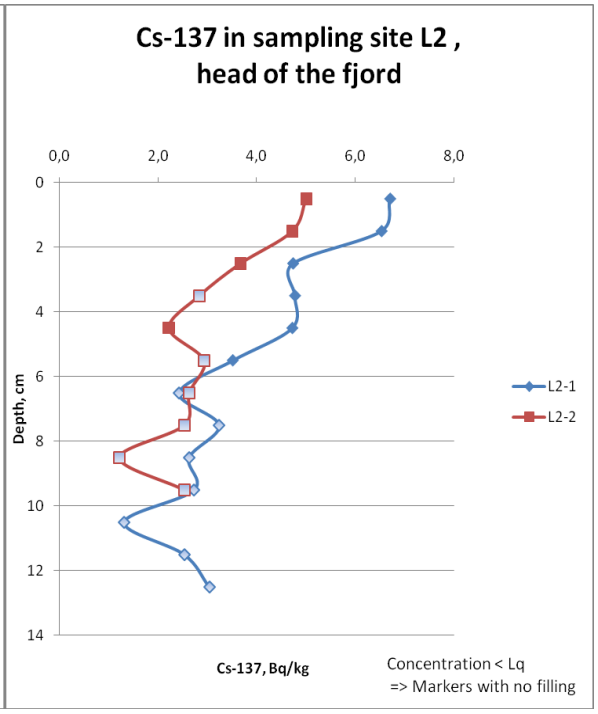


**Figure 3.3: Cs-137 in cores from the head of Laksefjorden, sampling site L2 (2008).**

**Table 3.2: Cs-137 in all layers in the cores from the Laksefjord.**

| | L1-1 | | L1-2 | | L2-1 | | L2-2 | |
|---|---|---|---|---|---|---|---|---|
| Depth | Cs-137, Bq/kg (d.w.) | Uncertainty, Bq/kd (d.w.) | Cs-137, Bq/kg (d.w.) | Uncertainty, Bq/kd (d.w.) | Cs-137, Bq/kg (d.w.) | Uncertainty, Bq/kd (d.w.) | Cs-137, Bq/kg (d.w.) | Uncertainty, Bq/kd (d.w.) |
| 0-1 cm | 5.7 | 0.8 | 5.7 | 1.0 | 6.7 | 1.2 | 5.0 | 0.9 |
| 1-2 cm | 5.7 | 0.8 | 2.9 | 0.7 | 6.5 | 1.2 | 4.7 | 1.0 |
| 2-3 cm | 3.4 | 1.2 | 1.7 | 0.5 | 4.7 | 1.0 | 3.7 | 0.8 |
| 3-4 cm | < 3.8 | | < 2.7 | | 4.8 | 1.0 | < 2.8 | |
| 4-5 cm | 1.2 | 0.5 | < 3.0 | | 4.7 | 0.9 | 2.2 | 0.8 |
| 5-6 cm | < 2.3 | | < 3.0 | | 3.5 | 0.7 | < 2.9 | |
| 6-7 cm | < 3.5 | | < 3.0 | | < 2.4 | | < 2.6 | |
| 7-8 cm | < 3.0 | | < 3.5 | | < 3.2 | | < 2.5 | |
| 8-9 cm | < 1.6 | | < 1.5 | | < 2.6 | | < 1.2 | |
| 9-10 cm | < 2.9 | | < 2.9 | | < 2.7 | | < 2.5 | |
| 10-11 cm | < 2.7 | | < 3.1 | | < 1.3 | | | |
| 11-12 cm | < 3.1 | | < 2.9 | | < 2.5 | | | |
| 12-13 cm | | | < 3.0 | | < 3.0 | | | |
| 13-14 cm | | | < 1.3 | | | | | |
| 14-15 cm | | | < 2.7 | | | | | |

In the Sognefjord the Cs-137 activity concentration in the outer part of the fjords differs considerably from the activity concentrations in the inner part of the fjord. In the outlet of the

fjord, sampling sites S1 (2007) and S3 (2008), the Cs-137 activity concentration in 0-1 cm layer is from 27.9 to 36.2 Bq/kg (d.w.), with decreasing concentrations with increasing depths in the sediments, Figure 3.4, 3.5 and Table 3.3.

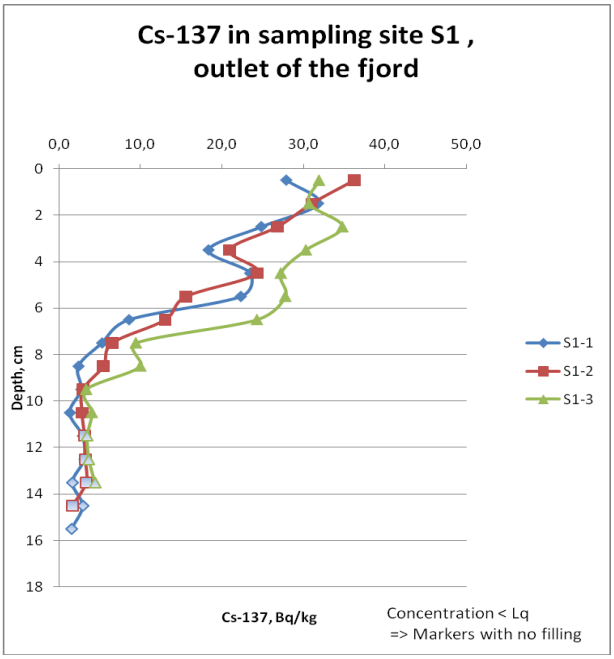


**Figure 3.4: Cs-137 in cores from the outlet of Sognefjorden, sampling site S1 (2007).**

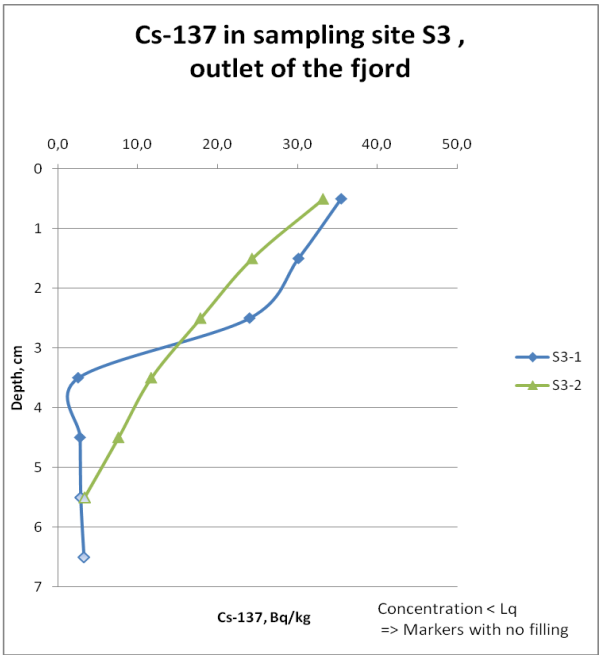


**Figure 3.5: Cs-137 in cores from the outlet of Sognefjorden, sampling site S3 (2008).**

**Table 3.3: Cs-137 in all layers in the cores from the outlet of the Sognefjord.**

| Depth | S1-1 Cs-137, Bq/kg (d.w.) | Uncertainty, Bq/kd (d.w.) | S1-2 Cs-137, Bq/kg (d.w.) | Uncertainty, Bq/kd (d.w.) | S1-3 Cs-137, Bq/kg (d.w.) | Uncertainty, Bq/kd (d.w.) | S3-1 Cs-137, Bq/kg (d.w.) | Uncertainty, Bq/kd (d.w.) | S3-2 Cs-137, Bq/kg (d.w.) | Uncertainty, Bq/kd (d.w.) |
|---|---|---|---|---|---|---|---|---|---|---|
| 0-1 cm | 28 | 4 | 36 | 4 | 32 | 3 | 36 | 3 | 33 | 3 |
| 1-2 cm | 32 | 5 | 31 | 3 | 31 | 3 | 30 | 3 | 24 | 2 |
| 2-3 cm | 25 | 3 | 27 | 2 | 35 | 3 | 24 | 3 | 17.9 | 2.0 |
| 3-4 cm | 18.4 | 2.0 | 21 | 2 | 30 | 3 | 2.6 | 0.5 | 11.7 | 1.2 |
| 4-5 cm | 23.5 | 2.4 | 24 | 2 | 27 | 3 | 2.8 | 0.9 | 7.6 | 1.1 |
| 5-6 cm | 22.3 | 2.3 | 15.6 | 2.0 | 28 | 3 | < 2.9 | | < 3.3 | |
| 6-7 cm | 8.6 | 1.3 | 13.0 | 1.9 | 24 | 2 | < 3.3 | | | |
| 7-8 cm | 5.3 | 1.1 | 6.6 | 1.3 | 9.5 | 2.6 | | | | |
| 8-9 cm | 2.4 | 0.9 | 5.4 | 1.3 | 10.0 | 1.6 | | | | |
| 9-10 cm | 2.7 | 1.0 | 2.9 | 0.6 | 3.4 | 0.6 | | | | |
| 10-11 cm | 1.3 | 0.3 | 2.8 | 1.0 | 4.1 | 1.1 | | | | |
| 11-12 cm | < 2.9 | | < 3.1 | | < 3.5 | | | | | |
| 12-13 cm | < 3.1 | | < 3.2 | | < 3.7 | | | | | |
| 13-14 cm | < 1.7 | | < 3.3 | | < 4.4 | | | | | |
| 14-15 cm | < 2.9 | | < 1.7 | | | | | | | |
| 15-16 cm | < 1.6 | | | | | | | | | |

The quantification limit is reached at 11 to 14 cm depth for sampling site S1, but for sampling site S3 the quantification limit is reached at 5 to 6 cm depth. There seem to be no difference in the Cs-137 activity concentrations in the upper layers in cores between the two years.

In the head of the fjord, sampling sites S2 (2007) and S4 (2008), the Cs-137 activity concentration in upper (0-1cm) layer is from 327 to 242 Bq/kg (d.w.), with decreasing concentrations with increasing depths in the sediments, Figure 3.6, 3.7 and Table 3.4. The quantification limit is reached at 11 to 14 cm depth for sampling site S2, but for sampling site S4 the quantification limit is not reached in these 8 and 9 cm long cores respectively. There seems to be no difference in Cs-137 activity concentrations in the upper layers in cores between the two years.

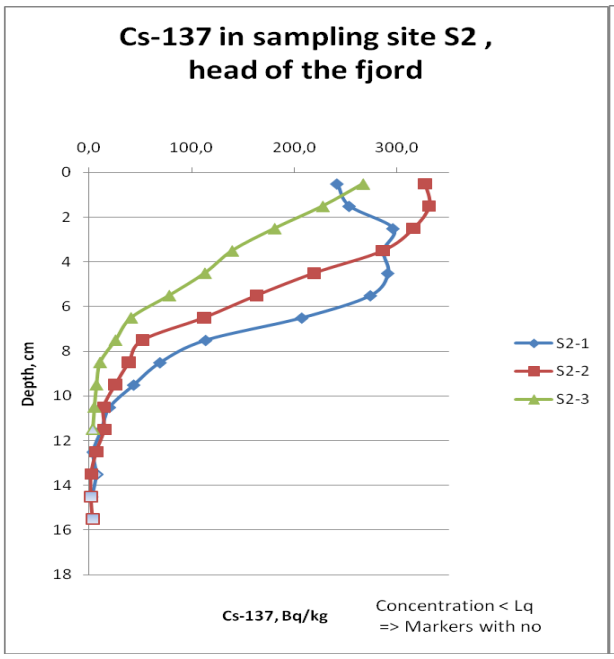


**Figure 3.6: Cs-137 in cores from the head of Sognefjorden, sampling site S2 (2007).**

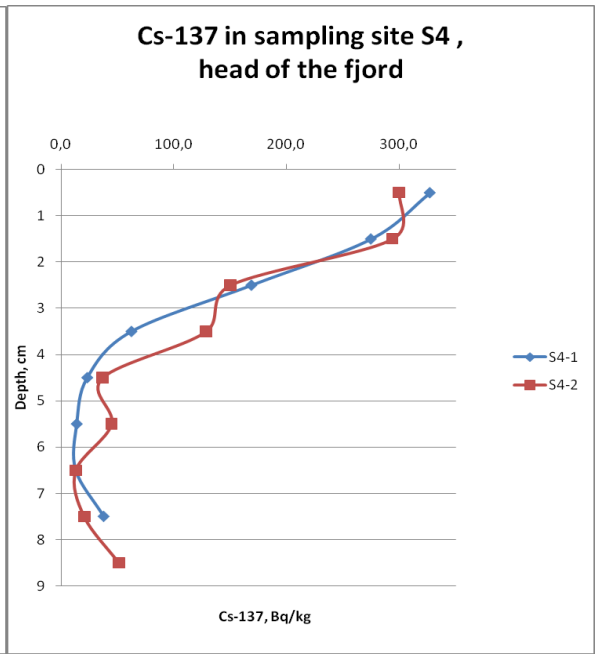


**Figure 3.7: Cs-137 in cores from the head of Sognefjorden, sampling site S4 (2008).**

**Table 3.4: Cs-137 in all layers in the cores from the head of the Sognefjord.**

| Depth | *S2-1* Cs-137, Bq/kg (d.w.) | Uncertainty, Bq/kd (d.w.) | *S2-2* Cs-137, Bq/kg (d.w.) | Uncertainty, Bq/kd (d.w.) | *S2-3* Cs-137, Bq/kg (d.w.) | Uncertainty, Bq/kd (d.w.) | *S4-1* Cs-137, Bq/kg (d.w.) | Uncertainty, Bq/kd (d.w.) | *S4-2* Cs-137, Bq/kg (d.w.) | Uncertainty, Bq/kd (d.w.) |
|---|---|---|---|---|---|---|---|---|---|---|
| 0-1 cm | 242 | 25 | 327 | 28 | 267 | 24 | 327 | 30 | 300 | 27 |
| 1-2 cm | 254 | 24 | 331 | 30 | 228 | 20 | 275 | 24 | 294 | 26 |
| 2-3 cm | 296 | 28 | 316 | 29 | 181 | 17 | 169 | 15 | 150 | 14 |
| 3-4 cm | 287 | 26 | 286 | 25 | 140 | 14 | 63 | 7 | 129 | 12 |
| 4-5 cm | 291 | 27 | 219 | 19 | 113 | 10 | 23 | 3 | 37 | 4 |
| 5-6 cm | 274 | 26 | 163 | 14 | 78 | 7 | 13.9 | 1.4 | 45 | 5 |
| 6-7 cm | 207 | 22 | 112 | 10 | 41 | 4 | 13.0 | 1.3 | 13.0 | 1.6 |
| 7-8 cm | 114 | 12 | 52 | 5 | 26 | 4 | 37.8 | 3.7 | 20.6 | 2.1 |
| 8-9 cm | 69 | 6 | 39 | 4 | 11.0 | 1.1 | | | 51.3 | 4.8 |
| 9-10 cm | 44 | 6 | 26 | 3 | 7.5 | 1.3 | | | | |
| 10-11 cm | 20.0 | 1.9 | 14.4 | 1.7 | 5.4 | 0.6 | | | | |
| 11-12 cm | 12.1 | 1.6 | 14.8 | 1.8 | < 3.8 | 1.2 | | | | |
| 12-13 cm | 4.1 | 1.2 | 7.2 | 1.3 | | | | | | |
| 13-14 cm | < 6.9 | 1.1 | 2.2 | 0.4 | | | | | | |
| 14-15 cm | < 2.8 | 1.1 | < 2.0 | | | | | | | |
| 15-16 cm | | | < 3.6 | | | | | | | |

All data collected used in calculating the Cs-137 activity concentrations are presented in Appendix IV Table A19 to A32.

## 3.4 Pb-210 and Ra-226 content

The content of Pb-210 and Ra-226 in 11 of the sediment-cores are presented in Figures 3.8 to 3.11. The results from all cores show a similar pattern. In the top layer is the fresh Pb-210 fallout, with a subsequent decrease down into the sediments because the fallout Pb-210 is buried and decays with a half life of 22.3 years. The content of Ra-226 is not changing with increasing depths, as this nuclide is a part of the U-238 decay chain in the sediments, according to chapter 2.8.

At a certain depth the Pb-210 content equals the Ra-226 content. This is the content of supported Pb-210 according to chapter 2.8. The Pb-210 content will not decrease below this because decay of Ra-226 in the sediments will be a constant supply of Pb-210.

All data collected used for calculating the Pb-210 and Ra-226 content, results and uncertainties are presented in Appendix V Table A33 to A43.

In Figure 3.8 are the content of Pb-210 and Ra-226 in L1-1 (blue) and L1-2 (red) cores from the outlet of the Laksefjord. The two cores are taken from the same grab sample. The results

show good agreement between the depths, to about 8 centimeters, at which the unsupported Pb-210 reaches zero. Figure 3.9 shows the content of Pb-210 and Ra-226 in L2-1 (blue) and L2-2 (red) cores from the head of the Laksefjord. The two cores are taken from the same grab sample. The results shows good agreement on Ra-226 results between the two cores. However there seems to be a large difference in the Pb-210 content. The depth at which the unsupported Pb-210 reaches zero are different for the two cores; 6 cm in core L2-2 and 10 cm in core L2-1.

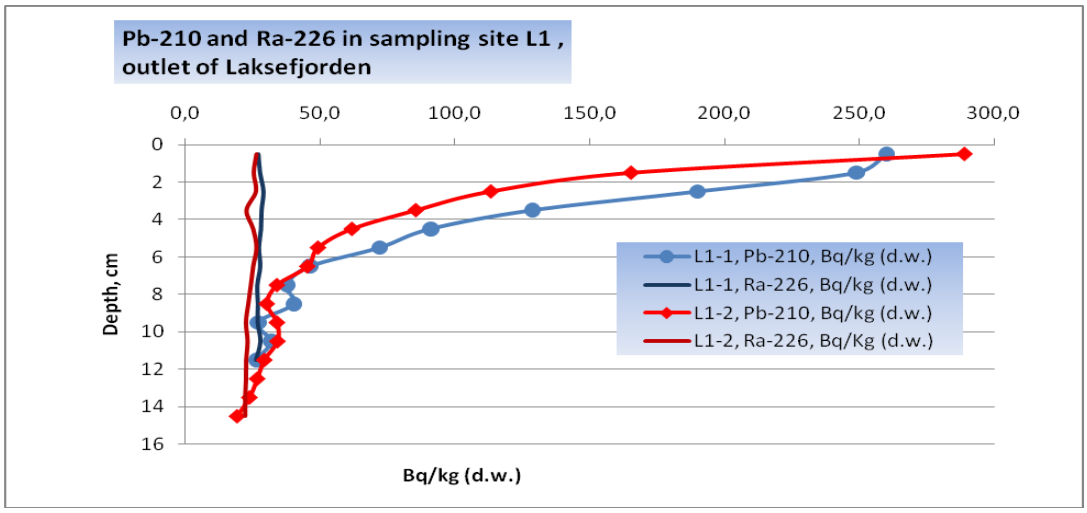


**Figure 3.8: Pb-210 and Ra-226 in cores from the outlet of Laksefjorden, sampling site L1.**

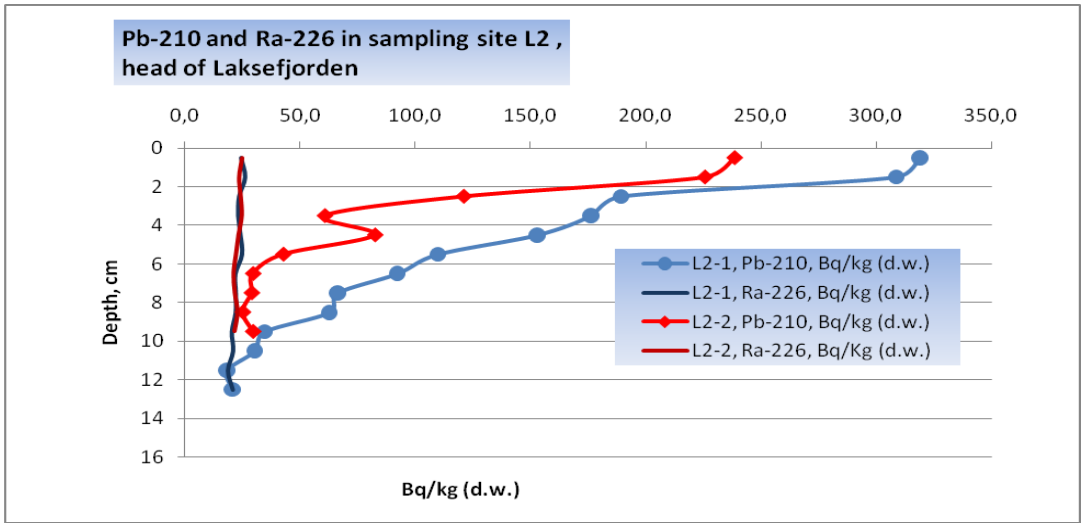


**Figure 3.9: Pb-210 and Ra-226 in cores from the head of Laksefjorden, sampling site L2.**

Figure 3.10 shows the content of Pb-210 and Ra-226 in S1-1 (blue), S1-2 (red), S1-3 (green) and S3-1 (yellow) cores from the outlet of the Sognefjord. Three of the cores are taken from the same grab sample. Core S3-1 is taken at approximately the same position one year later.

The results shows good agreement on Ra-226 results between the four cores. The content of Ra-226 and thus supported Pb-210 is the same in the four cores. The Pb-210 results from two of three cores from the same grab sample shows good agreement. The third core from the same grab sample shows the same pattern but at a slightly different depth.

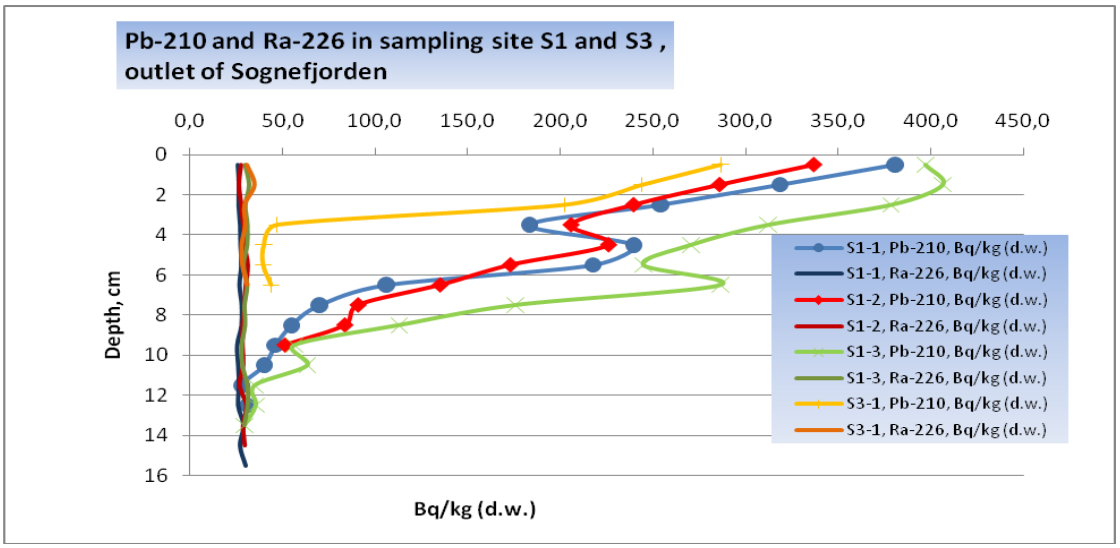


**Figure 3.10: Pb-210 and Ra-226 in cores from the outlet of Sognefjorden, sampling site S1 and S3.**

The depth at which the unsupported Pb-210 reaches zero are for two of the cores 11 cm, while one of them does not reach zero. The core S3-1, taken one year later, does not reach zero unsupported Pb-210, but the curve turns at about 4 cm depth. Below this depth there seems to be a constant Pb-210 content. It is then reasonable to assume that this is the layer where the unsupported Pb-210 is zero. This assumption is made when dating this core.

In the three cores from grab sample S1, the Pb-210 content is not decreasing uniformly down through the sediment cores. At 4 cm depth (S1-1 and S1-2) and 6 cm depth (S1-3) the Pb-210 content is higher than the layer above.

In Figure 3.11 are the content of Pb-210 and Ra-226 in the S2-1 (blue), S2-2 (red) and S4-2 (green) cores from the head of the Sognefjord. The two cores taken from the same grab sample, S2-1 and S2-2 show good agreement in Pb-210 content, but the earlier seen, Figure 3.10, pattern of Pb-210 not decreasing uniformly is not seen here. Core S4-2 is taken at approximately the same position and one year later.

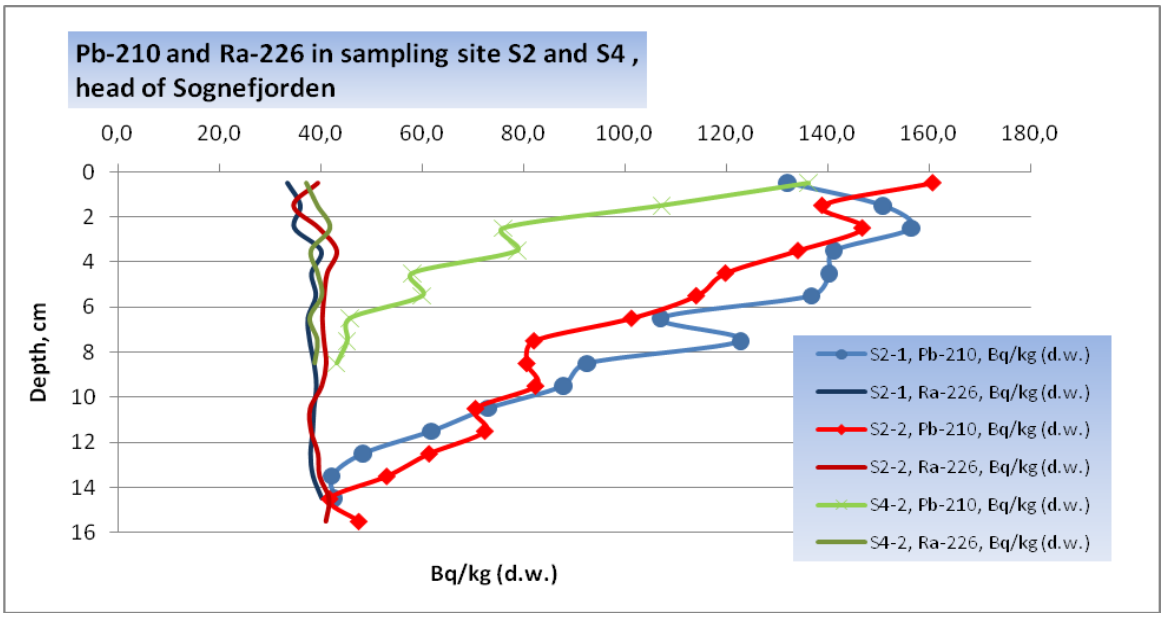


**Figure 3.11: Pb-210 and Ra-226 in cores from the head of Sognefjorden, sampling site S2 and S4.**

The results shows good agreement in Ra-226 results between the three cores. The depth at which the unsupported Pb-210 reaches zero are for both cores from the same grab sample about 14 cm. The core S4-2, taken one year later, reaches zero unsupported Pb-210 at about 8 cm. The latter core is not long enough to clearly show the Pb-210 minimum.

## 3.5 Dating

The slices from 11 of the cores were dated according to Goldberg (1963) described in Chapter 2.8., using the content of Pb-210 corrected for content of Ra-226. The age of sediment layers were determined both with CRS and CIC models (Appleby and Oldfield, 1977) in order to have a better platform when judging the results.

Table 3.5 to 3.8 show the Cs-137 content in the core slices, as compared to the year of deposition. The uncertainty in the dating was estimated according to Binford (1989). Ninety-five percent confidence intervals range from 1-2 years at 10 years of age (10-20%), 10-20 (10-20%) years at 100 years and 8-90 (5-60%) at 150 years old.

The CRS and CIC models gave different results; and the difference was larger than the estimated uncertainty.

In the cores from the Laksefjord, the Cs-137 measured was found in the upper layers. The oldest layer with Cs-137 were dated (CRS) to 1958 (L1-1), 1986 (L1-2), 1967 (L2-1) and 1947 (L2-2) and (CIC) 1966 (L1-1), 1973 (L1-2), 1969 (L2-1) and 1967 (L2-2).

In all the cores from the outlet of the Sognefjord, Cs-137 are measured above quantification limit at depths which was deposited before and partly long before nuclear industry started; S1-1 (1882), S1-2 (1913), S1-3 (1891) and S3-1(1931).

From the head of the Sognefjord, Cs-137 are measured above quantification limit in depths which was deposited before and partly long before nuclear industry started; S2-1 (1880), S2-2 (1892) and S4-2 (prior to 1903).

**Table 3.5: Age of the core slices from outlet of Laksefjorden compared to Cs-137 content, 20% uncertainty in parentheses.**

| Core | L1-1 | | |
|---|---|---|---|
| Depth | Cs-137, Bq/kg (d.w.) | CRS-model Year | CIC-model Year |
| 0-1 cm | 5,7 | 2008 ( -1) | 2008 ( -1) |
| 1-2 cm | 5,7 | 1998 ( +/-2) | 2006 (+/-1) |
| 2-3 cm | 3,4 | 1987 ( +/-4) | 1996 (+/-2) |
| 3-4 cm | 2,3 | 1972 ( +/-7) | 1981 (+/-5) |
| 4-5 cm | 1,2 | 1958 (+/-10) | 1966 (+/-8) |
| 5-6 cm | < 2,3 | 1940 (+/-14) | 1956 (+/-10) |
| 6-7 cm | < 3,5 | 1922 (+/-17) | 1928 (+/-16) |
| 7-8 cm | < 3,0 | 1907 (+/-20) | 1912 (+/-19) |
| 8-9 cm | < 1,6 | 1891 (+/-23) | 1918 (+/-18) |
| 9-10 cm | < 2,9 | | |
| 10-11 cm | < 2,7 | | |
| 11-12 cm | < 3,1 | | |

| Core | L1-2 | | |
|---|---|---|---|
| Depth | Cs-137, Bq/kg (d.w.) | CRS-model Year | CIC-model Year |
| 0-1 cm | 5,7 | 2008 (-1) | 2008 (-1) |
| 1-2 cm | 2,9 | 1996 (+/-2) | 1988 (+/-4) |
| 2-3 cm | 1,7 | 1986 (+/-4) | 1973 (+/-7) |
| 3-4 cm | < 2,7 | 1977 (+/-6) | 1963 (+/-9) |
| 4-5 cm | < 3,0 | 1966 (+/-8) | 1946 (+/-12) |
| 5-6 cm | < 3,0 | 1955 (+/-11) | 1931 (+/-15) |
| 6-7 cm | < 3,0 | 1947 (+/-12) | 1927 (+/-16) |
| 7-8 cm | < 3,5 | 1938 (+/-14) | 1904 (+/-21) |
| 8-9 cm | < 1,5 | 1930 (+/-16) | 1894 (+/-23) |
| 9-10 cm | < 2,9 | 1924 (+/-17) | 1909 (+/-20) |
| 10-11 cm | < 3,1 | 1911 (+/-19) | 1908 (+/-20) |
| 11-12 cm | < 2,9 | | |
| 12-13 cm | < 3,0 | | |
| 13-14 cm | < 1,3 | | |
| 14-15 cm | < 2,7 | | |

**Table 3.6: Age of the core slices from the head of Laksefjorden compared to Cs-137 content, 20% uncertainty in parantheses.**

| Core | L2-1 | | |
|---|---|---|---|
| Depth | Cs-137, Bq/kg (d.w.) | CRS-model Year | CIC-model Year |
| 0-1 cm | 6,7 | 2008 ( -1) | 2008 ( -1) |
| 1-2 cm | 6,5 | 2002 (+/-1) | 2007 (+/-1) |
| 2-3 cm | 4,7 | 1994 (+/-3) | 1990 (+/-4) |
| 3-4 cm | 4,8 | 1987 (+/-4) | 1987 (+/-4) |
| 4-5 cm | 4,7 | 1978 (+/-6) | 1982 (+/-5) |
| 5-6 cm | 3,5 | 1967 (+/-8) | 1969 (+/-8) |
| 6-7 cm | < 2,4 | 1957 (+/-10) | 1962 (+/-9) |
| 7-8 cm | < 3,2 | 1939 (+/-12) | 1948 (+/-12) |
| 8-9 cm | < 2,6 | 1925 (+/-17) | 1945 (+/-13) |
| 9-10 cm | < 2,7 | 1893 (+/-23) | 1912 (+/-19) |
| 10-11 cm | < 1,3 | | |
| 11-12 cm | < 2,5 | | |
| 12-13 cm | < 3,0 | | |

| Core | L2-2 | | |
|---|---|---|---|
| Depth | Cs-137, Bq/kg (d.w.) | CRS-model Year | CIC-model Year |
| 0-1 cm | 5,0 | 2008 ( -1) | 2008 ( -1) |
| 1-2 cm | 4,7 | 1995 (+/-3) | 2006 (+/-1) |
| 2-3 cm | 3,7 | 1976 (+/-6) | 1983 (+/-5) |
| 3-4 cm | < 2,8 | 1957 (+/-10) | 1952 (+/-11) |
| 4-5 cm | 2,2 | 1947 (+/-12) | 1967 (+/-8) |
| 5-6 cm | < 2,9 | 1926 (+/-16) | 1934 (+/-15) |
| 6-7 cm | < 2,6 | 1910 (+/-20) | 1905 (+/-21) |
| 7-8 cm | < 2,5 | 1890 (+/-24) | 1901 (+/-21) |
| 8-9 cm | < 1,2 | | |
| 9-10 cm | < 2,5 | | |

**Table 3.7: Age of the core slices from the outlet of Sognefjorden compared to Cs-137 content, 20% uncertainty in parentheses.**

| Core | S1-1 | | |
|---|---|---|---|
| Depth | Cs-137, Bq/kg (d.w.) | CRS-model Year | CIC-model Year |
| 0-1 cm | 27,9 | 2007 ( -1) | 2007 ( -1) |
| 1-2 cm | 31,8 | 1999 (+/-2) | 2001 (+/-1) |
| 2-3 cm | 24,8 | 1992 (+/-3) | 1993 (+/-3) |
| 3-4 cm | 18,4 | 1984 (+/-5) | 1981 (+/-5) |
| 4-5 cm | 23,5 | 1977 (+/-6) | 1991 (+/-3) |
| 5-6 cm | 22,3 | 1963(+/-9) | 1987 (+/-4) |
| 6-7 cm | 8,6 | 1943 (+/-13) | 1959 (+/-10) |
| 7-8 cm | 5,3 | 1926 (+/-16) | 1939 (+/-14) |
| 8-9 cm | 2,4 | 1913 (+/-19) | 1925 (+/-16) |
| 9-10 cm | 2,7 | 1901 (+/-21) | 1917 (+/-18) |
| 10-11 cm | 1,3 | 1881 (+/-25) | 1905 (+/-20) |
| 11-12 cm | < 2,9 | | |
| 12-13 cm | < 3,1 | | |
| 13-14 cm | < 1,7 | | |
| 14-15 cm | < 2,9 | | |
| 15-16 cm | < 1,6 | | |

| Core | S1-2 | | |
|---|---|---|---|
| Depth | Cs-137, Bq/kg (d.w.) | CRS-model Year | CIC-model Year |
| 0-1 cm | 36,2 | 2007 ( -1) | 2007 ( -1) |
| 1-2 cm | 31,0 | 2003 (+/-1) | 2001 (+/-1) |
| 2-3 cm | 26,8 | 1996 (+/-2) | 1995 (+/-2) |
| 3-4 cm | 20,9 | 1986 (+/-4) | 1989 (+/-4) |
| 4-5 cm | 24,3 | 1977 (+/-6) | 1993 (+/-3) |
| 5-6 cm | 15,6 | 1966 (+/-8) | 1982 (+/-5) |
| 6-7 cm | 13,0 | 1959 (+/-10) | 1973 (+/-7) |
| 7-8 cm | 6,6 | 1948 (+/-12) | 1956 (+/-10) |
| 8-9 cm | 5,4 | 1939 (+/-14) | 1952 (+/-11) |
| 9-10 cm | 2,9 | 1923 (+/-17) | 1925 (+/-16) |
| 10-11 cm | 2,8 | 1912 (+/-19) | 1921 (+/-17) |
| 11-12 cm | < 3,1 | 1898 (+/-22) | 1909 (+/-20) |
| 12-13 cm | < 3,2 | | |
| 13-14 cm | < 3,3 | | |
| 14-15 cm | < 1,7 | | |

| Core | S1-3 | | |
|---|---|---|---|
| Depth | Cs-137, Bq/kg (d.w.) | CRS-model Year | CIC-model Year |
| 0-1 cm | 31,9 | 2007 ( -1) | 2007 ( -1) |
| 1-2 cm | 30,6 | 2003 (+/-1) | 2008 (-2) |
| 2-3 cm | 34,7 | 1996 (+/-2) | 2005 (+/-1) |
| 3-4 cm | 30,3 | 1990 (+/-4) | 1999 (+/-2) |
| 4-5 cm | 27,2 | 1982 (+/-3) | 1993 (+/-3) |
| 5-6 cm | 27,8 | 1974 (+/-7) | 1990 (+/-3) |
| 6-7 cm | 24,3 | 1965 (+/-8) | 1995 (+/-2) |
| 7-8 cm | 9,5 | 1947 (+/-12) | 1978 (+/-6) |
| 8-9 cm | 10,0 | 1927 (+/-16) | 1960 (+/-9) |
| 9-10 cm | 3,4 | 1905 (+/-20) | 1926 (+/-16) |
| 10-11 cm | 4,1 | 1890 (+/-23) | 1932 (+/-15) |
| 11-12 cm | < 3,5 | | |
| 12-13 cm | < 3,7 | | |
| 13-14 cm | < 4,4 | | |

| Core | S3-1 | | |
|---|---|---|---|
| Depth | Cs-137, Bq/kg (d.w.) | CRS-model Year | CIC-model Year |
| 0-1 cm | 35,5 | 2008 ( -1) | 2008 ( -1) |
| 1-2 cm | 30,1 | 1992 (+/-3) | 2002 (+/-1) |
| 2-3 cm | 24,0 | 1978 (+/-5) | 1996 (+/-2) |
| 3-4 cm | 2,6 | 1893 (+/-13) | 1922 (+/-17) |
| 4-5 cm | 2,8 | | 1911 (+/-19) |
| 5-6 cm | < 2,9 | | 1909 (+/-20) |
| 6-7 cm | < 3,3 | | 1913 (+/-19) |

**Table 3.8: Age of the core slices from the head of Sognefjorden compared to Cs-137 content, 20% uncertainty in parentheses.**

| Core | S2-1 | | |
|---|---|---|---|
| Depth | Cs-137, Bq/kg (d.w.) | CRS-model Year | CIC-model Year |
| 0-1 cm | 241,6 | 2007 (-1) | 2007 (-1) |
| 1-2 cm | 253,5 | 2004 (+/-1) | 2012 (-6) |
| 2-3 cm | 296,1 | 2001 (+/-1) | 2014 (-7) |
| 3-4 cm | 286,5 | 1997 (+/-2) | 2008 (-2) |
| 4-5 cm | 291,1 | 1991 (+/-3) | 2008 (-2) |
| 5-6 cm | 274,2 | 1985 (+/-4) | 2007 (-1) |
| 6-7 cm | 207,4 | 1976 (+/-6) | 1996 (+/-2) |
| 7-8 cm | 113,8 | 1969 (+/-8) | 2002 (+/-1) |
| 8-9 cm | 69,3 | 1957 (+/-10) | 1988 (+/-4) |
| 9-10 cm | 43,6 | 1946 (+/-12) | 1985 (+/-4) |
| 10-11 cm | 20,0 | 1930 (+/-15) | 1973 (+/-7) |
| 11-12 cm | 12,1 | 1910 (+/-19) | 1961 (+/-9) |
| 12-13 cm | 4,1 | 1889 (+/-24) | 1935 (+/-14) |
| 13-14 cm | < 6,9 | | 1902 (+/-21) |
| 14-15 cm | < 2,8 | | 1889 (+/-24) |

| Core | S2-2 | | |
|---|---|---|---|
| Depth | Cs-137, Bq/kg (d.w.) | CRS-model Year | CIC-model Year |
| 0-1 cm | 327,2 | 2007 ( -1) | 2007 ( -1) |
| 1-2 cm | 331,2 | 2002 (+/-1) | 2002 (+/-1) |
| 2-3 cm | 315,9 | 1998 (+/-2) | 2003 (+/-1) |
| 3-4 cm | 286,1 | 1993 (+/-3) | 1998 (+/-2) |
| 4-5 cm | 219,3 | 1987 (+/-4) | 1993 (+/-3) |
| 5-6 cm | 163,2 | 1981 (+/-5) | 1991 (+/-3) |
| 6-7 cm | 111,9 | 1974 (+/-7) | 1985 (+/-4) |
| 7-8 cm | 52,3 | 1968 (+/-8) | 1973 (+/-7) |
| 8-9 cm | 38,8 | 1961 (+/-9) | 1971 ( +/-7) |
| 9-10 cm | 25,6 | 1954 (+/-11) | 1973 (+/-7) |
| 10-11 cm | 14,4 | 1942 (+/-13) | 1965 (+/-8) |
| 11-12 cm | 14,8 | 1930 (+/-15) | 1967 (+/-8) |
| 12-13 cm | 7,2 | 1913 (+/-19) | 1953 (+/-11) |
| 13-14 cm | 2,2 | 1891 (+/-23) | 1937 (+/-14) |
| 14-15 cm | < 2,0 | | |
| 15-16 cm | < 3,6 | | |

| Core | S4-2 | | |
|---|---|---|---|
| Depth | Cs-137, Bq/kg (d.w.) | CRS-model Year | CIC-model Year |
| 0-1 cm | 299,9 | 2008 ( -1) | 2008 ( -1) |
| 1-2 cm | 293,8 | 2000 (+/-2) | 1996 (+/-2) |
| 2-3 cm | 150,2 | 1987 (+/-4) | 1974 (+/-7) |
| 3-4 cm | 128,6 | 1976 (+/-6) | 1980 (+/-6) |
| 4-5 cm | 36,8 | 1955 (+/-11) | 1955 (+/-11) |
| 5-6 cm | 44,8 | 1940 (+/-14) | 1957 (+/-10) |
| 6-7 cm | 13,0 | 1921 (+/-17) | 1928 (+/-16) |
| 7-8 cm | 20,6 | 1903 (+/-21) | 1918 (+/-18) |
| 8-9 cm | 51,3 | | 1908 (+/-20) |

# 4. Discussion

## 4.1 Inaccuracy in sampling and sample preparation

All samples in this work are collected from a boxcorer grab sample. An ideal grab sampling with a boxcorer is described; Chapter 2.2; When the boxcorer hits the bottom it may however, depending on the bottom conditions, penetrate with tilt and thus take a sample in a certain angle into the sediment, instead of a clean vertical cut. Further, when placing the grab sample on the sampling platform (research vessel) in order to do sub sampling with tubes, it will be set straight and the result is a core in a certain angle downwards into the sediments; Figure 4.1. The result of this inaccuracy will be slices non-parallel to the sediment surface. The range of this inaccuracy is difficult to estimate, but may cause single sample slices containing material from more than the one centimeter layer and slices adjacent to each other containing some material from the same layer. This could also be the reason for obtaining different length of the cores from the same grab sample.

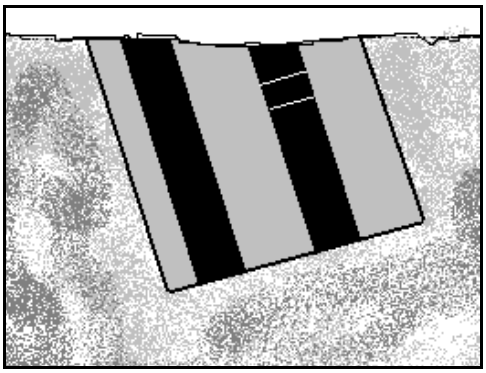

**Figure 4.1 Schematic drawing of boxcorer sampling, subsampling of cores (in black) and 1cm slices (white lines).**

Compression of the seabed with the sampling device, when taking the grab sample and when sub sampling the cores, may also cause inaccuracy as the compression will not be equal throughout the grab sample and the core. When sub sampling cores in tubes, material will be transported along the walls of the tubes both when pressing it into the sediment and when pushing the core out of the tube. This may cause some contamination of single sediment slices from slices below or above. To reduce this effect, the tubes chosen were 10 cm in diameter. The relative amount of sediment next to the tube walls will then be less compared to

sediments in tubes with a smaller diameter. But cores moved along the tube walls will still lead to disturbance of the sedimentation layers, moving Cs-137 and Pb-210 along the core.

Cutting the cores may also add inaccuracy to the samples, as measuring and cutting layers of one centimeter thickness in this wet material was difficult. The result may have been better if the cores had not been thawed completely. The water content was between 40% and 65%, Appendix II Table 5, and the sediments were soft and lost their initial form when pushed out of the tubes. Based on this experience, the uncertainty in the sliced layers can be estimated to +/- 1 cm.

The result of inaccuracy when cutting the cores is visible in the profile-curves. In the Pb-210 profile in Figure 3.10, the S1-3 profile-curve is further down than the S1-1 and S1-2 profile-curves, and moving the S1-3 profile curve upwards one centimeter will improve the coherence between the three cores from the S1 grab sample. This is also seen in the other profiles; Figure 3.2 to 3.11, and will cause deviation in the age estimate of a specific depth in cores from the same grab sample.

Loss of sediment material during the cutting process may also be a problem. This is roughly estimated to be 5 % in each core. An evenly distributed loss from each slice will not affect the dating. But if not evenly distributed, however, it would cause inaccuracy in the dating. If the majority of sediment loss was from the upper slices, it would cause dating the lower slices to be too young, or contrary; if the majority of loss was from the lower slices it would cause dating the lower slices to be too old. In this work this inaccuracy is not known, but is estimated to be within the total uncertainty described; Chapter 2.8. The loss of material will also influence the recalculation from activity per. weight to activity per. area.

The slicing of core L2-2 was not entirely successful. The core fell partly out of the tube during the cutting process, and this could add an uncertainty in the following analysis of this specific core.

The cores were relatively short, between 6 cm and 16 cm. All but two cores, (S4-1 and S4-2), were long enough to reach down to depths where the Cs-137 activity concentrations was below the quantification limit.

Marine sediments contain a certain amount of seawater when sampled. The seawater is dried out when preparing the samples prior to measuring leaving the salt in the dry sample. This salt

is not a part of the sample but adds weight to it. The salinity in the water above the sediments in this study is estimated to 35 ‰ (pers. comm. Dr. Lars Asplin, IMR, Norway), leaving 35 g salt per liter water dried out. An estimated content of salt in the samples based on the dry weight data; Appendix IV Table A19 to A32; is 5 %.

The sample weights in this study are not corrected for salt-content since a majority of the comparative studies are not salt-content corrected (NRPA, 2001) (NRPA, 2003, 2004, 2005, 2006, 2007, 2008, 2009f). In some of the comparative studies, there is no information about salt-content correction.

The deviation in measurements between parallel cores from the same grab sample could partly be caused by the sampling and sample preparation, but is also because one should expect that Cs-137 is not homogenous distributed within the sediments.

## 4.2 Evaluating the dating

In this work the age of the sediment layers are calculated using both the CRS-model and CIC-model (Appleby and Oldfield, 1977), giving different results. The models should give the same results if the accumulation rate is constant over time. If the accumulation rate is not constant, the CRS-model should be preferred (Appleby and Oldfield, 1977). However, both these models presume that disturbance of the sediments has not occurred. This seems not to be the fact in the sampling areas in the Sognefjord, since the Pb-210 content in those cores does not decrease uniformly with depth.

The result of the dating must be reviewed as the method is a result from models which includes assumptions on of how nature acts. The Cs-137 in the cores could be a supplementary method to the Pb-dating, as the known sources, in specific events, have caused steep changes in the Cs-137 concentrations in the environment. None of the cores measured for Cs-137 gave any indication of age of layer. Cs-137 was found in layers dated to long before 1950 in all cores from the Sognefjord, and using the deepest layer containing Cs-137 as a reference to 1952 cannot be done.

The data material with its uncertainty is not sufficiently good to lead to any conclusion on which dating model giving the best result in this work. On the other hand, if doing the exercise of correcting the Cs-137 activity concentrations for decay according to the calculated age (CRS) of the sediment layers, as done for core S2-1; Figure 4.2; the Chernobyl peak are

most likely revealed. This is an indication of the confidence of using the CRS-model in the dating on this core.

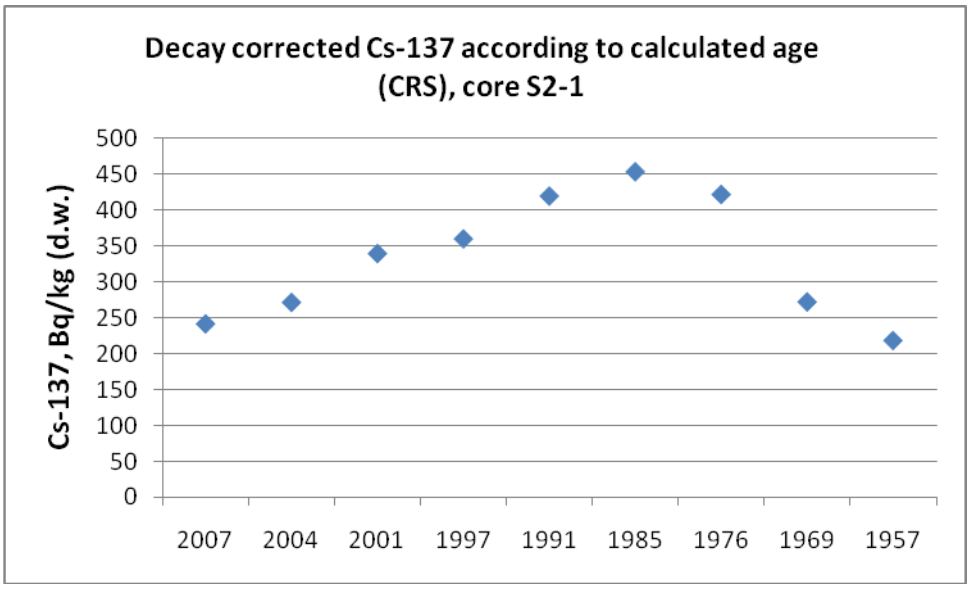


**Figure 4.2: Cs-137 decay-corrected according to the age of sediment.**

In all cores, the Ra-226 content in all the sample slices from the same core was similar. This is expected; Chapter 2.8. The Pb-210 content decreased with increasing depth reaching the Ra-226 value; this was the case for 10 of the 11 cores analyzed for date. This is again as expected**;** the unsupported Pb-210 will decay and the remaining Pb-210 is in equilibrium with Ra-226; Chapter 2.8**.** The 11$^{th}$ core (S3-1) reached a minimum content of Pb-210 which was somewhat higher than the Ra-226 content. The reason for this is unknown. The dating of this core is done after correction for the difference between Ra-226 and minimum content of Pb-210.

Dating the cores showed that Cs-137 in layers deposited before nuclear era started and is not a good indication of the accuracy of the dating in this work. However, Cs-137 in old layers can be the actual situation as seen in other investigations; Chapter 4.3.2.

At sampling site L2 there was a large difference in the Pb-210 content in the two cores. As mentioned; Chapter 4.1; the slicing of L2-2 was not successful. This might well have caused disturbance in the core layers in L2-2, causing the difference in the two cores, Figure 3.8.

At sampling site S1 there is not a linear decrease of the Pb-210 content with increasing depth of the profile. At 4 cm depth (S1-1 and S1-2) and 6 cm depth (S1-3) the Pb-210 content is higher than in the slices above. This indicates that the sediment layers have been disturbed, most likely at the time these layers where deposited. This is evident in all the three cores from

the same grab sample, indicating that mixing of samples is not likely. The CRS-dating will not reflect this, but can be seen in the CIC-dating; Table 3.7.
In order to assure the quality of the dating method used, it is necessary to participate in an intercomparison test in Pb-210 and Ra-226 measurements and dating cores. This is not completed in this work, but will be a necessary action further on.

## 4.3 Cs-137 results

### 4.3.1 Cs-137 activity concentrations in surface sediment

In the Laksefjord the Cs-137 activity concentration found in surface sediments in the present study (from 5.0 to 6.7 Bq/kg (d.w.)) are in good agreement with other observations from the Laksefjord, showing Cs-137 activity concentrations in surface sediments from 2.0 to 9.1 Bq/kg (d.w.) (NRPA, 2004) (NRPA, 2006) (NRPA, 2008) (NRPA, 2009f); Appendix I table A4. In samples from 1995 (H. Nies, 1999) and 2006 (Boitsov, 2009), Cs-137 activity concentrations in Barents Sea surface sediments were from 1.5 to 5.8 Bq/kg. In Føyn and Sværen (1995) the Cs-137 activity concentrations in surface sediments from the Barents Sea from 1991, 1992 and 1993 were between < 1.0 and 8.6 Bq/kg (d.w.).
It is not possible to see any time-trend (the last 15-20 years) comparing present and earlier measurements.
In the Sognefjord the Cs-137 activity concentration found in surface sediments from the outlet of the fjord in the present study (from 27.9 to 36.2 Bq/kg (d.w.) at S1 and S3) are in good agreement with other observations. Samples from the outlet of the Sognefjord collected by IMR in 2005 (NRPA, 2007) and 2008 (preliminary results) contained 45.4 and 36.0 Bq/kg (d.w.) respectively in surface sediment; Appendix I Table A2.
The activity concentrations in the samples from 2007 and 2008 are similar. It is not possible to see any time trend comparing present and earlier investigations; (45.4 in 2005, 32 (average) in 2007 and 34.4 (average) in 2008, all in Bq/kg d.w.).
No other measurements on Cs-137 content in sediments from the outer part of the Sognefjord, is known.
The activity concentration inside the sill of the Sognefjord differs distinctly from the levels outside the fjord. Surface sediments collected in 2004 and 2005 from the area outside the

Sognefjord showed activity concentrations from 1.9 to 3.8 Bq/kg (d.w.) (NRPA, 2007) and 1.5 Bq/kg (d.w.) (NRPA, 2006**).** A depth profile across the Norwegian Trench and all along the Sognefjord to the Lusterfjord is shown in Figure 4.3. The depth in the fjord is considerably deeper than outside the sill and also much deeper than the Norwegian trench.

The deepest part of the North Sea, Skagerrak and the Norwegian Trench are areas where sediments accumulate (Becks, 2000), but fjords can act as sediment traps (Syvitski et.al., 1987). It is therefore likely to believe that the deepest part of the Sognefjord is an area where the sediments accumulate even more than in the deepest part of the North Sea with a following increased content of Cs-137.

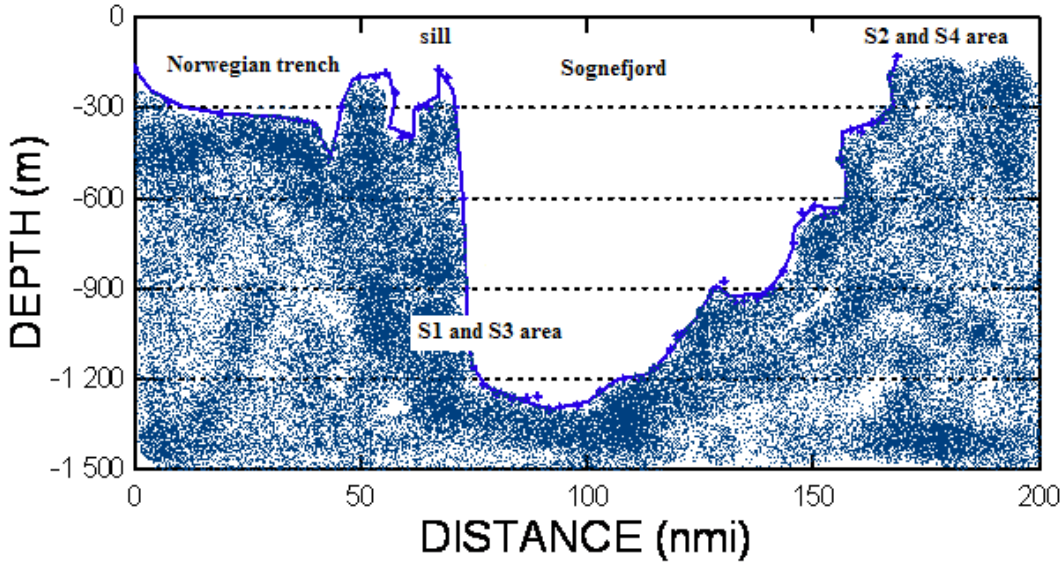


**Figure 4.3. Depth profile across the Norwegian trench, the Sognefjord and into the S2 and S4 area.**

The Cs-137 activity concentration in the surface sediment layer (0-1 cm) in the head of the Sognefjord in this study is from 241.6 to 327.4 Bq/kg (d.w.) at the two sampling sites S2 (3 cores in 2007) and S4 (2 cores in 2008). The activity concentrations in the samples from 2007 and 2008 are similar. These results are in good agreement with earlier measurements from the same area; Cs-137 activity concentrations in 2005 and 2008 were 415 Bq/kg (d.w.) (NRPA, 2007) and 323 Bq/kg (d.w.) (preliminary results) respectively in surface sediments at the same location; Appendix I Table A2. Prior to 2005 there are no investigations on Cs-137 in sediments from this part of the fjord. The one single sample from 2005 (415 Bq/kg (d.w.))

is not enough data material to indicate a decrease in the surface sediment activity concentration from 2005 to 2007 and 2008.

The samples in the head of the Sognefjord have like the Irish Sea and the Baltic extraordinary activity concentrations of Cs-137, Chapter 1.3.4.

The 6 sampling sites in this study represent three different levels of Cs-137 activity concentrations: the Laksefjord in northern Norway with the lowest concentrations, the outlet of the Sognefjord with approximately 6 times the Laksfjord level and the head of the Sognefjord with approximately 60 times the Laksefjord level; giving the relation 1:6:60. Chernobyl fallout in the three areas differed as shown in Figure 1.1; 1-2 kBq/$m^2$ in the area surrounding the Laksefjord, 2-5 kBq/$m^2$ in the area surrounding the outlet of the Sognefjord and 10-25 kBq/$m^2$ in the area surrounding the head of the Sognefjord. This gives the following relation: 1:3:12.This strongly implies that there are other factors influencing the Cs-137 activity concentrations than the direct Chernobyl fallout.

### 4.3.2 Cs-137 activity concentrations as function of age

In all the cores from the Laksefjord, the youngest sediments had the highest Cs-137 activity concentrations. One core (L2-2) have Cs-137 down in a layer dated (CRS) to 1947. But Cs-137 did not exist this early. This sample was from the core in which the slicing was not successful, and there might well have been a disturbance of the core layers causing this. The three remaining cores have their oldest layer containing Cs-137 (1958, 1986, 1967 (CRS)) (1966, 1973, 1969 (CIC)) more in accordance with the development of nuclear industry. There is, however, a large difference between cores taken from the same grab sample. There seems to be no difference in the Cs-137 activity concentrations in the cores from the two sampling sites, as the difference between cores from the same grab sample is larger.

Two cores (S1-1 and S1-3) from the outlet of the Sognefjord have their maximum Cs-137 activity concentrations in layers beneath the surface layer, both from the sampling conducted in 2007. The two other cores from the outlet of Sognefjorden have the maximum Cs-137 activity concentrations in the upper one centimeter. The uncertainty in each measurement is however too large to conclude that the maximum value is higher than from the adjacent years. From surface layers there is a significant decrease in Cs-137 activity concentrations with increasing depth, indicating a continuous support of Cs-137 with time.

The oldest layers containing Cs-137 in the outlet of the fjord were dated to 1881, 1912, 1890 and 1893 (CRS) and 1905, 1921, 1932 and 1911 (CIC). This is not in accordance with the start of the nuclear industry; again, Cs-137 did not exist in environment at the time.

Two cores (S2-1 and S2-2) from the head of the Sognefjord have their maximum Cs-137 activity concentrations in layers beneath the surface layer, both from the sampling conducted in 2007. The two other cores from the head of the Sognefjord have their maximum Cs-137 activity concentrations in the upper one centimeter. From surface layers there is a significant decrease in Cs-137 activity concentrations with increasing depth, indicating a continuous support of Cs-137 with time.

The oldest layers containing Cs-137 in the head of the fjord were dated to 1889, 1913 and prior to 1903 (CRS) and 1935, 1937 and 1908 (CIC). This is not in accordance with the start of the nuclear industry; again, Cs-137 did not exist in environment at the time.

When examining the contents of Pb-210 and Ra-226 in figure 3.8 to figure 3.11 the Pb-210 content is following the expected decay of unsupported Pb-210, indicating relative correctness of the dating. The uncertainty in age of sediment layers are also increasing with increasing depths.

As described; Chapter 4.1, the sampling method and slicing method is quite rough and could cause some contamination between layers. Bioturbation or mechanical disturbance can cause vertical transport of Cs-137 in the sediments. Downward diffusion of Cs-137 in interstitial water (Appleby and Oldfield, 1977) could also cause Cs-137 in layers before the nuclear industry. Cs-137 activity concentrations found in layers deeper than expected are also observed by others (Grøttheim, 1998) (Holby and Evans, 1996) (Ritchie and McHenry, 1990).

Other investigations of Cs-137 in sediment cores from Norwegian coastal areas are shown in Figure 4.4. In a) are shown the Cs-137 activity concentrations in a sediment core from Framvaren (1989), on the coast of southern Norway (Keith-Roach et. al., 2004). The Cs-137 activity concentration shows a peak at approximately 12 cm depth. In b) are shown the Cs-137 activity concentrations in a sediment core from the west coast of Norway (Bergen area) (2001) (Asplin et.al., 2003). In c) are shown Cs-137 activity concentrations in a sediment core from the coast of northern Norway (2006) (Boitsov et. al., 2009), with a maximum Cs-137 activity concentration at approximately 8 cm depth. In d) are shown the Cs-137 activity concentration in a sediment core from the head of the Oslofjord (Skagerrak area) (2007) (Skei, 2008), with a maximum Cs-137 activity concentration in a layer dated to 1985.

In three of these cores the Cs-137 peak from Chernobyl are found at a certain sediment depth.

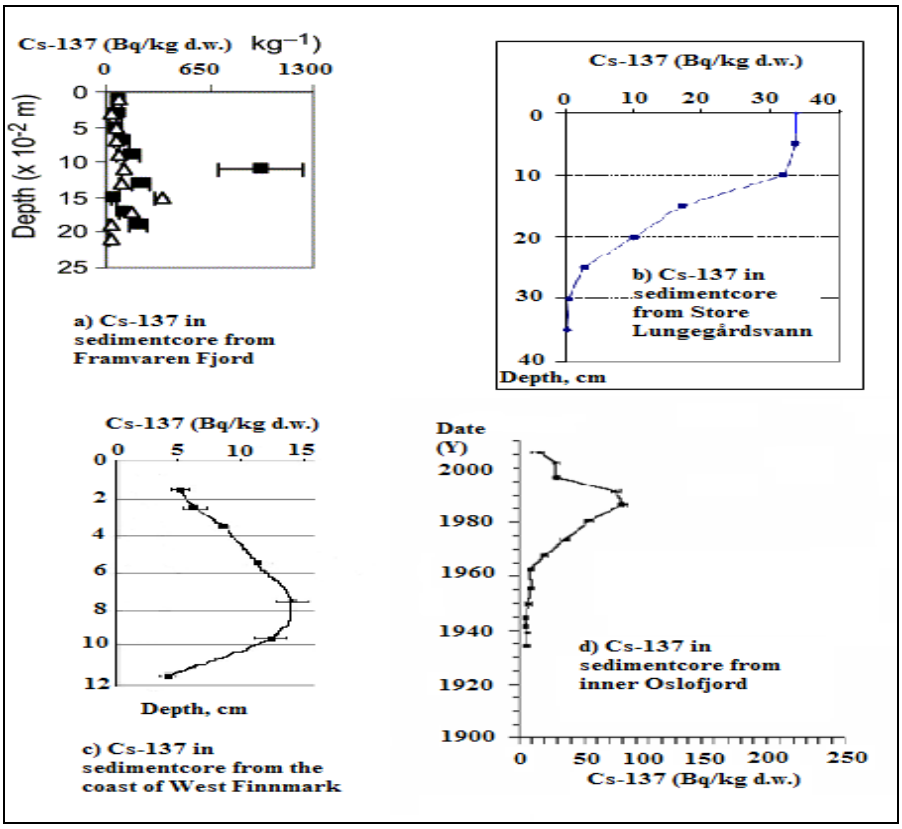


**Figure 4.4: Cs-137 i in cores from Norwegian coastal areas.**

This is not the case in the sediment cores in this work. These cores have the Cs-137 maximum content in the top layers. This is also seen in core b). This fjord on the west coast of Norway has the Cs-137 maximum content in the top layers. The activity concentration distribution is similar to the cores in this work and the activity concentrations in surface sediments are similar to the surface sediments from the outlet of the Sognefjord.

### 4.3.3 Cs-137 activity concentrations in relations to sources

Dating the sediment cores was done in order to investigate if time of deposition of Cs-137 could indicate which source was dominating the levels at the three sampling areas. In none of the 14 sediment cores analyzed, there where peaks in years clearly indicating a dominating source present.

Global fallout of Cs-137 in Norway from atmospheric nuclear weapons tests was considerable. The country average of Cs-137 in air each year from 1955 to 1985 is shown in figure 4.5 (Bergan, 2000). Two peaks are observed; one in the late 1950s and one in 1961-1962. This is well correlated to the release from nuclear weapons testing. The precipitation;

Figure 1.2; was higher in the area surrounding the outlet of the Sognefjord than the head of the fjord and in the Laksefjord area, and thus also received more Cs-137 during the late 1950's and early 1960's (Bergan, 2000). This could cause a signal in the sediment cores.

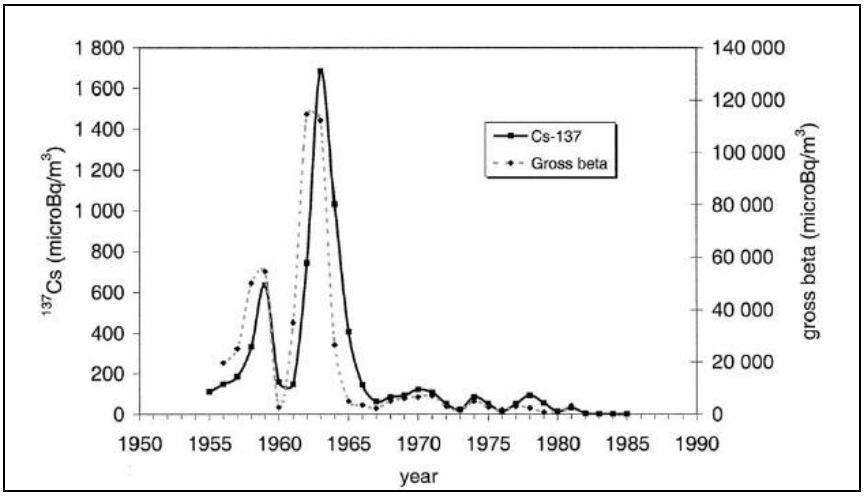


**Figure 4.5: Total beta (right axis) and Cs-137 (left axis) in air, country average each year during the period 1955 to 1985 (Bergan, 2000).**

Discharges from the nuclear fuel reprocessing plant, Sellafield, have contained various amounts of Cs-137, Figure 4.6; (Thørring, 2006b).

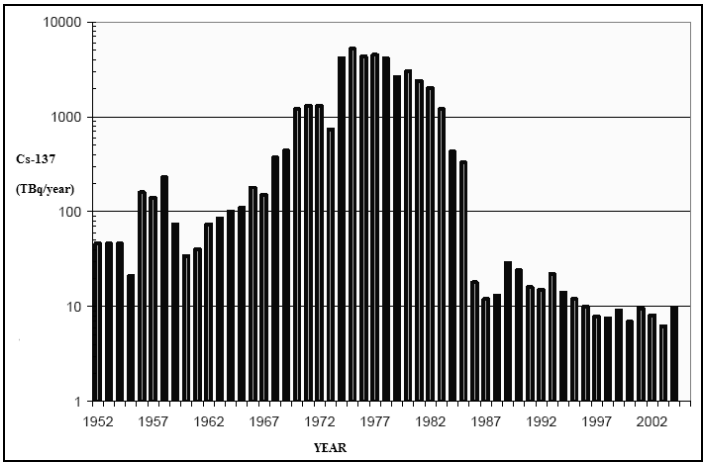


**Figure 4.6: Annual Cs-137 discharges from Sellafield (data from: Jackson et. al., 2000, OSPAR, 2006 and BNFL, 2004).**

The Cs-137 discharges peaked in the seventies with a rapid decrease in 1985, and nearly all the reported Cs-137 discharge from Sellafield was in solution as $Cs^+$ (Mitchell et al., 1996).

Following Chernobyl (1986), there has been a continuous outflow of Chernobyl contaminated seawater from Baltic. Baltic water exchange through the Danish Straits carries annually 30 TBq Cs-137 into the Kattegat (Thørring, 2006b). Cs-137 from Sellafield and Chernobyl Baltic reaches and follows the Norwegian coastal current, Figure 1.4 and Figure 1.5. The Cs-137 will thus reach the west coast (inlet of the Sognefjord) in 3 to 4 years and the Barents Sea (inlet of the Laksefjord) in 5 to 6 years (Dahlgaard, 1995). These events could also cause signals in the sediment cores.

There are no signals in any of the core layers from Laksefjord which could specifically be connected to the mentioned sources. The upper youngest layers have the highest content of Cs-137 indicating a continuous supply. The Laksefjord has a rapid exchange of water with the Norwegian Coastal current (Wassmann et. al, 1999). The Cs-137 activity concentrations in the surface sediments are the same inside the fjord as outside which also reflect this. This also indicates that run-off is not a major recent source. The levels of Cs-137 in surface seawater in Norwegian areas from 2008 are shown in Figure 1.7. Surface water outside the inlet of the Sognefjord has an activity concentration of about 7.5 $Bq/m^3$ (preliminary results). Surface water south west of the inlet to the Laksefjord has an activity concentration of about 1.9 $Bq/m^3$ (preliminary results). According to Nies (1999), the surface water in 1995 from the Norwegian coast is decreasing northerly from 9.6 $Bq/m^3$ (west coast) to 3.8 $Bq/m^3$ (Lofoten) In (Kautsky, 1987) the surface water in 1985 from the Norwegian coast is decreasing northerly from 62,2 $Bq/m^3$ (west coast) to 25,2 $Bq/m^3$(south west Barents Sea). A decrease in the Cs-137 activity concentrations in sediment cores from the Sognefjord to the Laksefjord as seen in this study is therefore expected.

The water in the Sognefjord has a relatively long residence time; it is changed approximately every eight year with water in the Norwegian coastal current, carrying Sellafield discharges and Chernobyl Baltic. Global fallout from weapons tests was considerable in this area, which also received Chernobyl fallout. The Cs-137 could also have its origin from remobilization of Cs-137 from shallower parts inside the fjord, as sediments are transported to deeper areas over time. The signals from weapons test fall out are most likely masked by more recent sources.

The profiles of Cs-137 activity concentrations in the S1 cores show a small peak at approximately 5 cm depth dated to 1977-1977-1974 (CRS) indicating Sellafield or 1991-1993-1990 (CIC) indicating Chernobyl. Thus it is impossible to conclude on source from the

present dating. But the peak at 5 cm depth is followed by a peak in the accompanying Pb-210 profile. The Pb-210 profile indicates that the layer at 5 cm depth are younger than the layers above and thus contains more Cs-137 (assuming a downward decrease). Disturbance of the sediments can then have caused the peak and not extra supply from an external source.
When a conservative tracer in the Norwegian coastal current such as Cs-137 reaches coastal areas with a higher content of particulate material and subsequently particulates from erosion of land in special, it will be bound to particles with clay mineral (Coughtrey and Thorne, 1983) and be transferred into the sediments. This will happen in any fjord with settling clay particles. This could be a reason to the elevated levels of Cs-137 in the Sognefjord. There is a large difference in the activity concentrations in the two sampled areas inside the fjord (1:10). There are no other results from head of other fjord arms in this fjord which could have indicated a fjord head sedimentation pattern. Samples taken in the head of a few other fjords along the Norwegian coastal current show a similar pattern, with a maximum of 365 Bq/kg (d.w.) in the Velfjord (NRPA, 2004), but there are samples from more fjords in which this pattern is not observed.; Figure 1.11. This comparison indicates that Sellafield discharges and Chernobyl Baltic are not the sources for the elevated Cs-137 activity concentrations in the head of the Sognefjord. Chernobyl fallout onto the land area surrounding the head of the Sognefjord is the most likely the source and the reason for the elevated Cs-137 activity concentrations. The fjords with no elevated Cs-137 activity concentrations are all receiving drain-off from areas which was less affected by the Chernobyl fallout.

Nevertheless, drain-off of Chernobyl fallout from the catchment area on land can be relatively small after 21 years. Saxen and Ilus (2001) showed that in the 11 years period after the Chernobyl accident, the amount of Cs-137 removed from catchment areas on land in Finland was very low. More than 97 % was retained in the catchment area. The amount of Cs-137 removed by drain-off was highest the 1-2 first years after the Chernobyl accident. The same work shows that only 6 % of the Cs-137 in Baltic was from river outlet. Though the land areas surrounding Baltic and the Sognefjord are different, it is likely to believe that a large ratio of the fallout also will be retained in the catchment areas surrounding the Sognefjord.

In the head of a fjord there will be a focusing of material from river run-off. In the area where S2 and S4 cores where taken, the catchment area delivering the drain-off are 1 134 $km^2$ (Fortunsvassdraget) while the sea area initially receiving this drain-off is only 61 $km^2$ (NVE

atlas, 2010). This gives a land/sea area ratio of 18.6. This land area received 10 to 25 kBq/$m^2$ (NRPA, 2009b) indicating that if all Cs-137 is drained into the fjord, it will receive in the range 186 kBq/$m^2$ to 465 kBq/$m^2$, in addition to the direct Chernobyl fallout. However, if only 3 % (Saxen and Ilus, 2001) will drain off from this area, the amounts will be in range 5.6 kBq/$m^2$ to 14.0 kBq/$m^2$, in addition to the direct fallout.

The Cs-137 activity concentrations in this work are in Bq pr. weight. Recalculation of the Cs-activity concentrations to Bq/$m^2$ can be done by the equation:

[Amount] Cs-137/$m^2$ = [Activity concentration] Cs-137/kg · [sediment] kg/$m^2$, (d.w.).

The core areas where 78.5 $cm^2$ , and the weight of each slice is given in Appendix II, Table A5. The loss of material during core cutting process is estimated to 5 %; giving the recalculated values shown in Table 4.1.

**Table 4.1: Cs-137 activity concentrations in kBq/ m2.**

| Cores | Activity concentrations, Cs-137 | | Sampling site |
|---|---|---|---|
| S2-1 | 19 | kBq/$m^2$ | Head of the Sognefjord |
| S2-2 | 19 | kBq/$m^2$ | Head of the Sognefjord |
| S2-3 | 10 | kBq/$m^2$ | Head of the Sognefjord |
| S4-1 | 10 | kBq/$m^2$ | Head of the Sognefjord |
| S4-2 | 12 | kBq/$m^2$ | Head of the Sognefjord |

In the two sampling sites in the head of the Sognefjord, the Cs-137 activity concentrations are in range 10 to 19 kBq/m2. This corresponds to approximately 4 % of the Chernobyl fallout on land. If again comparing with the Baltic, currently 70 % of the Cs-137 found there are located in sediments (Ikkaheimonen, Outola, 2009). But the salinity in Baltic is much less than in the Sognefjord. It is thus expected that the relative amount of Cs-137 in the fjord water is larger than in the Baltic, as the distribution factor ($K_d$ = Bq ·$kg^{-1}$ sediment/Bq·$kg^{-1}$ water) is decreasing with increasing salinity (Christensen, 1998). But the budget is not complete since direct Chernobyl fallout is a part of the total inventory, and so is the Cs-137 brought here by the ocean currents.

A work done by Brydsten and Jansson (1988) on particle transport in a river ending in the Baltic with Cs-137 from Chernobyl as tracer; shows that material transported in a river are

settled in the estuary and are redistributed further away until it reaches an area where it settles. Spring flow was the greatest controlling factor for the deposition of particles in the estuary of a river. Sampling distance to a river mouth is thus important when assessing Cs-137 activity concentrations in a fjord. This was not controlled in this work.

## 4.4 Particle size distribution

The particle size analysis on surface sediments showed that the sediments were mainly clay and silt. The sampling sites in the head of the Sognefjord had the highest content of particles < 63um, followed by the Laksefjord and the outlet of the Sognefjord ; 99.4%, 96% and 91.2% respectively The differences between the three sampling areas was so small that firm conclusions on this parameter cannot me made. All these three areas have sediments containing a large fraction of particles which can bind Cs-137.

## 4.5 $^{238}$Pu/239+$^{240}$Pu ratio

The $^{238}$Pu/$^{239+240}$Pu ratio in the surface sediment layers from the 6 sampling sites were all in the range 0.025 to 0.067. Plutonium and Cs-137 does not act the same way in nature (Vintro, 2009), however the $^{238}$Pu/$^{239+240}$Pu ratio will give an indication of the source of plutonium in an area. The ratios measured indicates that weapons test fall out is the plutonium-source in all the 6 sampling sites; as the ratio from weapons test fallout was 0.033, and the ratios from the other known sources were considerably higher (Becks, 2000).

## 4.6 Conclusion

The results in this thesis are in good agreement with other investigations from the same areas. However, comparison of the Cs-137 activity concentrations in this work with recent studies from other areas requires recalculation as the results in this study is given as activity concentrations per. weight sediment while in the most recent studies, the results are given in activity per. area.

Dating the cores does not give as reliable results as expected. Special effort in sampling and sample preparing could probably improve this. There are no sediment layers in the cores which indicate a specific source. Correcting the Cs-137 activity concentrations according to the age found can give an indication of the source at specific layers.

The contents of Cs-137 in sediments are relatively high the Sognefjord. Sediment cores from the head and the outlet of the fjord show an overall decrease in the Cs-137 activity concentrations with increasing depths, indicating a continuous supply. This can be caused by a combination of run-off and a relatively long water residence time. The Sognefjord with is unusual depths can be a huge sediment trap with a low mobility of bottom sediments. The nuclide is found several centimeters into the sediments; in layer deposited before nuclear industry. It is not possible to conclude whether this is caused by bioturbation, diffusion of Cs-137 in interstitial water or by the sampling procedure. The elevated levels in the outlet of the Sognefjord can have its origin from Chernobyl fallout, Chernobyl Baltic and Sellafield. The origin of the Cs-137 in the Laksefjord is most likely Sellafield discharges and Chernobyl Baltic due to a rapid water exchange between the Laksefjord and the Norwegian coastal current.

It is not likely that the elevated Cs-137 activity concentrations in the head of the Sognefjord have its origin from Sellafield or Chernobyl Baltic. Chernobyl fallout on land area surrounding the Sognefjord is most likely the source. The Cs-137 can be focused in the head of fjords due to the ratio between the drain-off area and the area receiving the drain-off. There are also relatively high levels of Cs-137 in some other Norwegian fjords. These fjords are also located in areas which received a large amount of Chernobyl fallout. Fjords located in areas which received a relatively moderate amount of Chernobyl fallout does not show these elevated levels.

How this radio nuclide is bound in the sediments is not investigated here. Speciation should be done in order to see in which physicochemical forms this nuclide exists in the sediments and thus predict whether this nuclide is mobile and thus bioavailable. Analysis of Cs-137 in seawater, river run-off, precipitating particles and sediments in the estuary could be further investigated in order to find the development of this radio nuclide in the Sognefjord. Cs-137 earlier bound in Irish Sea sediment is now remobilized. Cook et. al. (1997) has calculated an annual loss of 86 TBq Cs-137, from the Irish Sea. Could also this happen in the Sognefjord, or is the Cs-137 irreversibly bound to the sediments which will be buried as time pass on?

# 5. References


Aarkrog, A., 1994. Source terms and inventories of anthropogenic radionuclides, in: Holm, E. (Ed.), Radioecology - Lectures in environmental radioactivity. World Scientific Publishing Co. Pte. Ltd., Singapore, Utopia Press, ISBN 981-02-1778-1: 23-38.

Andersson Sørlie, A., Strand, P., Selnæs, T.D., 1992. Brukerveilledning for Canberra serie 10 pluss. Arbeidsdokument SIS 1992:5.

Andersson, T., Meili, M., 1994. Dahlgaard, H. (ed.).The role of lake-specific abiotic and biotic factors for the transfer of radiocesium fallout to fish. Studies in Environmental Science 62. Nordic Radioecology. The transfer of Radionuclides through Nordic ecosystem to man. Elsevier Science B.V., Amsterdam. ISBN: 0-444-81617 -8: 79-92.

Appleby, P.G., Oldfield, F., 1978. The Calculation of lead-210 dates assuming a constant rate of supply of unsupported 210Pb to the sediment. Catena Vol.5: 1-8.

Asplin, L., Dahl, E., 2003. Havets miljø 2003. Fisken og havet, særnr.2-2003.

Becks, J.P., 2000. Storage and distribution of plutonium, 241Am, 137Cs and 210Pbxs in North Sea Sediments. Continental Self Reasearch ,20: 1941-1964.

Bergan, T.D., 2002. Radioactive fallout in Norway from atmospheric nuclear weapons tests. Journal of environmental radioactivity , 60, 189-208.

Binford, M.W., 1990. Calculation and uncertainty analysis of 210Pb dates for PIRLA project lake sediment cores. Journal of Paleolimnology, 3: 253-267.

Bjørnes, H., Hovde, P., 1978. Fysiske målinger. Universitetsforlaget. ISBN 82-00-26802-0

BNFL, 2004. Discharges and monitoring of the environment in the UK. Annual report 2003. Warrington: British Nuclear Fuels, BNFL, 2004.

Boitsov, S., Jensen, H.K.B., Klungsøyr, J., 2009. Natural background and anthropogenic inputs of polycyclic aromatic hydrocarbons (PAH) in sediments of South-Western Barents Sea. MareanoMarine Environmental Research, 68: 236-245.

Bowen, H.J.M., 1979. Environmental chemistry of the elements. Academic Press. London, 333.

Brungot, A.L., Amundsen, I., 2003. LORAKON: Kvalitetskontroll 2000 og 2001. Strålevernrapport 2003:4 Østerås: Statens Strålevern.

Brydsten, L., Jansson, M., 1989. Studies of Estuarine Sediment Dynamics Using $^{137}Cs$ from the Tjernobyl Accident as a Tracer. Estuarine, Coastal and Shielf Science, 28: 249-259.

Buchanan, J.B.,1984. Sediment analysis. Pp 41-65 in: Holme, N.A., McIntyre, A.D. (Eds.). Methods for the study of marine benthos. Blackwell Scientific Publications, Oxford.

Christensen, G.C., Bergan, T.D.S., Berge, D., Bækken, T., 1998. A comparison of sea water and fresh water in a study of sediment-water exchange of radionuclides. Radiation Protection Dosimetry, 75: 107-109.

Cook, G.T., MacKenzie, A.B., McDonald, P., Jones, S.R., 1997. Remobilization of Sellafield –Dervived Radionuclides and Transport from the North-east Irish Sea. Journal of Environmental Radioactivity, 35: 227-241.

Coughtrey, P.J., Thorne, M.C., 1983. Cesium in aquatic ecosystems. In: Radionuclide distribution and transport in terrestrial and aquatic ecosystems. Vol. 1,AA Balkema Publ., Rotterdam: pp 496.

Currie, L.A., 1968. Limits for Qualitative Detection and Quantitative Determination, Application to Radiochemistry. Analytical Chemistry, 40: 586-593.

Cutshall, N.H., Larsen, I.L., Olsen, C.R., 1983. Direct analysis of 210Pb in sediment samples: Self-absorption corrections. Nuclear Instruments and Methods 206: 309-312.

Dahl, E., Hansen, P. K., Haug, T., Karlsen, Ø., 2007. Kyst og havbruk 2007. Fisken og havet, særnr.2-2007.

Dahlgaard, H., 1995. Transfer of European Coastal Pollution to the Arctic: Radioactive Tracers. Marine Pollution Bulletin, 31: 3-7.

Dahlgaard, H., 2002. Baltic 137Cs outflow through the Danish Straits indicates remobilization, in: Strand, P., Børrezen, P., Jølle, T., (Eds.), International conference on radioactivity in the environment, Monaco 2002. Extended abstract. Østerås: Norwegian Radiation Protection Authority: 516-520.

Department of Food and Rural Affairs, 2003. Artificial Sources of Radiation. Exposure from liquid effluents.
http://www.defra.gov.uk/evidence/statistics/environment/radioact/radliquid.htm#rafg0910
Page last modified: 16 September 2003.

Evans, S., 1991. Impacts of the Chernobyl fallout in the Baltic ecosystem, in: Moberg L., (ed.), The Chernobyl fallout in Sweden. Swedish Radiation Protection Institute, Stockholm: 109-127.

Føyn, L., Sværen, I., 1995. Distribution and sedimentation of radionuclides in the Barents Sea. ICES C.M. 1995. Mini11.

Gjøsæter, H., Huse, G., Robbertstad, Y., Skogen, M., 2008 Havets ressurser og miljø 2008. Fisken og havet, særnr. I-2008.

Goldberg, E.D., 1963. Geochronology with Pb-210 in radioactive dating. International Atomic Energy Agency. Symposium Proceedings, Vienna 1962: 121-131.

Grøttheim, S., 1998. A preliminary report on radioactive contamination in the northern marine environment. Studies on distribution of radiocaesium, plutonium and americium in sea water and sediments. Norwegian Radiation Protection Authority.

Hermansen, H.O., 1974. Sognefjordens hydrografi og vannutveksling. Hovedfagsoppgave i fysisk oseanografi. Del I med tekst (56s.) + Del 2 med 46 figurer.

Holby, O., Evans, S., 1996. The Vertical Distribution of Chernobyl-Derived Radionuclides in a Baltic Sea Sediment. Journal of Environmental Radioactivity, 33: 129-145.

IAEA, 1985. Sediment Kds and concentration factors for radio-nuclides in the Marine Environment. Report coded STI/DOC/10/247, International Atomic Energy Agency, Vienna, Austria.

IAEA, 1991. Reference sheet IAEA-368 Radionuclides in Pacific Ocean sediment.

IAEA, 2000. Report on the intercomparison run IAEA-384 Radionuclides in Fangataufa Lagoon Sediment.

IAEA, 2001. Worldwide Marine Radioactive studies (WOMARS). IAEA-MEL, Report R1/01, Monaco.

IAEA, 2005. Report on the worldwide Intercomparison Exercise IAEA-385 Radionuclides in Irish Sea Sediments.

Ikkaheimonen, T.K., Outola, I., 2009. Radioactivity in the Baltic SEa: inventories and temporal trends of 137Cs and 90Sr in water and sediments. Journal of Radioanalytical Chemistry, 282: 419-425.

Jackson, D., Lambers, B., Gray, J., 2000. Radiation doses to members of the public near Sellafield, Cumbria, from liquid discharges 1952-1998. Journal of Radiological Protection, 20: 139-167.

Jones, D.G., Kershaw, P.J., McMahon, C.A., Milodowski, A.E., Murray, M., Hunt, G.J., 2007. Changing patterns of radionuclide distribution in Irish Sea subtidal sediments. Journal of Environment radioactivity, 96: 63-74.

Kautsky, H., 1987. Investigations on the Distribution of 137Cs, 134Cs and 90Sr and the Water Mass Transport Times in the Northern North Atlantic and the North Sea. Deutsches Hydrographicses zeitung, 40: 49-69.

Keith-Roach, M., J., Roos, P., 2004. Redox-dependent behaviour of technetium-99 entering a permanently stratified anoxic fjord (Framvaren fjord, Norway). Estuarine, Coastal and Shelf Science. 60: 151-161.

Matishov, D.G., Matishov, G.G., 2004. Radioecology in Northern European Seas. Springer-Verlag Berlin Heidelberg New York: 103-160. ISBN 3-540-20197-1.

Matthäus, W., Schinke, H., 1999. The influence of river runoff on deep water conditions of the Baltic Sea. Hydrobiologia, 393: 1-10.

Mitchell, P.I., Kershaw, P.J., Vintró, L., 1996. Radioactivity in the Irish Sea: past practices, present status and future perspectives. In: Guéguéniat, P., Germain, P. and Métivier, H., Editors, 1996. Radionuclides in the Oceans, Les éditions de physique, les Ulis, France: 155–175.

Nies, H., Harms, I.H., Karcher, M.J., Dethleff, D., Bahe, C., 1999. Antropogenic radioactivity in the Arctic Ocean- Review of the results from the joint German project. The Science of Total Environment 237/238: 181-191.

NRPA, 2001.Radioactivity in the Marine Environment (RAME) 1999. NRPA Report 2001:9 Østerås: Norwegian Radiation Protection Authority.

NRPA, 2003 Radioactivity in the Marine Environment 2000 and 2001. Results from the Norwegian National Monitoring Programme (RAME). StrålevernRapport 2003:8 Østerås: Norwegian Radiation Protection Authority.

NRPA, 2004. Radioactivity in the Marine Environment 2002. Results from the Norwegian National Monitoring Programme (RAME). StrålevernRapport 2004:10 Østerås: Norwegian Radiation Protection Authority.

NRPA, 2005. Radioactivity in the Marine Environment 2003. Results from the Norwegian National Monitoring Programme (RAME). StrålevernRapport 2005:20 Østerås: Norwegian Radiation Protection Authority.

NRPA, 2006. Radioactivity in the Marine Environment 2004. Results from the Norwegian National Monitoring Programme (RAME). StrålevernRapport 2006:14 Østerås: Norwegian Radiation Protection Authority.

NRPA, 2007. Radioactivity in the Marine Environment 2005. Results from the Norwegian National Monitoring Programme (RAME). StrålevernRapport 2007:10 Østerås: Norwegian Radiation Protection Authority.

NRPA, 2008. Radioactivity in the Marine Environment 2006. Results from the Norwegian National Monitoring Programme (RAME). StrålevernRapport 2008:14 Østerås: Norwegian Radiation Protection Authority.

NRPA, 2009a: NRPA website: Kilder til radioaktiv forurensning; oppdatert: 18.11.2009. http://www.nrpa.no/eway/default.aspx?pid=239&trg=Center_6304&LeftMiddle_6254=6262:0:15,4840:1:0:0:::0:0&CenterAndRight_6254=6304:0:15,4892&Center_6304=6312:80110::0:6314:1:::0:0

NRPA 2009b: NRPA website: Tsjernobyl-ulykken; oppdatert: 03.12.2009. http://www.nrpa.no/eway/default.aspx?pid=239&trg=Center_6304&LeftMiddle_6254=6262:0:15,4840:1:0:0:::0:0&CenterAndRight_6254=6304:0:15,4892&Center_6304=6312:80090::0:6321:2:::0:0

NRPA, 2009c: NRPA website: Grenseverdier for radioaktivt cesium i Norge; oppdatert 25.11.2009. http://www.nrpa.no/eway/default.aspx?pid=239&trg=Center_6304&LeftMiddle_6254=6262:0:15,4840:1:0:0:::0:0&CenterAndRight_6254=6304:0:15,4898&Center_6304=6312:80036::0:6321:3:::0:0

NRPA, 2009d: NRPA website: Atmosfæriske prøvesprengninger; oppdatert: 20.10.2009. http://www.nrpa.no/eway/default.aspx?pid=239&trg=Center_6304&LeftMiddle_6254=6262:0:15,4840:1:0:0:::0:0&CenterAndRight_6254=6304:0:15,4892&Center_6304=6312:80037::0:6322:1:::0:0

NRPA, 2009e: NRPA website: Fisk; oppdatert: 25.11.2009. http://www.nrpa.no/eway/default.aspx?pid=239&trg=Center_6304&LeftMiddle_6254=6262:0:15,4840:1:0:0:::0:0&CenterAndRight_6254=6304:0:15,4894&Center_6304=6312:80365::0:6322:1:::0:0

NRPA, 2009f. Radioactivity in the Marine Environment 2007. Results from the Norwegian National Monitoring Programme (RAME). StrålevernRapport 2009:15 Østerås: Norwegian Radation Protection Authority.

NVE-Atlas, 2010: Norwegian Water Resources and Energy Directorate
http://www.nve.no/no/Vann-og-vassdrag/Databaser-og-karttjenester/
http://arcus.nve.no/website/nve/viewer.htm

OSPAR, 2006. Liquid discharges from nuclear installations in 2004. Radioactive substances series. Publication number 297/2006. London: OSPAR Commision, 2006.

Povinec, P.P., 2003. Temporal and spatial trends in the distribution of Cs-137 in surface of Northern European Seas – a record of 40 years of investigation. Deep-Sea Research II 50: 2785-2801.

Richie, J.C., McHenry, J.R., 1990 Application of radioactive fallout cesium-137 for measuring soil erosion and sediment accumulation rates and patterns: a review. Journal of Environmental Quality, 19: 215-233.

Salbu, B., Krekling, T., Oughton, D., 1998. Characterisation of radioactive particles in the environment. Analyst, 123: 843-849.

Saxen, R., Ilus, E., 2001. Discharge of 137Cs and 90Sr by Finnish rivers to the Baltic Sea in 1986-1996. Journal of Environmental Radioactivity, 54: 275-291.

Schøtzig, U., Schraeder, H., 1993. Halbwertszeiten und Photonen-Emissionswahrscheinlichkeiten von haufig verwendeten Radionukliden. Physikalisch-Technische Bundesanstalt, Braunschweig. ISBN 3-89429-349-7.

SFT, 2010: Forurensede sedimenter.
http://www.klif.no/publikasjoner/vann/1957/ta1957_01_02.html

Skei, J., Nilsson, H., 2008. Kjemiske analyser av sedimentkjerner fra deponiområdet ved Malmøykalven og randområdene. NIVA, s.54.

Smith, J.T., Beresford, N.A., 2005. Radioactive fallout and environmental transfers, in: Smith, J., Beresford, N.A. (Eds.), Chernobyl - Catastrophe and Consequences. Praxis Publishing Ltd, Chichester, UK: 35-80.

STUK-B 91. Mustonen, R., (Ed.), 2008. Strålingsovervakning av miljøn I Finland. Årsrapport 2007. STUK-B 91. Helsingfors. 67s.

Svendsen, S.W., 2006. Master Thesis in Physical Oceanography: Stratification and circulation in Sognefjorden. University of Bergen.

Sværen, I., 2010. R1: Bestemmelse av radioaktivt cesium i sedimenter og biota, målt med gamma-spektroskopi på HPGe-detektor. Intern metode. Havforskningsinstituttet.

Syvitski, J.P.M., Burell, D.C., Skei, J.M., 1987. Fjords: processes and products. New York: Springer Verlag. 379p.

Tadjiki, S., Erten, H.N., 1994. Radiochronology of sediments from the Mediterranean Sea using natural Pb-210 and fallout C-137. Journal of radioanalytical and nuclear chemistry, 181: 447-459.

Thørring, H., 2006a: Statens Strålevern: Stråleverninfo 2006:11: Radioaktive stoffer i norske matvarer etter Tsjernobyl-ulykken. http://www.nrpa.no/dav/11dfeb42a3.pdf

Thørring, H., Gäfvert, T., Iosjpe, M., Rudjord, A.L., 2006b. Tilførsel av radioaktive stoffer til norske kyst- og havområder. StrålevernRapport 2006:23. Østerås: Statens Strålevern, 2006.

UNSCEAR, 1993. Sources and effects of ionizing radiation, United Nations Scientific Committee on Effects of Atomic Radiation, UNSCEAR 1993 Report to the General Assembly, with Scientific Annexes; United Nations, New York.

UNSCEAR, 2000. Report to the General Assembly. Sources and effects of ionizing radiation. Volume II, Annex J. United Nations, New York: 453-551.

Varga, Z., 2007. Origin and release date assessment of environmental plutonium by isotopic composition. Analytical and Bioanalytical Chemistry, 389: 725-732.

Vintro, L. L., 2009. Marine Radioecology. Lecture in European Master in Radioecology 2009/2010. UMB.

Wassmann, P., Svendsen, H., Kecka, A., Reigstad, M., 1996. Selected aspects of the physical oceanography and particle fluxes in fjords of northern Norway. Journal of Marine Systems, 8: 53-71.

Zaborska, A., Carroll, J., Papucci C., Torricelli, L., Carroll, M.L., Walkusz-Miotk, J., Pempkowiak, J., 2008. Recent sediment accumulation rates for the Western margin of the Barents Sea. Deep Sea Research Part II, 55: 2352-2360.

***APPENDIX I***

**Appendix I Table A1:**

*Cs-137 activity concentrations in surface sediment samples from the Skagerrak area (NRPA, 2003) (NRPA, 2006) (NRPA, 2007).*

| **Fjord** | **Year** | | | |
|---|---|---|---|---|
| | | | | |
| Iddefjorden | 2001 | | 37, 24, 31 | 3 sampling sites |
| Iddefjorden | 2004 | | 33.3 | |
| Iddefjorden | 2005 | | 30.8 | |
| Bunnefjorden | 2001 | | 3.2 | |
| Bunnefjorden | 2004 | | <1.0 | |
| Bunnefjorden | 2005 | | 3.2 | |
| Oslofjorden | 2001 | | 40 | |
| Oslofjorden | 2004 | | 40.4, 30 | 2 sampling sites |
| Oslofjorden | 2005 | | 12.5, 31.7 | 2 sampling sites |
| ***Drammensfjorden indre*** | ***2001*** | | ***290*** | |
| Drammensfjorden midt | 2001 | | 10 | |
| Drammensfjorden ytre | 2001 | | 7.9, 7.7 | 2 sampling sites |
| Drammensfjorden ytre | 2004 | | 14.2 | |
| Drammensfjorden ytre | 2005 | | 28.8 | |
| Tønsbergfjorden | 2004 | | 13.7 | |
| Tønsbergfjorden | 2005 | | 11.9 | |
| Larvikfjorden | 2004 | | 20.4 | |
| Frierfjorden | 2001 | | 7.2 | |
| Grenland | 2004 | | 20.6, 21.3, 3.3, 2.3 | 4 sampling sites |
| Grenland | 2005 | | 13.3, 7.4 | 2 sampling sites |
| Eidangerfjorden | 2001 | | 9.7 | |
| Kragerø | 2004 | | 19.1 | |
| Kragerø | 2005 | | 22.4 | |
| Risør | 2004 | | <0.7 | |
| Risør | 2005 | | 2.3 | |

**Appendix I Table A2:**

*Cs-137 activity concentrations in surface sediment samples from the west coast of Norway (including preliminary results) (NRPA, 2001) (NRPA, 2003) (NRPA, 2004) (NRPA, 2007).*

| **Fjord** | **Year** | | | |
|---|---|---|---|---|
| | | | | |
| Sørfjorden | 2005 | | 23.1 | |
| Fensfjorden | 2002 | | 11 | |
| Masfjorden | 2002 | | 2 | |
| ***Sognefjorden head*** | ***2005*** | | ***415*** | |
| ***Sognefjorden head*** | ***2008*** | | ***323*** | |
| Sognefjorden mouth | 2005 | | 45.4 | |
| Sognefjorden mouth | 2008 | | 34.4 | |
| ***Nordfjord*** | ***1999*** | | ***102*** | |
| Innvik | 2001 | | 9.4 | |
| Nordfjord indre | 2002 | | 19, 20 | 2 sampling sites |
| Geirangerfjorden | 2002 | | 40 | |
| Stor/Sulafjord | 2002 | | 7.8 | |
| Storfjorden | 2005 | | 16.2 | |
| ***Sunndalsfjorden*** | ***2002*** | | ***85*** | |
| Frøyfjorden | 2002 | | 6 | |
| Romsdalsfjorden | 1999 | | 41 | |
| Romsdalsfjorden | 2001 | | 18.3 | |
| Moldefjorden | 2005 | | 27.4 | |

**Appendix I Table A3:**

*Cs-137 activity concentrations in surface sediment samples from Trøndelag to Lofoten (NRPA, 2001) (NRPA, 2003) (NRPA, 2004) (NRPA, 2005) (NRPA, 2007) (NRPA, 2008) (NRPA, 2009).*

| **Fjord** | **Year** | | | |
|---|---|---|---|---|
| | | | | |
| ***Trondheimsfjorden*** | ***2001*** | | ***67*** | |
| ***Beistadfjorden*** | ***1999*** | | ***102*** | |
| Beistadfjorden | 2001 | | 6.2 | |
| ***Namsfjorden*** | ***1999*** | | ***330*** | |
| Namsfjorden | 2001 | | 83 | |
| Namsfjorden | 2002 | | 186 | |
| Bindalsfjorden | 2001 | | 48 | |
| Tosenfjorden | 2001 | | 30 | |
| ***Velfjorden*** | ***2002*** | | ***365*** | |
| ***Vefsenfjorden*** | ***2002*** | | ***317*** | |
| Ranafjorden | 1999 | | 2 | |
| ***Ranafjorden*** | ***2001*** | | ***126*** | |
| Glomfjord | 2001 | | 16.9 | |
| Glomfjord | 2005 | | 5.6 | |
| Sørfolla | 1999 | | 5.7 | |
| Follafjordene | 2002 | | 3.1, 7.7, 11, 8.6, 11.8 | 5 sampling sites |
| Ofotfjorden | 1999 | | 14.3 | |
| Ofotfjorden | 2001 | | 3.9 | |
| Tysfjord | 2002 | | 5.6, 2.5 | 2 sampling sites |
| Ofotfjorden | 2003 | | 15.9 | |
| Ofotfjprden | 2006 | | 5.9 | |
| Ofotfjorden | 2007 | | 9 | |

**Appendix I Table A4:**

*Cs-137 activity concentrations in surface sediment samples from Lofoten to the Russian border (NRPA, 2001) (NRPA, 2003) (NRPA, 2004) (NRPA, 2005) (NRPA, 2006) (NRPA, 2007) (NRPA, 2008) (NRPA 2009).*

| **Fjord** | **Year** | | | |
|---|---|---|---|---|
| | | | | |
| Vågsfjorden-Astafjorden | 2006 | | 16.4 | |
| Vågsfjorden-Astafjorden | 2007 | | 10.5 | |
| Balsfjorden | 2001 | | 16 | |
| Balsfjorden | 2006 | | 12.7 | |
| Tromsø | 2004 | | 13.1, 20.2, 4.2, 8.8 | 4 sampling sites |
| Tromsø | 2005 | | 7 | |
| Tromsø | 2006 | | 2.6 | |
| Tromsø | 2007 | | 11.1 | |
| Ullsfjorden | 2006 | | 10.8 | |
| Ullsfjorden | 2007 | | 10.3 | |
| Malangen | 2002 | | 16,5.6 | 2 sampling sites |
| Malangen | 2005 | | 7.5 | |
| Malangen | 2006 | | 6.6 | |
| Malangen | 2007 | | 14 | |
| Lyngenfjorden ytre | 2002 | | 12, 6.1, 7.7 | 3 sampling sites |
| Lyngen | 2006 | | 8.3 | |
| Lyngen | 2007 | | 5.9 | |
| Kvænangen | 2006 | | 8.5 | |
| Kvænangen | 2007 | | 1.9 | |
| Altafjorden | 1999 | | 20.1 | |
| Altafjorden | 2001 | | 14.5 | |
| Altafjorden | 2004 | | 13.1 | |
| Altafjorden | 2005 | | 8.9 | |
| Altafjorden | 2006 | | 10.6 | |
| Altafjorden | 2007 | | 10.1 | |
| Porsangerfjorden | 1999 | | 7.2 | |
| Porsangerfjorden | 2001 | | 12.4 | |
| Porsangerfjorden | 2004 | | 9.8, 9 | |
| Porsangerfjorden | 2005 | | 9.9 | |
| Porsangerfjorden | 2006 | | 7.4 | |
| Porsangerfjorden | 2007 | | 9, 6.5 | 2 sampling sites |
| Laksefjorden | 2002 | | 2, 6.2 | 2 sampling sites |
| Laksefjorden | 2004 | | 9.1, 4.7 | 2 sampling sites |
| Laksefjorden | 2006 | | 6.6 | |
| Laksefjorden | 2007 | | 7.4 | |
| Tanafjorden | 1999 | | 13.8 | |
| Tanafjorden | 2001 | | 9.9 | |
| Tanafjorden | 2003 | | 10.9 | |
| Tanafjorden | 2004 | | 3.5 | |
| Tanafjorden | 2005 | | 9.2 | |
| Tanafjorden | 2006 | | 8.6 | |
| Tanafjorden | 2007 | | 5.7 | |
| Varangerfjorden | 2003 | | 4.6 | |
| Varangerfjorden indre | 2004 | | 4.5, 5.6 | 2 sampling sites |
| Varangerfjorden | 2006 | | 5.2 | |
| Varangerfjorden | 2007 | | 6, 7.6, 4 | 3 sampling sites |

***APPENDIX II***

**Appendix II Table A5: Overview of samples; weighing data and dry weight calculations in each layer; from corers S1-1, S1-2 and S1-3.**

| Corer | S1-1 | | | | | | S1-2 | | | | | | S1-3 | | | | | |
|---|---|---|---|---|---|---|---|---|---|---|---|---|---|---|---|---|---|---|
| Date | 20.11.07 | | | | | | 20.11.07 | | | | | | 20.11.07 | | | | | |
| Layer | Empty cont., g | Gross wet weight, g | Gross dry weight, g | Net wet weight, g | Net dry weight, g | % dry weight | Empty cont., g | Gross wet weight, g | Gross dry weight, g | Net wet weight, g | Net dry weight, g | % dry weight | Empty cont., g | Gross wet weight, g | Gross dry weight, g | Net wet weigh,. g | Net dry weight, g | % dry weight |
| 0-1 cm | 2.5 | 150.0 | 61.7 | 147.5 | 59.2 | 40.1 | 2.5 | 91.4 | 35.3 | 88.9 | 32.8 | 36.9 | 2.5 | 134.4 | 49.0 | 131.9 | 46.5 | 35.3 |
| 1-2 cm | 2.5 | 114.1 | 51.7 | 111.6 | 49.2 | 44.1 | 2.5 | 126.6 | 56.8 | 124.1 | 54.3 | 43.8 | 2.5 | 140.3 | 64.1 | 137.8 | 61.6 | 44.7 |
| 2-3 cm | 2.5 | 117.3 | 53.9 | 114.8 | 51.4 | 44.8 | 2.6 | 162.7 | 74.6 | 160.1 | 72 | 45.0 | 2.5 | 132.3 | 59.5 | 129.8 | 57.0 | 43.9 |
| 3-4 cm | 2.5 | 131.9 | 61.8 | 129.4 | 59.3 | 45.8 | 2.5 | 120.9 | 55.7 | 118.4 | 53.2 | 44.9 | 2.5 | 140.0 | 64.6 | 137.5 | 62.1 | 45.2 |
| 4-5 cm | 2.5 | 138.6 | 64.7 | 136.1 | 62.2 | 45.7 | 2.5 | 106.5 | 50.1 | 104 | 47.6 | 45.8 | 2.5 | 138.1 | 65.4 | 135.6 | 62.9 | 46.4 |
| 5-6 cm | 2.5 | 121.3 | 59.1 | 118.8 | 56.6 | 47.6 | 2.5 | 84.8 | 34.7 | 82.3 | 32.2 | 39.1 | 2.5 | 121.6 | 58.3 | 119.1 | 55.8 | 46.9 |
| 6-7 cm | 2.5 | 134.8 | 67.8 | 132.3 | 65.3 | 49.4 | 2.5 | 104.1 | 52.2 | 101.6 | 49.7 | 48.9 | 2.5 | 138.1 | 65.1 | 135.6 | 62.6 | 46.2 |
| 7-8 cm | 2.5 | 111.6 | 56.8 | 109.1 | 54.3 | 49.8 | 2.5 | 100.6 | 50.5 | 98.1 | 48 | 48.9 | 2.5 | 153.3 | 73.0 | 150.8 | 70.5 | 46.8 |
| 8-9 cm | 2.5 | 118.3 | 61.0 | 115.8 | 58.5 | 50.5 | 2.5 | 144.0 | 71.6 | 141.5 | 69.1 | 48.8 | 2.5 | 150.6 | 72.6 | 148.1 | 70.1 | 47.3 |
| 9-10 cm | 2.5 | 144.6 | 75.2 | 142.1 | 72.7 | 51.2 | 2.5 | 147.0 | 76.2 | 144.5 | 73.7 | 51.0 | 2.5 | 150.3 | 76.9 | 147.8 | 74.4 | 50.3 |
| 10-11 cm | 2.5 | 133.1 | 71.0 | 130.6 | 68.5 | 52.5 | 2.5 | 139.1 | 72.5 | 136.6 | 70 | 51.2 | 2.5 | 157.3 | 83.1 | 154.8 | 80.6 | 52.1 |
| 11-12 cm | 2.5 | 158.6 | 84.9 | 156.1 | 82.4 | 52.8 | 2.5 | 167.3 | 88.7 | 164.8 | 86.2 | 52.3 | 2.5 | 176.4 | 91.5 | 173.9 | 89.0 | 51.2 |
| 12-13 cm | 2.5 | 156.6 | 85.1 | 154.1 | 82.6 | 53.6 | 2.5 | 148.1 | 76.9 | 145.6 | 74.4 | 51.1 | 2.5 | 154.9 | 82.8 | 152.4 | 80.3 | 52.7 |
| 13-14 cm | 2.5 | 133.9 | 71.2 | 131.4 | 68.7 | 52.3 | 2.5 | 155.8 | 82.1 | 153.3 | 79.6 | 51.9 | 2.5 | 118.5 | 64.0 | 116.0 | 61.5 | 53.0 |
| 14-15 cm | 2.5 | 168.0 | 90.1 | 165.5 | 87.6 | 52.9 | 2.5 | 155.3 | 83.7 | 152.8 | 81.2 | 53.1 | | | | | | |
| 15-16 cm | 2.5 | 146.2 | 80.6 | 143.7 | 78.1 | 54.3 | | | | | | | | | | | | |
| Length | 16 cm | | | | | | 15 cm | | | | | | 14 cm | | | | | |

**Continued Appendix II Table A5: Overview of samples; weighing data and dry weight calculations in each layer; corers S2-1, S2-2 and S2-3**

| Corer | S2-1 | | | | | | S2-2 | | | | | | S2-3 | | | | | |
|---|---|---|---|---|---|---|---|---|---|---|---|---|---|---|---|---|---|---|
| Date | 18.11.07 | | | | | | 18.11.07 | | | | | | 18.11.07 | | | | | |
| Layer | Empty cont., g | Gross wet weight, g | Gross dry weight, g | Net wet weight, g | Net dry weight, g | % dry weight | Empty cont., g | Gross wet weight, g | Gross dry weight, g | Net wet weight, g | Net dry weight, g | % dry weight | Empty cont., g | Gross wet weight, g | Gross dry weight, g | Net wet weight, g | Net dry weight, g | % dry weight |
| 0-1 cm | 2.5 | 141.4 | 66.80 | 138.9 | 64.3 | 46.3 | 2.6 | 163.3 | 76.7 | 160.7 | 74.1 | 46.1 | 2.5 | 108.2 | 49.1 | 105.7 | 46.6 | 44.1 |
| 1-2 cm | 2.5 | 105.5 | 52.90 | 103.0 | 50.4 | 48.9 | 2.6 | 132.1 | 67.9 | 129.5 | 65.3 | 50.4 | 2.5 | 161.0 | 82.2 | 158.5 | 79.7 | 50.3 |
| 2-3 cm | 2.5 | 110.9 | 56.20 | 108.4 | 53.7 | 49.5 | 2.5 | 153.3 | 82 | 150.8 | 79.5 | 52.7 | 2.5 | 126.3 | 69.0 | 123.8 | 66.5 | 53.7 |
| 3-4 cm | 2.5 | 149.6 | 79.10 | 147.1 | 76.6 | 52.1 | 2.5 | 148.0 | 81.9 | 145.5 | 79.4 | 54.6 | 2.5 | 139.9 | 79.0 | 137.4 | 76.5 | 55.7 |
| 4-5 cm | 2.5 | 138.7 | 75.10 | 136.2 | 72.6 | 53.3 | 2.6 | 143.0 | 80.8 | 140.4 | 78.2 | 55.7 | 2.5 | 131.3 | 76.0 | 128.8 | 73.5 | 57.1 |
| 5-6 cm | 2.5 | 144.7 | 79.20 | 142.2 | 76.7 | 53.9 | 2.6 | 130.3 | 75.1 | 127.7 | 72.5 | 56.8 | 2.5 | 137.7 | 80.8 | 135.2 | 78.3 | 57.9 |
| 6-7 cm | 2.5 | 135.6 | 76.30 | 133.1 | 73.8 | 55.4 | 2.6 | 131.2 | 76.2 | 128.6 | 73.6 | 57.2 | 2.5 | 164.5 | 97.3 | 162.0 | 94.8 | 58.5 |
| 7-8 cm | 2.5 | 136.2 | 77.60 | 133.7 | 75.1 | 56.2 | 2.6 | 150.2 | 88.3 | 147.6 | 85.7 | 58.1 | 2.5 | 143.7 | 85.3 | 141.2 | 82.8 | 58.6 |
| 8-9 cm | 2.5 | 142.2 | 81.70 | 139.7 | 79.2 | 56.7 | 2.6 | 146.3 | 86.6 | 143.7 | 84 | 58.5 | 2.5 | 140.8 | 84.0 | 138.3 | 81.5 | 58.9 |
| 9-10 cm | 2.5 | 137.2 | 79.20 | 134.7 | 76.7 | 56.9 | 2.5 | 156.1 | 92.8 | 153.6 | 90.3 | 58.8 | 2.5 | 108.4 | 65.3 | 105.9 | 62.8 | 59.3 |
| 10-11 cm | 2.5 | 142.5 | 82.70 | 140.0 | 80.2 | 57.3 | 2.5 | 142.0 | 84.6 | 139.5 | 82.1 | 58.9 | 2.5 | 131.7 | 80.1 | 129.2 | 77.6 | 60.1 |
| 11-12 cm | 2.5 | 117.0 | 69.30 | 114.5 | 66.8 | 58.3 | 2.5 | 125.4 | 75.8 | 122.9 | 73.3 | 59.6 | 2.5 | 118.1 | 71.2 | 115.6 | 68.7 | 59.4 |
| 12-13 cm | 2.5 | 180.4 | 108.00 | 177.9 | 105.5 | 59.3 | 2.6 | 131.0 | 78.6 | 128.4 | 76 | 59.2 | | | | | | |
| 13-14 cm | 2.5 | 166.0 | 99.50 | 163.5 | 97.0 | 59.3 | 2.5 | 167.0 | 100.6 | 164.5 | 98.1 | 59.6 | | | | | | |
| 14-15 cm | 2.5 | 134.4 | 80.2 | 131.9 | 77.7 | 58.9 | 2.6 | 118.3 | 71.4 | 115.7 | 68.8 | 59.5 | | | | | | |
| 15-16 cm | | | | | | | 2.5 | 119.8 | 72.7 | 117.3 | 70.2 | 59.8 | | | | | | |
| Length | 15 cm | | | | | | 16 cm | | | | | | 12 cm | | | | | |

**Continued Appendix II Table A5: Overview of samples; weighing data and dry weight calculations in each layer; from corers S3-1and S3-2**

| Corer | S3-1 | | | | | | S3-2 | | | | | |
|---|---|---|---|---|---|---|---|---|---|---|---|---|
| Date | 20.11.07 | | | | | | 20.11.07 | | | | | |
| Layer | Empty cont., g | Gross wet weight, g | Gross dry weight, g | Net wet weight, g | Net dry weight, g | % dry weight | Empty cont., g | Gross wet weight, g | Gross dry weight, g | Net wet weight, g | Net dry weight, g | % dry weight |
| 0-1 cm | 2.6 | 94.8 | 46.0 | 92.2 | 43.4 | 47.1 | 2.5 | 96.1 | 47.0 | 93.6 | 44.5 | 48.9 |
| 1-2 cm | 2.6 | 64.4 | 32.8 | 61.8 | 30.2 | 48.9 | 2.6 | 102.1 | 50.0 | 99.5 | 47.4 | 49.0 |
| 2-3 cm | 2.6 | 127.0 | 62.6 | 124.4 | 60.0 | 48.2 | 2.5 | 106.8 | 52.9 | 104.3 | 50.4 | 49.5 |
| 3-4 cm | 2.6 | 139.4 | 68.1 | 136.8 | 65.5 | 47.9 | 2.5 | 99.6 | 49.0 | 97.1 | 46.5 | 49.2 |
| 4-5 cm | 2.5 | 147.5 | 72.9 | 145.0 | 70.4 | 48.6 | 2.5 | 139.0 | 70.6 | 136.5 | 68.1 | 50.8 |
| 5-6 cm | 2.6 | 139.0 | 71.0 | 136.4 | 68.4 | 50.1 | 2.5 | 134.9 | 64.8 | 132.4 | 62.3 | 48.0 |
| 6-7 cm | 2.6 | 191.5 | 93.4 | 188.9 | 90.8 | 48.1 | | | | | | |
| Lenght | 7 cm | | | | | | 6 cm | | | | | |

**Continued Appendix II Table A5: Overview of samples; weighing data and dry weight calculations in each layer; from corers S4-1and S4-2**

| Corer | S4-1 | | | | | | S4-2 | | | | | |
|---|---|---|---|---|---|---|---|---|---|---|---|---|
| Date | 20.11.07 | | | | | | 20.11.07 | | | | | |
| Layer | Empty cont., g | Gross wet weight, g | Gross dry weight, g | Net wet weight, g | Net dry weight, g | % dry weight | Empty cont., g | Gross wet weight, g | Gross dry weight, g | Net wet weight, g | Net dry weight, g | % dry weight |
| 0-1 cm | 2.6 | 182.1 | 86.9 | 179.5 | 84.3 | 47.0 | 2.50 | 129.80 | 59.6 | 127.30 | 57.10 | 44.9 |
| 1-2 cm | 2.6 | 131.2 | 68.9 | 128.6 | 66.3 | 51.6 | 2.50 | 180.50 | 94.4 | 178.00 | 91.90 | 51.6 |
| 2-3 cm | 2.5 | 157.9 | 86.7 | 155.4 | 84.2 | 54.2 | 2.50 | 195.20 | 109.7 | 192.70 | 107.20 | 55.6 |
| 3-4 cm | 2.6 | 162.7 | 92.3 | 160.1 | 89.7 | 56.0 | 2.50 | 180.20 | 105.6 | 177.70 | 103.10 | 58.0 |
| 4-5 cm | 2.5 | 110.6 | 64.9 | 108.1 | 62.4 | 57.7 | 2.50 | 160.70 | 94.7 | 158.20 | 92.20 | 58.3 |
| 5-6 cm | 2.5 | 166.4 | 98.7 | 163.9 | 96.2 | 58.7 | 2.50 | 110.80 | 65.3 | 108.30 | 62.80 | 58.0 |
| 6-7 cm | 2.5 | 154.6 | 92.6 | 152.1 | 90.1 | 59.2 | 2.50 | 158.40 | 92.9 | 155.90 | 90.40 | 58.0 |
| 7-8 cm | 2.6 | 128.8 | 76.9 | 126.2 | 74.3 | 58.9 | 2.50 | 163.40 | 96.8 | 160.90 | 94.30 | 58.6 |
| 8-9 cm | | | | | | | 2.50 | 135.00 | 81.3 | 132.50 | 78.80 | 59.5 |
| Length | 8 cm | | | | | | 9 cm | | | | | |

**Continued Appendix II Table A5: Overview of samples; weighing data and dry weight calculations in each layer; from corers L1-1and L2-1**

| Corer | L1-1 | | | | | | L1-2 | | | | | |
|---|---|---|---|---|---|---|---|---|---|---|---|---|
| Date | 03.11.08 | | | | | | 03.11.08 | | | | | |
| Layer | Empty cont., g | Gross wet weight, g | Gross dry weight, g | Net wet weight, g | Net dry weight, g | % dry weight | Empty cont., g | Gross wet weight, g | Gross dry weight, g | Net wet weight, g | Net dry weight, g | % dry weight |
| 0-1 cm | 2.5 | 131.2 | 55.4 | 128.7 | 52.9 | 41.1 | 2.5 | 82.7 | 44.9 | 80.2 | 42.4 | 52.9 |
| 1-2 cm | 2.5 | 110.9 | 49.2 | 108.4 | 46.7 | 43.1 | 2.5 | 92.7 | 51.1 | 90.2 | 48.6 | 53.9 |
| 2-3 cm | 2.5 | 124.2 | 56.2 | 121.7 | 53.7 | 44.1 | 2.5 | 98.7 | 55 | 96.2 | 52.5 | 54.6 |
| 3-4 cm | 2.5 | 126.4 | 58 | 123.9 | 55.5 | 44.8 | 2.5 | 112.0 | 62 | 109.5 | 59.5 | 54.3 |
| 4-5 cm | 2.5 | 147.8 | 69 | 145.3 | 66.5 | 45.8 | 2.5 | 142.7 | 79.2 | 140.2 | 76.7 | 54.7 |
| 5-6 cm | 2.5 | 111.1 | 53.7 | 108.6 | 51.2 | 47.1 | 2.5 | 120.8 | 67.5 | 118.3 | 65 | 54.9 |
| 6-7 cm | 2.5 | 128.5 | 63.6 | 126 | 61.1 | 48.5 | 2.5 | 118.6 | 66.4 | 116.1 | 63.9 | 55.0 |
| 7-8 cm | 2.5 | 143.5 | 72.4 | 141 | 69.9 | 49.6 | 2.5 | 153.7 | 86.5 | 151.2 | 84 | 55.6 |
| 8-9 cm | 2.5 | 169.9 | 85.7 | 167.4 | 83.2 | 49.7 | 2.5 | 139.9 | 78 | 137.4 | 75.5 | 54.9 |
| 9-10 cm | 2.5 | 189.8 | 95.6 | 187.3 | 93.1 | 49.7 | 2.5 | 139.9 | 77.8 | 137.4 | 75.3 | 54.8 |
| 10-11 cm | 2.5 | 166.1 | 84 | 163.6 | 81.5 | 49.8 | 2.5 | 174.9 | 98 | 172.4 | 95.5 | 55.4 |
| 11-12 cm | 2.5 | 131.0 | 68.4 | 128.5 | 65.9 | 51.3 | 2.5 | 154.7 | 86.6 | 152.2 | 84.1 | 55.3 |
| 12-13 cm | | | | | | | 2.5 | 139.5 | 77.1 | 137 | 74.6 | 54.5 |
| 13-14 cm | | | | | | | 2.5 | 150.1 | 81.5 | 147.6 | 79 | 53.5 |
| 14-15 cm | | | | | | | 2.5 | 107.0 | 58.1 | 104.5 | 55.6 | 53.2 |
| Length | 12 cm | | | | | | 15 cm | | | | | |

**Continued Appendix II Table A5: Overview of samples; weighing data and dry weight calculations in each layer; from corers L2-1and L2-2**

| Corer | L2-1 | | | | | | L2-2 | | | | | |
|---|---|---|---|---|---|---|---|---|---|---|---|---|
| Date | 18.11.07 | | | | | | 18.11.07 | | | | | |
| Layer | Empty cont., g | Gross wet weight, g | Gross dry weight, g | Net wet weight, g | Net dry weight, g | % dry weight | Empty cont., g | Gross wet weight, g | Gross dry weight, g | Net wet weight, g | Net dry weight, g | % dry weight |
| 0-1 cm | 2.5 | 89.9 | 47.9 | 87.4 | 45.4 | 51.9 | 2.5 | 177.7 | 94.8 | 175.2 | 92.3 | 52.7 |
| 1-2 cm | 2.5 | 96.0 | 51.7 | 93.5 | 49.2 | 52.6 | 2.5 | 176.2 | 93.6 | 173.7 | 91.1 | 52.4 |
| 2-3 cm | 2.5 | 95.6 | 52.8 | 93.1 | 50.3 | 54.0 | 2.5 | 185.5 | 103.8 | 183.0 | 101.3 | 55.4 |
| 3-4 cm | 2.5 | 117.1 | 65.2 | 114.6 | 62.7 | 54.7 | 2.5 | 171.0 | 96.8 | 168.5 | 94.3 | 56.0 |
| 4-5 cm | 2.5 | 130.4 | 72.9 | 127.9 | 70.4 | 55.0 | 2.5 | 128.6 | 72.7 | 126.1 | 70.2 | 55.7 |
| 5-6 cm | 2.5 | 120.0 | 67.1 | 117.5 | 64.6 | 55.0 | 2.5 | 164.8 | 93.5 | 162.3 | 91.0 | 56.1 |
| 6-7 cm | 2.5 | 164.0 | 92.2 | 161.5 | 89.7 | 55.5 | 2.5 | 265.8 | 148.2 | 263.3 | 145.7 | 55.3 |
| 7-8 cm | 2.5 | 127.3 | 71.7 | 124.8 | 69.2 | 55.4 | 2.5 | 140.3 | 77.1 | 137.8 | 74.6 | 54.1 |
| 8-9 cm | 2.5 | 157.8 | 88.9 | 155.3 | 86.4 | 55.6 | 2.5 | 155.4 | 84.4 | 152.9 | 81.9 | 53.6 |
| 9-10 cm | 2.5 | 157.0 | 87.8 | 154.5 | 85.3 | 55.2 | 2.5 | 177.3 | 94.4 | 174.8 | 91.9 | 52.6 |
| 10-11 cm | 2.5 | 171.6 | 95.8 | 169.1 | 93.3 | 55.2 | | | | | | |
| 11-12 cm | 2.5 | 188.3 | 105.8 | 185.8 | 103.3 | 55.6 | | | | | | |
| 12-13 cm | 2.5 | 147.0 | 82.9 | 144.5 | 80.4 | 55.6 | | | | | | |
| Length | 13 cm | | | | | | 10 cm | | | | | |

***APPENDIX III***

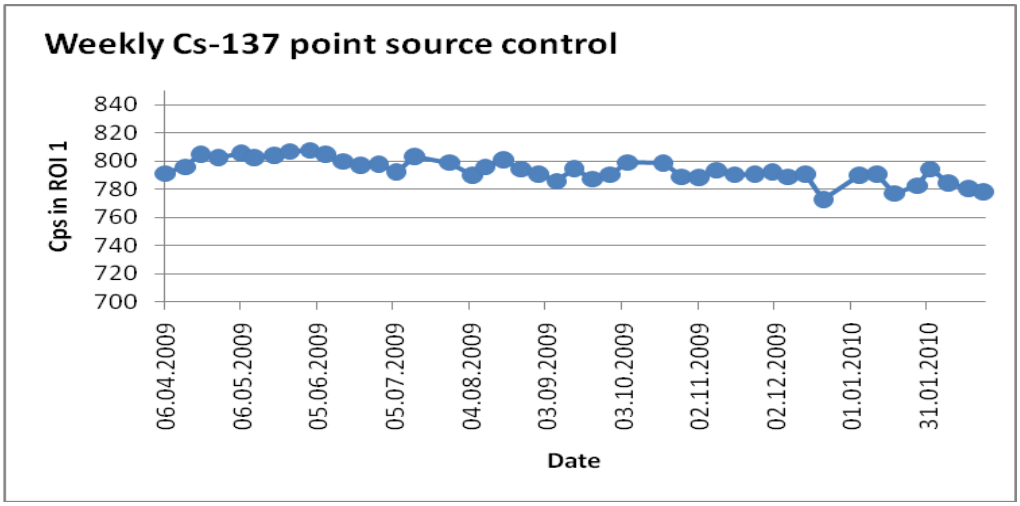


**Appendix III Figure A1: Weekly measurement of Cs-137 activity in point source.**

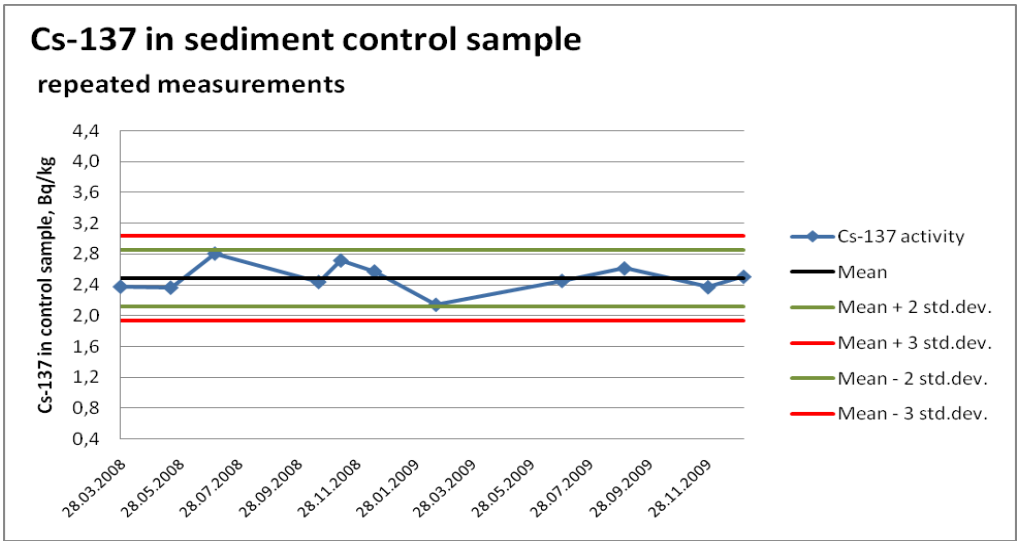


**Appendix III Figure A2: Every second month measurement of Cs-137 in sediment control sample.**

**Appendix III Table A6: External background in Cs-137 peak in sample measuring period.**

| Measuring date | Gross area in ROI 1 | Gross area in ROI 2 | Gross area in ROI 3 | Counting time, sec. | Internal background, cps | External background, cps |
|---|---|---|---|---|---|---|
| 17.02.2009 | 273 | 69 | 73 | 62 124 | 0.0047 | -0.0003 |
| 22.04.2009 | 334 | 94 | 78 | 87 667 | 0.0040 | -0.0002 |
| 25.05.2009 | 1782 | 427 | 479 | 434 212 | 0.0043 | -0.0002 |
| 06.07.2009 | 350 | 85 | 99 | 87 822 | 0.0043 | -0.0003 |
| 04.09.2009 | 379 | 82 | 113 | 90 173 | 0.0044 | -0.0002 |
| 26.11.2009 | 469 | 135 | 113 | 101 025 | 0.0050 | -0.0004 |
| 06.01.2010 | 349 | 82 | 91 | 81 254 | 0.0044 | -0.0001 |

## Appendix III Table A7: Cs-137 geometry factor measured every second month

| Calibration date | Reference date | Activity in the standard, Bq | Uncertainty in standard activity, Bq | Gross area in ROI 1 | Gross area in ROI 2 | Gross area in ROI 3 | Counting time, sec. | Internal background, cps | G, Bq/cps | sG, Bq/cps |
|---|---|---|---|---|---|---|---|---|---|---|
| 23.02.2009 | 01.10.2002 | 66.3 | 2.9 | 625 758 | 3641 | 2858 | 331 823 | 0.04 | **35.9** | **1.6** |
| 23.04.2009 | 01.10.2002 | 66.0 | 2.9 | 163 221 | 925 | 720 | 86 949 | 0.039 | **35.9** | **1.6** |
| 01.07.2009 | 01.10.2002 | 65.7 | 2.9 | 185 461 | 1073 | 819 | 98 573 | 0.039 | **35.7** | **1.6** |
| 02.09.2009 | 01.10.2002 | 65.4 | 2.9 | 341 320 | 1905 | 1521 | 182 749 | 0.038 | **35.8** | **1.6** |
| 01.12.2009 | 01.10.2002 | 65.1 | 2.9 | 139 930 | 769 | 626 | 75 885 | 0.038 | **36** | **1.6** |
| 12.01.2010 | 01.10.2002 | 64.9 | 2.9 | 161 308 | 899 | 660 | 87 579 | 0.036 | **35.9** | **1.6** |

## Appendix III Table A8: Background in Pb-210 peak in sample measuring period.

| Measured background; cps in 45,6 keV | | | | | | |
|---|---|---|---|---|---|---|
| | | | | | | |
| date | net area | + /- | mark peak ch-ch | counting time, sec. | **BK, cps** | uncertainty, cps |
| 17.02.2009 | -14 | 37 | 329-349 | 62 124 | -0.0002 | 0.0006 |
| 25.04.2009 | 230 | 51 | 333-345 | 434 212 | 0.0005 | 0.0001 |
| 22.05.2009 | 28 | 22 | 333-345 | 87 667 | 0.0003 | 0.0003 |
| 03.07.2009 | 54 | 23 | 333-345 | 87 822 | 0.0006 | 0.0003 |
| 04.09.2009 | 13 | 23 | 333-345 | 90 173 | 0.0001 | 0.0003 |
| 26.11.2009 | 110 | 46 | 329-349 | 101 025 | 0.0011 | 0.0005 |
| 06.01.2010 | -11 | 43 | 329-349 | 81 254 | -0.0001 | 0.0005 |
| | | | | | | |
| **=>** | **Mean background in 45.6 keV, cps** | | | | **0.0004** | **+ /- 0.0004** |

## Appendix III Table A9: Pb-210 standard calibration.

| Measured Pb-210 standard; **$R_{cal}$**, cps in 45,6keV | | | | | | |
|---|---|---|---|---|---|---|
| | | | | | | |
| date | net area | + /- | mark peak ch-ch | counting time, sec. | $R_{cal}$, Cps | uncertainty, cps |
| 02.06.2009 | 9713 032 | 3684 | 333-345 | 349 504 | 27.79 | 0.01 |
| 09.12.2009 | 3463 209 | 2015 | 329-349 | 98 118 | 35.30 | 0.02 |
| | | | | | | |
| The cps differs depending on mark peak results : 333-345 or 329 -349 | | | | | | |
| | | | | | | |
| | | **$R_{cal}$, cps** | uncertainty, cps | | | |
| => | roi: 333-345 | **27.80** | 0.01 | | (02.06.09) | |
| => | roi: 329-349 | **35.30** | 0.02 | | (09.12.09) | |
| => | each sample has to be marked with roi | | | | | |

**Appendix III Table A10: Pb-210 activity in standard at calibration date.**

| **Activity in the standard, $A_{std}$** | | | | | | |
|---|---|---|---|---|---|---|
| $A_0$ = | | 7460 | Bq | | | |
| $t_{1/2}$ | | 8145 | days | | | |
| Ref. date | | 01.07.2008 | | | | |
| Uncertainty | | 5 | % | | | |
| | | | | | | |
| Calibration date | Ref. date | days decayed | Activity on counting date, Bq | | uncertainty, Bq | |
| 02.06.2009 | 01.07.2008 | 336 | **7442** | | 362 | roi: 333-345 |
| 09.12.2009 | 01.07.2008 | 526 | **7438** | | 356 | roi: 329-349 |

**Appendix III Table A11: Pb-210 geometry factor, g.**

| **Geometry factor, $g_{Pb-210}$:** | | | | | | |
|---|---|---|---|---|---|---|
| | | | | | | |
| | | **$g_{Pb-210}$, Bq/cps** | | uncertainty, Bq/cps | | |
| => | roi: 333-345 | **267.7** | | 13.0 | | |
| => | roi: 329-349 | **210.7** | | 10.1 | | |

**Appendix III Table A12: Pointsource on top of the Pb-210 standard measured.**

| **Pointsource on top of the Pb-210 standard; $R_{cal+}$** | | | | | | |
|---|---|---|---|---|---|---|
| | | | | | | |
| **date** | net area | + /- | mark peak ch-ch | counting time, sec. | Cps | uncertainty, cps |
| 30.04.2009 | 240 871 | 596 | 333-345 | 600 | 401.5 | 1.0 |
| 26.02.2010 | 306 420 | 641 | 329-349 | 600 | 510.7 | 1.1 |
| | | | | | | |
| The cps differs depending on mark peak results : 333-345 or 329 -349 | | | | | | |
| | | | | | | |
| | | **$R_{cal+}$** | | uncertainty, cps | | |
| => | roi: 333-345 | **401.5** | | 1.0 | | |
| => | roi: 329-349 | **510.7** | | 1.1 | | |

**Appendix III Table A13: Measurement of point source on top of an empty container.**

| **Pointsource on top of an empty container; $R_s$** | | | | | | |
|---|---|---|---|---|---|---|
| | | | | | | |
| **date** | net area | + /- | mark peak ch-ch | counting time, sec. | Cps | uncertainty, cps |
| 14.03.2009 | 443 267 | 788 | 333-345 | 600 | 738.8 | 1.3 |
| 29.04.2009 | 3 794 425 | 2306 | 333-345 | 5120 | 741.1 | 0.5 |
| 29.04.2009 | 450 146 | 791 | 333-345 | 600 | 750.2 | 1.3 |
| 08.12.2009 | 584 216 | 808 | 329-349 | 600 | 973.7 | 1.3 |
| | | | | | | |
| The cps differs depending on mark peak results : 333-345 or 329 -349 | | | | | | |
| | | | | | | |
| | | **$R_s$, cps** | | uncertainty, cps | | |
| => | roi: 333-345 | **741.7** | | 0.5 | | |
| => | roi: 329-349 | **973.7** | | 1.3 | | |
| => | each sample has to be marked with roi | | | | | |

**Appendix III Table A14: Pb-210 geometry factor, G.**

| **Geometry factor, $G_{Pb\text{-}210}$:** | | | | | | |
|---|---|---|---|---|---|---|
| | | | uncertainty | | | |
| roi: 333-345 | **$KF_{Pb\text{-}210}$=** | 1.38 | 0.01 | | | |
| roi: 329-349 | **$KF_{Pb\text{-}210}$=** | 1.40 | 0.01 | | | |
| | | | | | | |
| | | **$G_{Pb\text{-}210}$, Bq/cps** | | uncertainty, Bq/cps | | |
| => | roi: 333-345 | **189.4** | | 9.5 | | |
| => | roi: 329-349 | **144.2** | | 7.3 | | |
| | | | | | | |

**Appendix III Table A15: Background in 295keV, 352keV and 609keV peaks in sample measuring period.**

| Measured background; cps in 295 keV, 352 keV and 609 keV | | | | | | |
|---|---|---|---|---|---|---|
| Date | 295 keV peak, cps | uncertainty | 352 keV peak, cps | uncertainty | 609 keV peak, cps | uncertainty |
| 22.04.2009 | 0.0009 | 0.0007 | 0.0035 | 0.0006 | 0.0033 | 0.0006 |
| 26.11.2009 | 0.0027 | 0.0006 | 0.0025 | 0.0006 | 0.0021 | 0.0005 |
| **Mean value** | **0.0018** | **0.0006** | **0.0030** | **0.0006** | **0.0027** | **0.0006** |

**Appendix III Table A16: Ra-226 activity in standard at calibration date.**

| Nuclide | Activity | Uncertainty | Date |
|---|---|---|---|
| **Ra-226** | **3540 Bq** | **5 %** | **01.07.08 (ref.date)** |
| **Ra-226** | **3539 Bq** | **5%** | **27.10.08** |
| **Ra-226** | **3539 Bq** | **5%** | **05.11.08** |
| **Ra-226** | **3538 Bq** | **5%** | **10.12.09** |
| **Ra-226** | **3537 Bq** | **5%** | **07.04.10** |

**Appendix III Table A17: Ra-226 geometry factors, G295keV, G352keV and G609keV**

| Measuring date | Net area in 609 keV peak | Uncertainty | Net area in 352 keV peak | Uncertainty | Net area in 295 keV keV peak | Uncertainty |
|---|---|---|---|---|---|---|
| 27.10.2008 | 48,2 | 0,1 | 69,6 | 0,1 | 42,2 | 0,1 |
| 05.11.2008 | 48,2 | 0,1 | 69,8 | 0,1 | 41,9 | 0,1 |
| 10.12.2009 | 48,2 | 0,1 | 69,5 | 0,1 | 42,1 | 0,1 |
| 07.04.2010 | 48,3 | 0,1 | 69,5 | 0,1 | 42,1 | 0,1 |
| **G-factor** | **609 keV peak** | **Uncertainty** | **352 keV peak** | **Uncertainty** | **295 keV peak** | **Uncertainty** |
| 27.10.2008 | 73,1 | 3,7 | 50,8 | 2,5 | 83,9 | 4,2 |
| 05.11.2008 | 73,4 | 3,7 | 50,7 | 2,5 | 84,5 | 4,2 |
| 10.12.2009 | 73,4 | 3,7 | 50,9 | 2,5 | 84,0 | 4,2 |
| 07.04.2010 | 73,2 | 3,7 | 50,9 | 2,5 | 84,0 | 4,2 |
| **Mean** | **73,3** | **7,4** | **50,8** | **5,0** | **84,1** | **8,4** |

***APPENDIX IV***

**Appendix IV Table A18: Results on sieving 0-1 cm slice from each sampling site.**

| Sampling site | % clay + silt (< 63 µm) | % sand ( >63 µm <2 mm) | % gravel (> 2 mm) |
|---|---|---|---|
| **L1** | **97,5** | **2,5** | **0,0** |
| **L2** | **96,2** | **3,8** | **0,0** |
| **S1** | **92,0** | **8,0** | **0,0** |
| **S2** | **99,3** | **0,7** | **0,0** |
| **S3** | **90,3** | **9,7** | **0,0** |
| **S4** | **99,4** | **0,6** | **0,0** |

**Appendix IV Table A19: Data and results from Cs-137 measurements on core L1-1.**

| Sample identity | Sampling date | Date of measurement | Sample weight, g | Geometry factor | sG | Gross area in ROI 1 | Gross area in ROI 2 | Gross area in ROI 3 | Counting time, sec. | Cs-137, Bq/kg | Uncertainty, Bq/kg |
|---|---|---|---|---|---|---|---|---|---|---|---|
| | | | | | | | | | | | |
| L1-1 0-1 cm | 03.11.2008 | 20.04.2009 | 34.6 | 35.9 | 1.6 | 2932 | 374 | 407 | 245981 | 5.7 | 0.8 |
| L1-1 1-2 cm | 03.11.2008 | 27.04.2009 | 36.7 | 35.9 | 1.6 | 3247 | 391 | 460 | 258873 | 5.7 | 0.8 |
| L1-1 2-3 cm | 03.11.2008 | 28.04.2009 | 34.4 | 35.9 | 1.6 | 763 | 115 | 141 | 74068 | 3.4 | 1.2 |
| L1-1 3-4 cm | 03.11.2008 | 29.04.2009 | 35.7 | 35.9 | 1.6 | 703 | 107 | 149 | 74857 | < 3.8 | |
| L1-1 4-5 cm | 03.11.2008 | 30.04.2009 | 38.1 | 35.9 | 1.6 | 2856 | 568 | 612 | 348683 | 1.2 | 0.5 |
| L1-1 5-6 cm | 03.11.2008 | 06.05.2009 | 37.0 | 35.9 | 1.6 | 1333 | 278 | 312 | 166805 | < 2.3 | |
| L1-1 6-7 cm | 03.11.2008 | 07.05.2009 | 37.3 | 35.9 | 1.6 | 702 | 158 | 185 | 88688 | < 3.5 | |
| L1-1 7-8 cm | 03.11.2008 | 08.05.2009 | 42.5 | 35.9 | 1.6 | 731 | 172 | 164 | 90242 | < 3.0 | |
| L1-1 8-9 cm | 03.11.2008 | 11.05.2009 | 45.1 | 35.9 | 1.6 | 1919 | 440 | 495 | 252171 | < 1.6 | |
| L1-1 9-10 cm | 03.11.2008 | 12.05.2009 | 43.2 | 35.9 | 1.6 | 589 | 148 | 154 | 80979 | < 2.9 | |
| L1-1 10-11 cm | 03.11.2008 | 13.05.2009 | 47.8 | 35.9 | 1.6 | 627 | 137 | 165 | 84026 | < 2.7 | |
| L1-1 11-12 cm | 03.11.2008 | 14.05.2009 | 41.4 | 35.9 | 1.6 | 559 | 130 | 157 | 84250 | < 3.1 | |

**Appendix IV Table A20: Data and results from Cs-137 measurements on core L1-2.**

| Sample identity | Sampling date | Date of measurement | Sample weight, g | Geometry factor | sG | Gross area in ROI 1 | Gross area in ROI 2 | Gross area in ROI 3 | Counting time, sec. | Cs-137, Bq/kg | Uncertainty, Bq/kg |
|---|---|---|---|---|---|---|---|---|---|---|---|
| L1-2 0-1 cm | 03.11.2008 | 04.11.2009 | 42.0 | 35.8 | 1.6 | 1216 | 125 | 170 | 94248 | 5.7 | 1.0 |
| L1-2 1-2 cm | 03.11.2008 | 06.11.2009 | 47.4 | 35.8 | 1.6 | 1912 | 293 | 328 | 167791 | 2.9 | 0.7 |
| L1-2 2-3 cm | 03.11.2008 | 09.11.2009 | 44.1 | 35.8 | 1.6 | 2226 | 401 | 435 | 250732 | 1.7 | 0.5 |
| L1-2 3-4 cm | 03.11.2008 | 10.11.2009 | 43.0 | 35.8 | 1.6 | 803 | 158 | 182 | 101639 | < 2.7 | |
| L1-2 4-5 cm | 03.11.2008 | 11.11.2009 | 44.9 | 35.8 | 1.6 | 709 | 137 | 155 | 81379 | < 3.0 | |
| L1-2 5-6 cm | 03.11.2008 | 12.11.2009 | 42.8 | 35.8 | 1.6 | 674 | 160 | 143 | 86258 | < 3.0 | |
| L1-2 6-7 cm | 03.11.2008 | 13.11.2009 | 45.4 | 35.8 | 1.6 | 689 | 165 | 148 | 83517 | < 3.0 | |
| L1-2 7-8 cm | 03.11.2008 | 03.11.2009 | 45.7 | 35.8 | 1.6 | 485 | 127 | 127 | 65440 | < 3.5 | |
| L1-2 8-9 cm | 03.11.2008 | 16.11.2009 | 47.2 | 35.8 | 1.6 | 1909 | 416 | 452 | 242163 | < 1.5 | |
| L1-2 9-10 cm | 03.11.2008 | 17.11.2009 | 45.6 | 35.8 | 1.6 | 673 | 133 | 169 | 84918 | < 2.9 | |
| L1-2 10-11 cm | 03.11.2008 | 18.11.2009 | 44.2 | 35.8 | 1.6 | 641 | 148 | 153 | 82518 | < 3.1 | |
| L1-2 11-12 cm | 03.11.2008 | 19.11.2009 | 43.8 | 35.8 | 1.6 | 673 | 125 | 161 | 88001 | < 2.9 | |
| L1-2 12-13 cm | 03.11.2008 | 20.11.2009 | 45.4 | 35.8 | 1.6 | 657 | 155 | 165 | 83986 | < 3.0 | |
| L1-2 13-14 cm | 03.11.2008 | 21.11.2009 | 47.7 | 35.8 | 1.6 | 2755 | 639 | 647 | 339097 | < 1.3 | |
| L1-2 14-15 cm | 03.11.2008 | 25.11.2009 | 48.0 | 35.8 | 1.6 | 627 | 142 | 136 | 84157 | < 2.7 | |

**Appendix IV Table A21: Data and results from Cs-137 measurements on core L2-1.**

| Sample identity | Sampling date | Date of measurement | Sample weight, g | Geometry factor | sG | Gross area in ROI 1 | Gross area in ROI 2 | Gross area in ROI 3 | Counting time, sec. | Cs-137, Bq/kg | Uncertainty, Bq/kg |
|---|---|---|---|---|---|---|---|---|---|---|---|
| L2-1 0-1 cm | 03.11.2008 | 21.04.2009 | 42.7 | 35.9 | 1.6 | 1188 | 137 | 132 | 80659 | 6.7 | 1.2 |
| L2-1 1-2 cm | 03.11.2008 | 10.06.2009 | 43.5 | 35.9 | 1.6 | 1289 | 155 | 162 | 81857 | 6.5 | 1.2 |
| L2-1 2-3 cm | 03.11.2008 | 11.06.2009 | 44.8 | 35.9 | 1.6 | 1063 | 130 | 156 | 81671 | 4.7 | 1.0 |
| L2-1 3-4 cm | 03.11.2008 | 12.06.2009 | 45.1 | 35.9 | 1.6 | 1099 | 138 | 155 | 84126 | 4.8 | 1.0 |
| L2-1 4-5 cm | 03.11.2008 | 13.06.2009 | 49.6 | 35.9 | 1.6 | 1527 | 189 | 219 | 107251 | 4.7 | 0.9 |
| L2-1 5-6 cm | 03.11.2008 | 15.06.2009 | 46.4 | 35.9 | 1.6 | 1817 | 255 | 292 | 154974 | 3.5 | 0.7 |
| L2-1 6-7 cm | 03.11.2008 | 16.06.2009 | 49.9 | 35.9 | 1.6 | 1026 | 182 | 217 | 101024 | < 2.4 | |
| L2-1 7-8 cm | 03.11.2008 | 17.06.2009 | 49.7 | 35.9 | 1.6 | 672 | 140 | 145 | 66798 | < 3.2 | |
| L2-1 8-9 cm | 03.11.2008 | 18.06.2009 | 49.1 | 35.9 | 1.6 | 893 | 142 | 167 | 86055 | < 2.6 | |
| L2-1 9-10 cm | 03.11.2008 | 19.06.2009 | 49.1 | 35.9 | 1.6 | 741 | 144 | 168 | 84405 | < 2.7 | |
| L2-1 10-11 cm | 03.11.2008 | 22.06.2009 | 51.6 | 35.9 | 1.6 | 2236 | 423 | 500 | 256847 | < 1.3 | |
| L2-1 11-12 cm | 03.11.2008 | 23.06.2009 | 52.8 | 35.9 | 1.6 | 697 | 139 | 165 | 83581 | < 2.5 | |
| L2-1 12-13 cm | 03.11.2008 | 25.06.2009 | 49.0 | 35.9 | 1.6 | 498 | 102 | 124 | 67315 | < 3.0 | |

**Appendix IV Table A22: Data and results from Cs-137 measurements on core L2-2.**

| Sample identity | Sampling date | Date of measurement | Sample weight, g | Geometry factor | sG | Gross area in ROI 1 | Gross area in ROI 2 | Gross area in ROI 3 | Counting time, sec. | Cs-137, Bq/kg | Uncertainty, Bq/kg |
|---|---|---|---|---|---|---|---|---|---|---|---|
| L2-2 0-1 cm | 03.11.2008 | 15.05.2009 | 50.2 | 35.9 | 1.6 | 1246 | 134 | 178 | 87572 | 5.0 | 0.9 |
| L2-2 1-2 cm | 03.11.2008 | 19.05.2009 | 48.6 | 35.9 | 1.6 | 1123 | 147 | 147 | 82279 | 4.7 | 1.0 |
| L2-2 2-3 cm | 03.11.2008 | 20.05.2009 | 51.1 | 35.9 | 1.6 | 1104 | 132 | 179 | 90314 | 3.7 | 0.8 |
| L2-2 3-4 cm | 03.11.2008 | 26.05.2009 | 49.9 | 35.9 | 1.6 | 770 | 154 | 158 | 78798 | < 2.8 | |
| L2-2 4-5 cm | 03.11.2008 | 28.05.2009 | 49.6 | 35.9 | 1.6 | 1037 | 141 | 228 | 92445 | 2.2 | 0.8 |
| L2-2 5-6 cm | 03.11.2008 | 29.05.2009 | 49.6 | 35.9 | 1.6 | 606 | 127 | 139 | 71836 | < 2.9 | |
| L2-2 6-7 cm | 03.11.2008 | 03.06.2009 | 55.8 | 35.9 | 1.6 | 649 | 135 | 144 | 72587 | < 2.6 | |
| L2-2 7-8 cm | 03.11.2008 | 04.06.2009 | 48.4 | 35.9 | 1.6 | 849 | 184 | 231 | 102055 | < 2.5 | |
| L2-2 8-9 cm | 03.11.2008 | 08.06.2009 | 48.6 | 35.9 | 1.6 | 2704 | 550 | 626 | 329124 | < 1.2 | |
| L2-2 9-10 cm | 03.11.2008 | 09.06.2009 | 51.9 | 35.9 | 1.6 | 757 | 153 | 189 | 87760 | < 2.5 | |

**Appendix IV Table A23: Data and results from Cs-137 measurements on core S1-1.**

| Sample identity | Sampling date | Date of measurement | Sample weight, g | Geometry factor | sG | Gross area in ROI 1 | Gross area in ROI 2 | Gross area in ROI 3 | Counting time, sec. | Cs-137, Bq/kg | Uncertainty, Bq/kg |
|---|---|---|---|---|---|---|---|---|---|---|---|
| S1-1 0-1 cm | 20.11.2007 | 28.07.2009 | 50.0 | 35.7 | 1.6 | 803 | 34 | 38 | 17416 | 27.9 | 3.6 |
| S1-1 1-2 cm | 20.11.2007 | 07.08.2009 | 42.3 | 35.7 | 1.6 | 522 | 22 | 13 | 12411 | 31.8 | 4.5 |
| S1-1 2-3 cm | 20.11.2007 | 11.08.2009 | 41.5 | 35.7 | 1.6 | 2906 | 130 | 152 | 83800 | 24.8 | 2.5 |
| S1-1 3-4 cm | 20.11.2007 | 12.08.2009 | 45.0 | 35.7 | 1.6 | 2391 | 132 | 160 | 80523 | 18.4 | 2.0 |
| S1-1 4-5 cm | 20.11.2007 | 13.08.2009 | 42.3 | 35.7 | 1.6 | 3092 | 153 | 199 | 88609 | 23.5 | 2.4 |
| S1-1 5-6 cm | 20.11.2007 | 14.08.2009 | 39.6 | 35.7 | 1.6 | 2888 | 135 | 185 | 93698 | 22.3 | 2.3 |
| S1-1 6-7 cm | 20.11.2007 | 19.08.2009 | 41.8 | 35.7 | 1.6 | 1545 | 151 | 177 | 90182 | 8.6 | 1.3 |
| S1-1 7-8 cm | 20.11.2007 | 20.08.2009 | 41.0 | 35.7 | 1.6 | 1017 | 116 | 150 | 80859 | 5.3 | 1.1 |
| S1-1 8-9 cm | 20.11.2007 | 21.08.2009 | 42.6 | 35.7 | 1.6 | 934 | 155 | 183 | 88118 | 2.4 | 0.9 |
| S1-1 9-10 cm | 20.11.2007 | 28.07.2009 | 45.0 | 35.7 | 1.6 | 795 | 141 | 127 | 74240 | 2.7 | 1.0 |
| S1-1 10-11 cm | 20.11.2007 | 05.08.2009 | 47.2 | 35.7 | 1.6 | 6418 | 1241 | 1337 | 674888 | 1.3 | 0.3 |
| S1-1 11-12 cm | 20.11.2007 | 06.08.2009 | 48.2 | 35.7 | 1.6 | 642 | 151 | 163 | 81850 | < 2.9 | |
| S1-1 12-13 cm | 20.11.2007 | 07.08.2009 | 48.6 | 35.7 | 1.6 | 564 | 133 | 143 | 71040 | < 3.1 | |
| S1-1 13-14 cm | 20.11.2007 | 10.08.2009 | 45.0 | 35.7 | 1.6 | 1678 | 383 | 496 | 242765 | < 1.7 | |
| S1-1 14-15 cm | 20.11.2007 | 18.08.2009 | 49.0 | 35.7 | 1.6 | 641 | 159 | 187 | 83599 | < 2.9 | |
| S1-1 15-16 cm | 20.11.2007 | 17.08.2009 | 46.8 | 35.7 | 1.6 | 1785 | 441 | 508 | 246471 | < 1.6 | |

**Appendix IV Table A24: Data and results from Cs-137 measurements on core S1-2.**

| Sample identity | Sampling date | Date of measurement | Sample weight, g | Geometry factor | sG | Gross area in ROI 1 | Gross area in ROI 2 | Gross area in ROI 3 | Counting time, sec. | Cs-137, Bq/kg | Uncertainty, Bq/kg |
|---|---|---|---|---|---|---|---|---|---|---|---|
| S1-2 0-1cm | 20.11.2007 | 08.10.2009 | 34.1 | 35.8 | 1.6 | 3398 | 147 | 141 | 84868 | 36.2 | 3.5 |
| S1-2 1-2cm | 20.11.2007 | 09.10.2009 | 39.3 | 35.8 | 1.6 | 3473 | 158 | 164 | 86209 | 31.0 | 3.0 |
| S1-2 2-3cm | 20.11.2007 | 15.10.2009 | 40.5 | 35.8 | 1.6 | 18752 | 831 | 952 | 519578 | 26.8 | 2.4 |
| S1-2 3-4cm | 20.11.2007 | 16.10.2009 | 33.8 | 35.8 | 1.6 | 2231 | 148 | 141 | 86632 | 20.9 | 2.3 |
| S1-2 4-5cm | 20.11.2007 | 19.10.2009 | 35.7 | 35.8 | 1.6 | 8179 | 411 | 496 | 272311 | 24.3 | 2.2 |
| S1-2 5-6cm | 20.11.2007 | 20.10.2009 | 29.9 | 35.8 | 1.6 | 1559 | 138 | 128 | 81232 | 15.6 | 2.0 |
| S1-2 6-7cm | 20.11.2007 | 21.10.2009 | 33.8 | 35.8 | 1.6 | 1279 | 100 | 134 | 67770 | 13.0 | 1.9 |
| S1-2 7-8cm | 20.11.2007 | 22.10.2009 | 34.8 | 35.8 | 1.6 | 1187 | 147 | 167 | 89023 | 6.6 | 1.3 |
| S1-2 8-9cm | 20.11.2007 | 23.10.2009 | 36.2 | 35.8 | 1.6 | 922 | 135 | 126 | 73433 | 5.4 | 1.3 |
| S1-2 9-10cm | 20.11.2007 | 26.10.2009 | 37.2 | 35.8 | 1.6 | 2538 | 403 | 470 | 255994 | 2.9 | 0.6 |
| S1-2 10-11cm | 20.11.2007 | 27.10.2009 | 36.3 | 35.8 | 1.6 | 841 | 146 | 143 | 90313 | 2.8 | 1.0 |
| S1-2 11-12cm | 20.11.2007 | 28.10.2009 | 41.1 | 35.8 | 1.6 | 650 | 142 | 133 | 84009 | < 3.1 | |
| S1-2 12-13cm | 20.11.2007 | 29.10.2009 | 39.5 | 35.8 | 1.6 | 622 | 137 | 151 | 86575 | < 3.2 | |
| S1-2 13-14cm | 20.11.2007 | 30.10.2009 | 39.5 | 35.8 | 1.6 | 570 | 133 | 151 | 85072 | < 3.3 | |
| S1-2 14-15cm | 20.11.2007 | 02.11.2009 | 41.3 | 35.8 | 1.6 | 1863 | 447 | 495 | 272196 | < 1.7 | |

**Appendix IV Table A25: Data and results from Cs-137 measurements on core S1-3.**

| Sample identity | Sampling date | Date of measurement | Sample weight, g | Geometry factor | sG | Gross area in ROI 1 | Gross area in ROI 2 | Gross area in ROI 3 | Counting time, sec. | Cs-137, Bq/kg | Uncertainty, Bq/kg |
|---|---|---|---|---|---|---|---|---|---|---|---|
| S1-3 0-1cm | 20.11.2007 | 17.04.2009 | 38.8 | 35.9 | 1.6 | 3121 | 156 | 124 | 76302 | 31.9 | 3.2 |
| S1-3 1-2cm | 20.11.2007 | 23.02.2010 | 32.4 | 35.8 | 1.6 | 2854 | 157 | 149 | 84489 | 30.6 | 3.1 |
| S1-3 2-3cm | 20.11.2007 | 25.02.2010 | 36.1 | 35.9 | 1.6 | 6874 | 278 | 300 | 171372 | 34.7 | 3.1 |
| S1-3 3-4cm | 20.11.2007 | 26.02.2010 | 35.8 | 35.9 | 1.6 | 2850 | 109 | 146 | 81151 | 30.3 | 3.0 |
| S1-3 4-5cm | 20.11.2007 | 01.03.2010 | 33.2 | 35.9 | 1.6 | 7801 | 399 | 476 | 251380 | 27.2 | 2.5 |
| S1-3 5-6cm | 20.11.2007 | 02.03.2010 | 32.2 | 35.9 | 1.6 | 2403 | 112 | 146 | 79277 | 27.8 | 2.9 |
| S1-3 6-7cm | 20.11.2007 | 03.03.2010 | 35.3 | 35.9 | 1.6 | 3239 | 166 | 198 | 109959 | 24.3 | 2.4 |
| S1-3 7-8cm | 20.11.2007 | 04.03.2010 | 36.8 | 35.9 | 1.6 | 3579 | 744 | 656 | 77067 | 9.5 | 2.6 |
| S1-3 8-9cm | 20.11.2007 | 05.03.2010 | 33.1 | 35.9 | 1.6 | 1149 | 107 | 128 | 76207 | 10.0 | 1.6 |
| S1-3 9-10cm | 20.11.2007 | 08.03.2010 | 40.1 | 35.9 | 1.6 | 2823 | 429 | 481 | 268255 | 3.4 | 0.6 |
| S1-3 10-11cm | 20.11.2007 | 09.03.2010 | 38.1 | 35.9 | 1.6 | 880 | 135 | 133 | 80850 | 4.1 | 1.1 |
| S1-3 11-12cm | 20.11.2007 | 10.03.2010 | 38.5 | 35.9 | 1.6 | 624 | 153 | 182 | 90468 | < 3.5 | |
| S1-3 12-13cm | 20.11.2007 | 11.03.2010 | 35.0 | 35.9 | 1.6 | 587 | 129 | 156 | 85929 | < 3.7 | |
| S1-3 13-14cm | 20.11.2007 | 12.03.2010 | 33.9 | 35.9 | 1.6 | 476 | 110 | 129 | 69883 | < 4.4 | |

**Appendix IV Table A26: Data and results from Cs-137 measurements on core S3-1.**

| Sample identity | Sampling date | Date of measurement | Sample weight, g | Geometry factor | sG | Gross area in ROI 1 | Gross area in ROI 2 | Gross area in ROI 3 | Counting time, sec. | Cs-137, Bq/kg | Uncertainty, Bq/kg |
|---|---|---|---|---|---|---|---|---|---|---|---|
| S3-1 0-1 cm | 23.11.2008 | 16.01.2009 | 49.2 | 35.5 | 1.6 | 11125 | 369 | 424 | 193821 | 35.5 | 3.3 |
| S3-1 1-2 cm | 23.11.2008 | 19.01.2009 | 30.1 | 35.5 | 1.6 | 2343 | 119 | 130 | 70594 | 30.1 | 3.4 |
| S3-1 2-3 cm | 23.11.2008 | 20.01.2009 | 45.2 | 35.5 | 1.6 | 3444 | 182 | 163 | 87360 | 24.0 | 2.5 |
| S3-1 3-4 cm | 23.11.2008 | 23.01.2009 | 45.1 | 35.5 | 1.6 | 2542 | 463 | 504 | 249091 | 2.6 | 0.5 |
| S3-1 4-5 cm | 23.11.2008 | 27.01.2009 | 44.8 | 35.5 | 1.6 | 926 | 148 | 164 | 82950 | 2.8 | 0.9 |
| S3-1 5-6 cm | 23.11.2008 | 29.01.2009 | 49.3 | 35.5 | 1.6 | 675 | 133 | 115 | 68467 | < 2.9 | |
| S3-1 6-7 cm | 23.11.2008 | 30.01.2009 | 40.4 | 35.5 | 1.6 | 780 | 154 | 171 | 86919 | < 3.3 | |

**Appendix IV Table A27: Data and results from Cs-137 measurements on core S3-2.**

| Sample identity | Sampling date | Date of measurement | Sample weight, g | Geometry factor | sG | Gross area in ROI 1 | Gross area in ROI 2 | Gross area in ROI 3 | Counting time, sec. | Cs-137, Bq/kg | Uncertainty, Bq/kg |
|---|---|---|---|---|---|---|---|---|---|---|---|
| S3-2 0-1 cm | 23.11.2008 | 02.02.2009 | 40.1 | 35.5 | 1.6 | 11837 | 474 | 499 | 263308 | 33.2 | 3.1 |
| S3-2 1-2 cm | 23.11.2008 | 05.05.2009 | 38.4 | 35.5 | 1.6 | 5981 | 323 | 351 | 176573 | 24.3 | 2.4 |
| S3-2 2-3 cm | 23.11.2008 | 06.02.2009 | 43.8 | 35.5 | 1.6 | 2538 | 153 | 173 | 85231 | 17.9 | 2.0 |
| S3-2 3-4 cm | 23.11.2008 | 09.02.2009 | 41.2 | 35.5 | 1.6 | 5267 | 479 | 483 | 244387 | 11.7 | 1.2 |
| S3-2 4-5 cm | 23.11.2008 | 10.02.2009 | 47.0 | 35.5 | 1.6 | 1701 | 182 | 176 | 97031 | 7.6 | 1.1 |
| S3-2 5-6 cm | 23.11.2008 | 11.02.2009 | 40.1 | 35.5 | 1.6 | 874 | 126 | 164 | 80973 | < 3.3 | |

**Appendix IV Table A28: Data and results from Cs-137 measurements on core S2-1.**

| Sample identity | Sampling date | Date of measurement | Sample weight, g | Geometry factor | sG | Gross area in ROI 1 | Gross area in ROI 2 | Gross area in ROI 3 | Counting time, sec. | Cs-137, Bq/kg | Uncertainty, Bq/kg |
|---|---|---|---|---|---|---|---|---|---|---|---|
| S2-1 0-1cm | 18.11.2007 | 06.03.2009 | 42.8 | 35.9 | 1.6 | 2673 | 24 | 27 | 8920 | 241.6 | 24.7 |
| S2-1 1-2cm | 18.11.2007 | 09.03.2009 | 42.0 | 35.9 | 1.6 | 2672 | 19 | 29 | 9164 | 253.5 | 23.6 |
| S2-1 2-3cm | 18.11.2007 | 10.03.2009 | 43.2 | 35.9 | 1.6 | 6621 | 55 | 54 | 18481 | 296.1 | 26.7 |
| S2-1 3-4cm | 18.11.2007 | 10.03.2009 | 44.3 | 35.9 | 1.6 | 3411 | 28 | 27 | 9887 | 286.5 | 26.0 |
| S2-1 4-5cm | 18.11.2007 | 10.03.2009 | 45.6 | 35.9 | 1.6 | 3721 | 14 | 27 | 10037 | 291.1 | 27.2 |
| S2-1 5-6cm | 18.11.2007 | 11.03.2009 | 45.9 | 35.9 | 1.6 | 2243 | 16 | 13 | 6508 | 274.2 | 26.1 |
| S2-1 6-7cm | 18.11.2007 | 11.03.2009 | 44.2 | 35.9 | 1.6 | 1325 | 25 | 12 | 5000 | 207.4 | 22.0 |
| S2-1 7-8cm | 18.11.2007 | 12.03.2008 | 48.9 | 35.9 | 1.6 | 1463 | 34 | 26 | 8956 | 113.8 | 11.9 |
| S2-1 8-9cm | 18.11.2007 | 13.03.2009 | 47.6 | 35.9 | 1.6 | 6745 | 193 | 203 | 68271 | 69.3 | 6.2 |
| S2-1 9-10cm | 18.11.2007 | 13.03.2009 | 46.8 | 35.9 | 1.6 | 1002 | 37 | 55 | 14582 | 43.6 | 5.5 |
| S2-1 10-11cm | 18.11.2007 | 16.03.2009 | 48.5 | 35.9 | 1.6 | 8950 | 584 | 712 | 238626 | 20.0 | 1.9 |
| S2-1 11-12cm | 18.11.2007 | 17.03.2009 | 49.0 | 35.9 | 1.6 | 1753 | 173 | 203 | 66930 | 12.1 | 1.6 |
| S2-1 12-13cm | 18.11.2007 | 19.03.2009 | 47.5 | 35.9 | 1.6 | 1060 | 163 | 186 | 64715 | 4.1 | 1.2 |
| S2-1 13-14cm | 18.11.2007 | 12.03.2009 | 48.3 | 35.9 | 1.6 | 889 | 156 | 192 | 64860 | < 6.9 | 1.1 |
| S2-1 14-15cm | 18.11.2007 | 11.03.2009 | 47.0 | 35.9 | 1.6 | 876 | 181 | 169 | 66882 | < 2.8 | 1.1 |

**Appendix IV Table A29: Data and results from Cs-137 measurements on core S2-2.**

| Sample identity | Sampling date | Date of measurement | Sample weight, g | Geometry factor | sG | Gross area in ROI 1 | Gross area in ROI 2 | Gross area in ROI 3 | Counting time, sec. | Cs-137, Bq/kg | Uncertainty, Bq/kg |
|---|---|---|---|---|---|---|---|---|---|---|---|
| S2-2 0-1cm | 18.11.2007 | 24.06.2009 | 38.3 | 35.9 | 1.6 | 30382 | 201 | 170 | 87994 | 327.2 | 28.4 |
| S2-2 1-2cm | 18.11.2007 | 24.06.2009 | 39.1 | 35.9 | 1.6 | 5196 | 38 | 36 | 14502 | 331.2 | 30.0 |
| S2-2 2-3cm | 18.11.2007 | 25.06.2009 | 40.8 | 35.9 | 1.6 | 4976 | 36 | 23 | 14021 | 315.9 | 28.6 |
| S2-2 3-4cm | 18.11.2007 | 06.07.2009 | 41.9 | 35.7 | 1.6 | 86168 | 710 | 641 | 257725 | 286.1 | 24.8 |
| S2-2 4-5cm | 18.11.2007 | 07.07.2009 | 38.6 | 35.7 | 1.6 | 19178 | 183 | 201 | 80479 | 219.3 | 19.2 |
| S2-2 5-6cm | 18.11.2007 | 08.07.2009 | 43.8 | 35.7 | 1.6 | 17563 | 221 | 265 | 85883 | 163.2 | 14.3 |
| S2-2 6-7cm | 18.11.2007 | 09.07.2009 | 39.6 | 35.7 | 1.6 | 11148 | 186 | 213 | 86406 | 111.9 | 9.9 |
| S2-2 7-8cm | 18.11.2007 | 10.07.2009 | 41.8 | 35.7 | 1.6 | 5849 | 192 | 203 | 85360 | 52.3 | 4.8 |
| S2-2 8-9cm | 18.11.2007 | 13.07.2009 | 39.2 | 35.7 | 1.6 | 13238 | 626 | 645 | 259157 | 38.8 | 3.5 |
| S2-2 9-10cm | 18.11.2007 | 14.07.2009 | 42.5 | 35.7 | 1.6 | 3461 | 202 | 226 | 87889 | 25.6 | 2.6 |
| S2-2 10-11cm | 18.11.2007 | 15.07.2009 | 46.1 | 35.7 | 1.6 | 2669 | 234 | 254 | 93160 | 14.4 | 1.7 |
| S2-2 11-12cm | 18.11.2007 | 16.07.2009 | 44.4 | 35.7 | 1.6 | 2185 | 180 | 200 | 79272 | 14.8 | 1.8 |
| S2-2 12-13cm | 18.11.2007 | 17.07.2009 | 44.1 | 35.7 | 1.6 | 1603 | 197 | 240 | 83127 | 7.2 | 1.3 |
| S2-2 13-14cm | 18.11.2007 | 27.07.2009 | 47.8 | 35.7 | 1.6 | 12131 | 2204 | 2484 | 869884 | 2.2 | 0.4 |
| S2-2 14-15cm | 18.11.2007 | 29.06.2009 | 41.2 | 35.9 | 1.6 | 2863 | 575 | 647 | 247286 | < 2.0 | |
| S2-2 15-16cm | 18.11.2007 | 26.06.2009 | 44.6 | 35.9 | 1.6 | 1089 | 191 | 240 | 80053 | < 3.6 | |

**Appendix IV Table A30: Data and results from Cs-137 measurements on core S2-3.**

| Sample identity | Sampling date | Date of measurement | Sample weight, g | Geometry factor | sG | Gross area in ROI 1 | Gross area in ROI 2 | Gross area in ROI 3 | Counting time, sec. | Cs-137, Bq/kg | Uncertainty, Bq/kg |
|---|---|---|---|---|---|---|---|---|---|---|---|
| S2-3 0-1 cm | 18.11.2007 | 16.03.2009 | 43.4 | 35.9 | 1.6 | 4801 | 34 | 40 | 14838 | 267.1 | 24.4 |
| S2-3 1-2 cm | 18.11.2007 | 18.03.2009 | 46.8 | 35.9 | 1.6 | 25899 | 232 | 212 | 86718 | 227.8 | 19.9 |
| S2-3 2-3 cm | 18.11.2007 | 18.03.2009 | 44.9 | 35.9 | 1.6 | 4584 | 59 | 43 | 19926 | 180.9 | 16.6 |
| S2-3 3-4 cm | 18.11.2007 | 31.01.2009 | 46.5 | 35.9 | 1.6 | 1421 | 22 | 7 | 7738 | 139.6 | 14.4 |
| S2-3 4-5 cm | 18.11.2007 | 02.04.2009 | 48.3 | 35.9 | 1.6 | 16449 | 256 | 282 | 104090 | 113.0 | 10.0 |
| S2-3 5-6 cm | 18.11.2007 | 20.03.2009 | 46.5 | 35.9 | 1.6 | 9825 | 218 | 239 | 90208 | 78.4 | 7.0 |
| S2-3 6-7 cm | 18.11.2007 | 31.03.2009 | 46.1 | 35.9 | 1.6 | 32712 | 1345 | 1421 | 527075 | 41.2 | 3.6 |
| S2-3 7-8 cm | 18.11.2007 | 20.03.2009 | 50.2 | 35.9 | 1.6 | 542 | 33 | 35 | 11407 | 26.0 | 4.3 |
| S2-3 8-9 cm | 18.11.2007 | 25.03.2009 | 48.4 | 35.9 | 1.6 | 10629 | 1050 | 1219 | 415845 | 11.0 | 1.1 |
| S2-3 9-10 cm | 18.11.2007 | 07.04.2009 | 45.6 | 35.9 | 1.6 | 1705 | 216 | 241 | 83534 | 7.5 | 1.3 |
| S2-3 10-11 cm | 18.11.2007 | 14.04.2009 | 47.3 | 35.9 | 1.6 | 10370 | 1409 | 1666 | 590590 | 5.4 | 0.6 |
| S2-3 11-12 cm | 18.11.2007 | 01.04.2009 | 48.3 | 35.9 | 1.6 | 1103 | 179 | 204 | 67295 | < 3.8 | 1.2 |

**Appendix IV Table A31: Data and results from Cs-137 measurements on core S4-1.**

| Sample identity | Sampling date | Date of measurement | Sample weight, g | Geometry factor | sG | Gross area in ROI 1 | Gross area in ROI 2 | Gross area in ROI 3 | Counting time, sec. | Cs-137, Bq/kg | Uncertainty, Bq/kg |
|---|---|---|---|---|---|---|---|---|---|---|---|
| S4-1 0-1 cm | 18.11.2007 | 25.02.2009 | 44.4 | 35.9 | 1.6 | 6577 | 38 | 47 | 16273 | 327.4 | 29.5 |
| S4-1 1-2 cm | 18.11.2007 | 27.02.2009 | 45.0 | 35.9 | 1.6 | 23686 | 200 | 177 | 68404 | 275.1 | 24.1 |
| S4-1 2-3 cm | 18.11.2007 | 02.03.2009 | 45.0 | 35.9 | 1.6 | 52313 | 597 | 647 | 241839 | 169.0 | 14.7 |
| S4-1 3-4 cm | 18.11.2007 | 02.03.2009 | 47.4 | 35.9 | 1.6 | 1450 | 40 | 48 | 15850 | 62.5 | 6.8 |
| S4-1 4-5 cm | 18.11.2007 | 03.03.2009 | 45.2 | 35.9 | 1.6 | 2673 | 188 | 190 | 66751 | 23.3 | 2.5 |
| S4-1 5-6 cm | 18.11.2007 | 06.03.2009 | 46.0 | 35.9 | 1.6 | 7407 | 690 | 743 | 258444 | 13.9 | 1.4 |
| S4-1 6-7 cm | 18.11.2007 | 09.03.2009 | 49.0 | 35.9 | 1.6 | 7240 | 678 | 763 | 249580 | 13.0 | 1.3 |
| S4-1 7-8 cm | 18.11.2007 | 10.03.2009 | 47.4 | 35.9 | 1.6 | 4030 | 183 | 207 | 66748 | 37.8 | 3.7 |

**Appendix IV Table A32: Data and results from Cs-137 measurements on core S4-2.**

| Sample identity | Sampling date | Date of measurement | Sample weight, g | Geometry factor | sG | Gross area in ROI 1 | Gross area in ROI 2 | Gross area in ROI 3 | Counting time, sec. | Cs-137, Bq/kg | Uncertainty, Bq/kg |
|---|---|---|---|---|---|---|---|---|---|---|---|
| S4-2 0-1 cm | 18.11.2007 | 12.02.2009 | 41.4 | 35.5 | 1.6 | 35340 | 241 | 256 | 100907 | 299.9 | 26.5 |
| S4-2 1-2 cm | 18.11.2007 | 13.02.2009 | 46.7 | 35.5 | 1.6 | 22315 | 170 | 169 | 58060 | 293.8 | 25.8 |
| S4-2 2-3 cm | 18.11.2007 | 13.02.2009 | 46.6 | 35.5 | 1.6 | 4471 | 61 | 71 | 22130 | 150.2 | 13.9 |
| S4-2 3-4 cm | 18.11.2007 | 16.02.2009 | 44.0 | 35.5 | 1.6 | 3631 | 65 | 50 | 21727 | 128.6 | 12.3 |
| S4-2 4-5 cm | 18.11.2007 | 18.02.2009 | 48.3 | 35.5 | 1.6 | 5051 | 216 | 247 | 86090 | 36.8 | 3.5 |
| S4-2 5-6 cm | 18.11.2007 | 19.02.2009 | 47.8 | 35.5 | 1.6 | 1583 | 59 | 69 | 23023 | 44.8 | 4.9 |
| S4-2 6-7 cm | 18.11.2007 | 24.02.2009 | 52.1 | 35.9 | 1.6 | 2277 | 195 | 208 | 78115 | 13.0 | 1.6 |
| S4-2 7-8 cm | 18.11.2007 | 25.02.2009 | 49.6 | 35.9 | 1.6 | 3303 | 209 | 274 | 85345 | 20.6 | 2.1 |
| S4-2 8-9 cm | 18.11.2007 | 26.02.2009 | 47.7 | 35.9 | 1.6 | 6593 | 203 | 250 | 83846 | 51.3 | 4.8 |

***APPENDIX V***

**Appendix V Table A33: Data and results from Pb-210 measurements on core L1-1.**

| Sample | | | | Measuring sample | | | | Measuring sample with Pb-210 point source on top | | | Results | |
|---|---|---|---|---|---|---|---|---|---|---|---|---|
| Sample identity | Sampling date | Date of measurement | Sample weight, kg | Mark peak ch | Net counts in 46,5keV roi | s (net counts in 46,5keV roi) | Counting time, sec. | Net counts in 46,5keV roi | Counting time, sec. | Correction factor | Pb-210 activity, Bq/kg (d.w.) | uncertainty |
| L1-1 0-1cm | 3.11.08 | 20.4.09 | 0.0346 | 333-345 | 8630 | 120 | 245981 | 248316 | 600 | 1.32 | 260.1 | 13.3 |
| L1-1 1-2cm | 3.11.08 | 27.4.09 | 0.0367 | 333-345 | 9051 | 124 | 258873 | 238701 | 600 | 1.34 | 248.9 | 12.7 |
| L1-1 2-3cm | 3.11.08 | 29.4.09 | 0.0344 | 333-345 | 1884 | 58 | 74068 | 245480 | 600 | 1.33 | 189.9 | 11.1 |
| L1-1 3-4cm | 3.11.08 | 30.4.09 | 0.0356 | 333-345 | 1337 | 51 | 74857 | 241989 | 600 | 1.34 | 128.8 | 8.1 |
| L1-1 4-5cm | 3.11.08 | 4.5.09 | 0.0381 | 333-345 | 4633 | 102 | 348683 | 229655 | 600 | 1.37 | 91.0 | 4.9 |
| L1-1 5-6cm | 3.11.08 | 6.5.09 | 0.0370 | 333-345 | 1733 | 65 | 166805 | 233480 | 600 | 1.36 | 72.1 | 4.5 |
| L1-1 6-7cm | 3.11.08 | 7.5.09 | 0.0373 | 333-345 | 611 | 45 | 88688 | 235247 | 600 | 1.35 | 46.3 | 4.3 |
| L1-1 7-8cm | 3.11.08 | 8.5.09 | 0.0425 | 333-345 | 563 | 44 | 90242 | 218926 | 600 | 1.40 | 37.8 | 3.7 |
| L1-1 8-9cm | 3.11.08 | 11.5.09 | 0.0451 | 333-345 | 1739 | 72 | 252171 | 210089 | 600 | 1.42 | 40.3 | 2.7 |
| L1-1 9-10cm | 3.11.08 | 12.5.09 | 0.0432 | 333-345 | 373 | 40 | 80979 | 214527 | 600 | 1.41 | 27.0 | 3.5 |
| L1-1 10-11cm | 3.11.08 | 13.5.09 | 0.0478 | 333-345 | 478 | 41 | 84026 | 196373 | 600 | 1.46 | 31.9 | 3.3 |
| L1-1 11-12cm | 3.11.08 | 14.5.09 | 0.0414 | 333-345 | 368 | 39 | 84250 | 216938 | 600 | 1.40 | 26.5 | 3.4 |

**Appendix V Table A34: Data and results from Pb-210 measurements on core L1-2.**

| Sample | | | | Measuring sample | | | | Measuring sample with Pb-210 point source on top | | | Results | |
|---|---|---|---|---|---|---|---|---|---|---|---|---|
| Sample identity | Sampling date | Date of measurement | Sample weight, kg | Mark peak ch | Net counts in 46,5keV roi | s(net counts in 46,5keV roi) | Counting time, sec. | Net counts in 46,5keV roi | Counting time, sec. | Correction factor | Pb-210 activity, Bq/kg (d.w.) | uncertainty |
| L1-2 0-1cm | 3.11.08 | 4.11.09 | 0.042 | 329-349 | 5328 | 98 | 94248 | 288862 | 600 | 1.39 | 288.9 | 14.7 |
| L1-2 1-2cm | 3.11.08 | 6.11.09 | 0.0474 | 329-349 | 5899 | 119 | 167791 | 262444 | 600 | 1.45 | 165.3 | 8.5 |
| L1-2 2-3cm | 3.11.08 | 9.11.09 | 0.0441 | 329-349 | 5741 | 132 | 250732 | 271362 | 600 | 1.43 | 113.4 | 6.0 |
| L1-2 3-4cm | 3.11.08 | 10.11.09 | 0.043 | 329-349 | 1741 | 77 | 101639 | 277979 | 600 | 1.42 | 85.6 | 5.5 |
| L1-2 4-5cm | 3.11.08 | 11.11.09 | 0.0449 | 329-349 | 1041 | 68 | 81379 | 266102 | 600 | 1.44 | 61.9 | 5.0 |
| L1-2 5-6cm | 3.11.08 | 12.11.09 | 0.0428 | 329-349 | 883 | 70 | 86258 | 294318 | 600 | 1.38 | 49.3 | 4.6 |
| L1-2 6-7cm | 3.11.08 | 13.11.09 | 0.0454 | 329-349 | 809 | 67 | 83517 | 272771 | 600 | 1.43 | 45.4 | 4.4 |
| L1-2 7-8cm | 3.11.08 | 3.11.09 | 0.0457 | 329-349 | 477 | 59 | 65440 | 260648 | 600 | 1.46 | 34.1 | 4.6 |
| L1-2 8-9cm | 3.11.08 | 16.11.09 | 0.0472 | 329-349 | 1652 | 114 | 242163 | 270096 | 600 | 1.43 | 30.3 | 2.6 |
| L1-2 9-10cm | 3.11.08 | 17.11.09 | 0.0456 | 329-349 | 620 | 68 | 84918 | 263669 | 600 | 1.45 | 34.1 | 4.2 |
| L1-2 10-11cm | 3.11.08 | 18.11.09 | 0.0442 | 329-349 | 590 | 66 | 82517 | 266001 | 600 | 1.44 | 34.3 | 4.3 |
| L1-2 11-12cm | 3.11.08 | 19.11.09 | 0.0438 | 329-349 | 540 | 68 | 88001 | 265922 | 600 | 1.44 | 29.4 | 4.1 |
| L1-2 12-13cm | 3.11.08 | 20.11.09 | 0.0454 | 329-349 | 491 | 66 | 83986 | 269654 | 600 | 1.44 | 26.8 | 3.9 |
| L1-2 13-14cm | 3.11.08 | 24.11.09 | 0.0477 | 329-349 | 1812 | 134 | 339097 | 250007 | 600 | 1.48 | 23.9 | 2.2 |
| L1-2 14-15cm | 3.11.08 | 25.11.09 | 0.048 | 329-349 | 377 | 69 | 84157 | 258394 | 600 | 1.46 | 19.3 | 3.9 |

**Appendix V Table A35: Data and results from Pb-210 measurements on core L2-1.**

| Sample | | | | Measuring sample | | | | Measuring sample with Pb-210 point source on top | | | Results | |
|---|---|---|---|---|---|---|---|---|---|---|---|---|
| Sample identity | Sampling date | Date of measurement | Sample weight, kg | Mark peak ch | Net counts in 46,5keV roi | s(net counts in 46,5keV roi) | Counting time, sec. | Net counts in 46,5keV roi | Counting time, sec. | Correction factor | Pb-210 activity, Bq/kg (d.w.) | uncertainty |
| L2-1 0-1cm | 3.11.08 | 21.4.09 | 0.0427 | 333-345 | 4088 | 81 | 80659 | 225745 | 600 | 1.38 | 318.9 | 16.9 |
| L2-1 1-2cm | 3.11.08 | 10.6.09 | 0.0435 | 333-345 | 4099 | 80 | 81857 | 228837 | 600 | 1.37 | 308.7 | 16.2 |
| L2-1 2-3cm | 3.11.08 | 11.6.09 | 0.0448 | 333-345 | 2583 | 67 | 81671 | 226628 | 600 | 1.38 | 189.2 | 10.5 |
| L2-1 3-4cm | 3.11.08 | 12.6.09 | 0.0451 | 333-345 | 2487 | 66 | 84126 | 224451 | 600 | 1.38 | 176.3 | 9.8 |
| L2-1 4-5cm | 3.11.08 | 13.6.09 | 0.0496 | 333-345 | 2976 | 73 | 107251 | 216267 | 600 | 1.40 | 152.8 | 8.4 |
| L2-1 5-6cm | 3.11.08 | 15.6.09 | 0.0464 | 333-345 | 2898 | 78 | 154974 | 214373 | 600 | 1.41 | 109.8 | 6.1 |
| L2-1 6-7cm | 3.11.08 | 16.6.09 | 0.0499 | 333-345 | 1674 | 59 | 101024 | 204078 | 600 | 1.44 | 92.2 | 5.6 |
| L2-1 7-8cm | 3.11.08 | 17.6.09 | 0.0497 | 333-345 | 800 | 44 | 66798 | 204339 | 600 | 1.44 | 66.2 | 5.0 |
| L2-1 8-9cm | 3.11.08 | 18.6.09 | 0.0491 | 333-345 | 969 | 49 | 86055 | 205001 | 600 | 1.44 | 62.8 | 4.5 |
| L2-1 9-10cm | 3.11.08 | 19.6.09 | 0.0491 | 333-345 | 542 | 43 | 84405 | 207612 | 600 | 1.43 | 34.6 | 3.4 |
| L2-1 10-11cm | 3.11.08 | 22.6.09 | 0.0516 | 333-345 | 1529 | 74 | 256847 | 208334 | 600 | 1.43 | 30.3 | 2.2 |
| L2-1 11-12cm | 3.11.08 | 23.6.09 | 0.0528 | 333-345 | 314 | 40 | 83581 | 198397 | 600 | 1.46 | 18.3 | 2.8 |
| L2-1 12-13cm | 3.11.08 | 25.6.09 | 0.049 | 333-345 | 269 | 35 | 67315 | 208492 | 600 | 1.43 | 20.7 | 3.2 |

**Appendix V Table A36: Data and results from Pb-210 measurements on core L2-2.**

| Sample | | | | Measuring sample | | | | Measuring sample with Pb-210 point source on top | | | Results | |
|---|---|---|---|---|---|---|---|---|---|---|---|---|
| Sample identity | Sampling date | Date of measurement | Sample weight, kg | Mark peak ch | Net counts in 46,5keV roi | s(net counts in 46,5keV roi) | Counting time, sec. | Net counts in 46,5keV roi | Counting time, sec. | Correction factor | Pb-210 activity, Bq/kg (d.w.) | uncertainty |
| L2-2 0-1cm | 3.11.08 | 15.5.09 | 0.0502 | 333-345 | 3691 | 79 | 87572 | 198996 | 600 | 1.46 | 238.5 | 12.7 |
| L2-2 1-2cm | 3.11.08 | 19.5.09 | 0.0486 | 333-345 | 3250 | 73 | 82279 | 209630 | 600 | 1.42 | 225.6 | 12.2 |
| L2-2 2-3cm | 3.11.08 | 20.5.09 | 0.0511 | 333-345 | 1997 | 63 | 90314 | 202293 | 600 | 1.45 | 121.0 | 7.1 |
| L2-2 3-4cm | 3.11.08 | 26.5.09 | 0.0499 | 333-345 | 873 | 47 | 78798 | 203918 | 600 | 1.44 | 60.8 | 4.5 |
| L2-2 4-5cm | 3.11.08 | 28.5.09 | 0.0496 | 333-345 | 1365 | 56 | 92445 | 202309 | 600 | 1.45 | 82.5 | 5.3 |
| L2-2 5-6cm | 3.11.08 | 29.5.09 | 0.0496 | 333-345 | 560 | 42 | 71836 | 199284 | 600 | 1.45 | 42.8 | 4.0 |
| L2-2 6-7cm | 3.11.08 | 3.6.09 | 0.0558 | 333-345 | 438 | 41 | 72587 | 188863 | 600 | 1.49 | 29.7 | 3.3 |
| L2-2 7-8cm | 3.11.08 | 4.6.09 | 0.0484 | 333-345 | 551 | 44 | 102055 | 208380 | 600 | 1.43 | 29.1 | 2.9 |
| L2-2 8-9cm | 3.11.08 | 8.6.09 | 0.0486 | 333-345 | 1556 | 80 | 329124 | 205962 | 600 | 1.43 | 25.2 | 1.9 |
| L2-2 9-10cm | 3.11.08 | 9.6.09 | 0.0519 | 333-345 | 518 | 42 | 87760 | 212125 | 600 | 1.42 | 29.6 | 3.0 |

**Appendix V Table A37: Data and results from Pb-210 measurements on core S1-1.**

| Sample | | | | Measuring sample | | | | Measuring sample with Pb-210 point source on top | | | Results | |
|---|---|---|---|---|---|---|---|---|---|---|---|---|
| Sample identity | Sampling date | Date of measurement | Sample weight, kg | Mark peak ch | Net counts in 46,5keV roi | s(net counts in 46,5keV roi) | Counting time, sec. | Net counts in 46,5keV roi | Counting time, sec. | Correction factor | Pb-210 activity, Bq/kg (d.w.) | uncertainty |
| S1-1 0-1cm | 20.11.07 | 28.7.09 | 0.05 | 333-345 | 1116 | 41 | 17416 | 196029 | 600 | 1.47 | 380.8 | 22.5 |
| S1-1 1-2cm | 20.11.07 | 7.8.09 | 0.0423 | 333-345 | 594 | 31 | 12411 | 221100 | 600 | 1.39 | 318.5 | 22.1 |
| S1-1 2-3cm | 20.11.07 | 11.8.09 | 0.0415 | 333-345 | 3133 | 73 | 83800 | 219511 | 600 | 1.39 | 253.9 | 13.3 |
| S1-1 3-4cm | 20.11.07 | 12.8.09 | 0.045 | 333-345 | 2326 | 65 | 80523 | 211405 | 600 | 1.42 | 183.4 | 10.0 |
| S1-1 4-5cm | 20.11.07 | 13.8.09 | 0.0423 | 333-345 | 3166 | 73 | 88609 | 216077 | 600 | 1.40 | 239.7 | 12.5 |
| S1-1 5-6cm | 20.11.07 | 14.8.09 | 0.0396 | 333-345 | 2909 | 72 | 93698 | 226028 | 600 | 1.38 | 217.7 | 11.5 |
| S1-1 6-7cm | 20.11.07 | 19.8.09 | 0.0418 | 333-345 | 1432 | 55 | 90182 | 218177 | 600 | 1.40 | 105.9 | 6.4 |
| S1-1 7-8cm | 20.11.07 | 20.8.09 | 0.041 | 333-345 | 837 | 47 | 80859 | 213568 | 600 | 1.41 | 70.0 | 5.2 |
| S1-1 8-9cm | 20.11.07 | 21.8.09 | 0.0426 | 333-345 | 746 | 45 | 88118 | 211918 | 600 | 1.42 | 54.8 | 4.2 |
| S1-1 9-10cm | 20.11.07 | 28.7.09 | 0.045 | 333-345 | 560 | 41 | 74240 | 208948 | 600 | 1.43 | 46.2 | 4.1 |
| S1-1 10-11cm | 20.11.07 | 5.8.09 | 0.0472 | 333-345 | 4566 | 121 | 674888 | 198567 | 600 | 1.46 | 40.1 | 2.2 |
| S1-1 11-12cm | 20.11.07 | 6.8.09 | 0.0482 | 333-345 | 406 | 41 | 81850 | 202233 | 600 | 1.45 | 27.9 | 3.3 |
| S1-1 12-13cm | 20.11.07 | 7.8.09 | 0.0486 | 333-345 | 395 | 38 | 71040 | 204786 | 600 | 1.44 | 31.2 | 3.5 |
| S1-1 13-14cm | 20.11.07 | 10.8.09 | 0.045 | 333-345 | 1203 | 68 | 242765 | 210255 | 600 | 1.42 | 29.4 | 2.2 |
| S1-1 14-15cm | 20.11.07 | 18.8.09 | 0.049 | 333-345 | 436 | 40 | 83599 | 199213 | 600 | 1.46 | 29.2 | 3.1 |
| S1-1 15-16cm | 20.11.07 | 17.8.09 | 0.0468 | 333-345 | 1284 | 71 | 246471 | 199622 | 600 | 1.45 | 30.5 | 2.3 |

**Appendix V Table A38: Data and results from Pb-210 measurements on core S1-2.**

| Sample | | | | Measuring sample | | | | Measuring sample with Pb-210 point source on top | | | Results | |
|---|---|---|---|---|---|---|---|---|---|---|---|---|
| Sample identity | Sampling date | Date of measurement | Sample weight, kg | Mark peak ch | Net counts in 46,5keV roi | s(net counts in 46,5keV roi) | Counting time, sec. | Net counts in 46,5keV roi | Counting time, sec. | Correction factor | Pb-210 activity, Bq/kg (d.w.) | uncertainty |
| S1-2 0-1cm | 20.11.07 | 8.10.09 | 0.0341 | 329-349 | 4588 | 92 | 84760 | 314303 | 600 | 1.34 | 336.9 | 16.9 |
| S1-2 1-2cm | 20.11.07 | 9.10.09 | 0.0393 | 329-349 | 4436 | 93 | 86103 | 295142 | 600 | 1.38 | 286.0 | 14.4 |
| S1-2 2-3cm | 20.11.07 | 15.10.09 | 0.0405 | 329-349 | 21968 | 218 | 518931 | 262954 | 600 | 1.45 | 239.6 | 11.3 |
| S1-2 3-4cm | 20.11.07 | 16.10.09 | 0.0338 | 329-349 | 2877 | 8 | 86543 | 321073 | 600 | 1.33 | 205.9 | 9.6 |
| S1-2 4-5cm | 20.11.07 | 19.10.09 | 0.0357 | 329-349 | 10176 | 150 | 272311 | 300296 | 600 | 1.37 | 226.2 | 11.0 |
| S1-2 5-6cm | 20.11.07 | 20.10.09 | 0.0299 | 329-349 | 2045 | 71 | 81232 | 331406 | 600 | 1.31 | 173.1 | 9.9 |
| S1-2 6-7cm | 20.11.07 | 21.10.09 | 0.0338 | 329-349 | 1456 | 65 | 67770 | 305333 | 600 | 1.36 | 135.3 | 8.5 |
| S1-2 7-8cm | 20.11.07 | 22.10.09 | 0.0348 | 329-349 | 1358 | 70 | 89023 | 317507 | 600 | 1.34 | 91.0 | 6.2 |
| S1-2 8-9cm | 20.11.07 | 23.10.09 | 0.0362 | 329-349 | 1075 | 63 | 73433 | 317740 | 600 | 1.34 | 83.8 | 6.1 |
| S1-2 9-10cm | 20.11.07 | 26.10.09 | 0.0372 | 329-349 | 2357 | 114 | 255994 | 302217 | 600 | 1.37 | 51.6 | 3.4 |
| S1-2 10-11cm | 20.11.07 | 27.10.09 | 0.0363 | 329-349 | 777 | 67 | 90313 | 299188 | 600 | 1.37 | 49.5 | 4.8 |
| S1-2 11-12cm | 20.11.07 | 28.10.09 | 0.0411 | 329-349 | 659 | 66 | 84009 | 282248 | 600 | 1.41 | 40.7 | 4.5 |
| S1-2 12-13cm | 20.11.07 | 29.10.09 | 0.0395 | 329-349 | 657 | 65 | 86575 | 287792 | 600 | 1.40 | 40.5 | 4.4 |
| S1-2 13-14cm | 20.11.07 | 30.10.09 | 0.0395 | 329-349 | 583 | 64 | 85072 | 278375 | 600 | 1.42 | 36.9 | 4.4 |
| S1-2 14-15cm | 20.11.07 | 2.11.09 | 0.0413 | 329-349 | 1566 | 118 | 272196 | 279859 | 600 | 1.41 | 29.2 | 2.6 |

**Appendix V Table A39: Data and results from Pb-210 measurements on core S1-3.**

| Sample | | | | Measuring sample | | | | Measuring sample with Pb-210 point source on top | | | Results | |
|---|---|---|---|---|---|---|---|---|---|---|---|---|
| Sample identity | Sampling date | Date of measurement | Sample weight, kg | Mark peak ch | Net counts in 46,5keV roi | s(net counts in 46,5keV roi) | Counting time, sec. | Net counts in 46,5keV roi | Counting time, sec. | Correction factor | Pb-210 activity, Bq/kg (d.w.) | uncertainty |
| S1-3 0-1cm | 20.11.07 | 17.4.09 | 0.0388 | 333-345 | 4233 | 81 | 76302 | 223684 | 600 | 1.38 | 397.2 | 20.3 |
| S1-3 1-2cm | 20.11.07 | 23.2.10 | 0.0324 | 329-349 | 5024 | 95 | 84489 | 293471 | 600 | 1.38 | 406.5 | 20.0 |
| S1-3 2-3cm | 20.11.07 | 25.2.10 | 0.0361 | 329-349 | 10554 | 138 | 171372 | 292355 | 600 | 1.39 | 378.7 | 18.0 |
| S1-3 3-4cm | 20.11.07 | 26.2.10 | 0.0358 | 329-349 | 4093 | 88 | 81151 | 292470 | 600 | 1.39 | 312.2 | 15.6 |
| S1-3 4-5cm | 20.11.07 | 1.3.10 | 0.0332 | 329-349 | 10471 | 148 | 251380 | 310246 | 600 | 1.35 | 270.5 | 12.9 |
| S1-3 5-6cm | 20.11.07 | 2.3.10 | 0.0322 | 329-349 | 2874 | 80 | 79277 | 303310 | 600 | 1.36 | 244.9 | 12.9 |
| S1-3 6-7cm | 20.11.07 | 3.3.10 | 0.0353 | 329-349 | 5019 | 100 | 109959 | 292749 | 600 | 1.39 | 286.4 | 14.2 |
| S1-3 7-8cm | 20.11.07 | 4.3.10 | 0.0368 | 329-349 | 2231 | 74 | 76907 | 285000 | 600 | 1.40 | 175.8 | 9.8 |
| S1-3 8-9cm | 20.11.07 | 5.3.10 | 0.0331 | 329-349 | 1330 | 68 | 76207 | 305030 | 600 | 1.36 | 113.0 | 7.6 |
| S1-3 9-10cm | 20.11.07 | 8.3.10 | 0.0401 | 329-349 | 2756 | 122 | 268255 | 276401 | 600 | 1.42 | 56.4 | 3.5 |
| S1-3 10-11cm | 20.11.07 | 9.3.10 | 0.0381 | 329-349 | 880 | 64 | 80850 | 272884 | 600 | 1.43 | 63.4 | 5.3 |
| S1-3 11-12cm | 20.11.07 | 10.3.10 | 0.0385 | 329-349 | 571 | 67 | 90468 | 276675 | 600 | 1.42 | 35.2 | 4.4 |
| S1-3 12-13cm | 20.11.07 | 11.3.10 | 0.035 | 329-349 | 517 | 62 | 85929 | 298698 | 600 | 1.37 | 35.6 | 4.6 |
| S1-3 13-14cm | 20.11.07 | 12.3.10 | 0.0339 | 329-349 | 346 | 55 | 69883 | 303495 | 600 | 1.36 | 29.5 | 4.9 |

**Appendix V Table A40: Data and results from Pb-210 measurements on core S2-1.**

| Sample | | | | Measuring sample | | | | Measuring sample with Pb-210 point source on top | | | Results | |
|---|---|---|---|---|---|---|---|---|---|---|---|---|
| Sample identity | Sampling date | Date of measurement | Sample weight, kg | Mark peak ch | Net counts in 46,5keV roi | s(net counts in 46,5keV roi) | Counting time, sec. | Net counts in 46,5keV roi | Counting time, sec. | Correction factor | Pb-210 activity, Bq/kg (d.w.) | uncertainty |
| S2-1 0-1cm | 18.11.07 | 23.9.09 | 0.048 | 333-345 | 1889 | 65 | 86226 | 204724 | 600 | 1.44 | 132.1 | 7.6 |
| S2-1 1-2cm | 18.11.07 | 23.9.09 | 0.042 | 333-345 | 372 | 27 | 17071 | 202497 | 600 | 1.44 | 150.9 | 12.9 |
| S2-1 2-3cm | 18.11.07 | 25.9.09 | 0.0432 | 333-345 | 393 | 29 | 17000 | 200493 | 600 | 1.45 | 156.5 | 13.5 |
| S2-1 3-4cm | 18.11.07 | 29.9.09 | 0.0443 | 333-345 | 1957 | 68 | 94106 | 186861 | 600 | 1.50 | 141.3 | 8.2 |
| S2-1 4-5cm | 18.11.07 | 30.9.09 | 0.0456 | 329-349 | 654 | 49 | 23621 | 254496 | 600 | 1.47 | 140.3 | 12.0 |
| S2-1 5-6cm | 18.11.07 | 2.10.09 | 0.0459 | 329-349 | 2384 | 94 | 87110 | 258844 | 600 | 1.46 | 136.8 | 8.2 |
| S2-1 6-7cm | 18.11.07 | 2.10.09 | 0.0442 | 329-349 | 400 | 42 | 19367 | 256970 | 600 | 1.47 | 107.0 | 11.9 |
| S2-1 7-8cm | 18.11.07 | 5.10.09 | 0.0489 | 329-349 | 407 | 37 | 15702 | 252529 | 600 | 1.48 | 122.8 | 12.1 |
| S2-1 8-9cm | 18.11.07 | 6.10.09 | 0.0476 | 329-349 | 1176 | 74 | 62537 | 243494 | 600 | 1.50 | 92.5 | 7.1 |
| S2-1 9-10cm | 18.11.07 | 7.10.09 | 0.0468 | 329-349 | 1571 | 87 | 88289 | 250573 | 600 | 1.48 | 87.8 | 6.2 |
| S2-1 10-11cm | 18.11.07 | 5.10.09 | 0.0485 | 329-349 | 3705 | 144 | 239405 | 254491 | 600 | 1.47 | 72.9 | 4.4 |
| S2-1 11-12cm | 18.11.07 | 1.10.09 | 0.049 | 329-349 | 804 | 73 | 63224 | 227339 | 600 | 1.55 | 61.9 | 6.2 |
| S2-1 12-13cm | 18.11.07 | 30.9.09 | 0.0475 | 329-349 | 728 | 74 | 71502 | 253999 | 600 | 1.47 | 48.3 | 5.3 |
| S2-1 13-14cm | 18.11.07 | 25.9.09 | 0.0483 | 329-349 | 119 | 20 | 14942 | 182582 | 600 | 1.69 | 42.2 | 7.3 |
| S2-1 14-15cm | 18.11.07 | 28.9.09 | 0.047 | 329-349 | 1892 | 84 | 242516 | 180337 | 600 | 1.70 | 42.6 | 2.7 |

**Appendix V Table A41: Data and results from Pb-210 measurements on core S2-2.**

| Sample | | | | Measuring sample | | | | Measuring sample with Pb-210 point source on top | | | Results | |
|---|---|---|---|---|---|---|---|---|---|---|---|---|
| Sample identity | Sampling date | Date of measurement | Sample weight, kg | Mark peak ch | Net counts in 46,5keV roi | s(net counts in 46,5keV roi) | Counting time, sec. | Net counts in 46,5keV roi | Counting time, sec. | Correction factor | Pb-210 activity, Bq/kg (d.w.) | uncertainty |
| S2-2 0-1cm | 18.11.07 | 24.6.09 | 0.0383 | 333-345 | 1951 | 65 | 87994 | 221444 | 600 | 1.39 | 160.8 | 9.3 |
| S2-2 1-2cm | 18.11.07 | 24.6.09 | 0.0391 | 333-345 | 287 | 26 | 14502 | 222855 | 600 | 1.39 | 139.0 | 14.2 |
| S2-2 2-3cm | 18.11.07 | 25.6.09 | 0.0408 | 333-345 | 300 | 25 | 14021 | 213984 | 600 | 1.41 | 146.9 | 14.1 |
| S2-2 3-4cm | 18.11.07 | 6.7.09 | 0.0419 | 333-345 | 5218 | 109 | 257725 | 217913 | 600 | 1.40 | 134.2 | 6.9 |
| S2-2 4-5cm | 18.11.07 | 7.7.09 | 0.0386 | 333-345 | 1350 | 58 | 80479 | 218508 | 600 | 1.40 | 119.9 | 7.7 |
| S2-2 5-6cm | 18.11.07 | 8.7.09 | 0.0438 | 333-345 | 1509 | 61 | 85883 | 204443 | 600 | 1.44 | 114.1 | 7.1 |
| S2-2 6-7cm | 18.11.07 | 9.7.09 | 0.0396 | 333-345 | 1270 | 56 | 86406 | 221469 | 600 | 1.39 | 101.3 | 6.6 |
| S2-2 7-8cm | 18.11.07 | 10.7.09 | 0.0418 | 333-345 | 1066 | 54 | 85360 | 215155 | 600 | 1.41 | 82.1 | 5.7 |
| S2-2 8-9cm | 18.11.07 | 13.7.09 | 0.0392 | 333-345 | 3025 | 92 | 259157 | 220962 | 600 | 1.39 | 80.6 | 4.5 |
| S2-2 9-10cm | 18.11.07 | 14.7.09 | 0.0425 | 333-345 | 1094 | 54 | 87889 | 204110 | 600 | 1.44 | 82.4 | 5.7 |
| S2-2 10-11cm | 18.11.07 | 15.7.09 | 0.0461 | 333-345 | 1062 | 57 | 93160 | 195703 | 600 | 1.47 | 70.5 | 5.1 |
| S2-2 11-12cm | 18.11.07 | 16.7.09 | 0.0444 | 333-345 | 903 | 51 | 79272 | 200793 | 600 | 1.45 | 72.4 | 5.4 |
| S2-2 12-13cm | 18.11.07 | 17.7.09 | 0.0441 | 333-345 | 803 | 51 | 83127 | 200005 | 600 | 1.45 | 61.4 | 4.9 |
| S2-2 13-14cm | 18.11.07 | 27.7.09 | 0.0478 | 333-345 | 7742 | 167 | 869884 | 190887 | 600 | 1.48 | 53.0 | 2.8 |
| S2-2 14-15cm | 18.11.07 | 29.6.09 | 0.0412 | 333-345 | 1614 | 83 | 247286 | 215150 | 600 | 1.41 | 41.7 | 3.0 |
| S2-2 15-16cm | 18.11.07 | 26.6.09 | 0.0446 | 333-345 | 612 | 48 | 80053 | 197427 | 600 | 1.46 | 47.5 | 4.5 |

**Appendix V Table A42: Data and results from Pb-210 measurements on core S3-1.**

| Sample | | | | Measuring sample | | | | Measuring sample with Pb-210 point source on top | | | Results | |
|---|---|---|---|---|---|---|---|---|---|---|---|---|
| Sample identity | Sampling date | Date of measurement | Sample weight, kg | Mark peak ch | Net counts in 46,5keV roi | s(net counts in 46,5keV roi) | Counting time, sec. | Net counts in 46,5keV roi | Counting time, sec. | Correction factor | Pb-210 activity, Bq/kg (d.w.) | uncertainty |
| S3-1 0-1cm | 23.11.08 | 15.4.09 | 0.0492 | 333-345 | 3743 | 79 | 75750 | 195753 | 600 | 1.47 | 286.5 | 15.3 |
| S3-1 1-2cm | 23.11.08 | 31.8.09 | 0.0301 | 333-345 | 7272 | 114 | 259065 | 240541 | 600 | 1.34 | 244.2 | 12.5 |
| S3-1 2-3cm | 23.11.08 | 28.8.09 | 0.0452 | 333-345 | 2503 | 67 | 81223 | 181670 | 600 | 1.51 | 202.1 | 11.2 |
| S3-1 3-4cm | 23.11.08 | 27.8.09 | 0.0451 | 333-345 | 578 | 42 | 75149 | 195522 | 600 | 1.47 | 47.0 | 4.3 |
| S3-1 4-5cm | 23.11.08 | 26.8.09 | 0.0448 | 333-345 | 646 | 47 | 99750 | 189937 | 600 | 1.49 | 40.0 | 3.7 |
| S3-1 5-6cm | 23.11.08 | 25.8.09 | 0.0493 | 333-345 | 567 | 43 | 85075 | 167173 | 600 | 1.57 | 39.5 | 3.7 |
| S3-1 6-7cm | 23.11.08 | 24.8.09 | 0.0404 | 333-345 | 530 | 41 | 81661 | 195982 | 600 | 1.47 | 43.8 | 4.2 |

**Appendix V Table A43: Data and results from Pb-210 measurements on core S4-1 (0-1cm) and S4-2 (1-9cm).**

| Sample | | | | Measuring sample | | | | Measuring sample with Pb-210 point source on top | | | Results | |
|---|---|---|---|---|---|---|---|---|---|---|---|---|
| Sample identity | Sampling date | Date of measurement | Sample weight, kg | Mark peak ch | Net counts in 46,5keV roi | s(net counts in 46,5keV roi) | Counting time, sec. | Net counts in 46,5keV roi | Counting time, sec. | Correction factor | Pb-210 activity, Bq/kg (d.w.) | uncertainty |
| S4-1 0-1cm | 22.11.08 | 16.4.09 | 0.0444 | 333-345 | 2214 | 71 | 98658 | 214967 | 600 | 1.41 | 136.3 | 7.9 |
| S4-2 1-2cm | 22.11.08 | 8.9.09 | 0.0467 | 329-349 | 1480 | 60 | 73411 | 192631 | 600 | 1.66 | 107.2 | 6.7 |
| S4-2 2-3cm | 22.11.08 | 14.9.09 | 0.0466 | 329-349 | 7695 | 146 | 529315 | 196974 | 600 | 1.64 | 76.0 | 3.9 |
| S4-2 3-4cm | 22.11.08 | 15.9.09 | 0.044 | 329-349 | 1059 | 53 | 74904 | 193795 | 600 | 1.65 | 78.7 | 5.5 |
| S4-2 4-5cm | 22.11.08 | 16.9.09 | 0.0483 | 329-349 | 1018 | 55 | 88768 | 190846 | 600 | 1.66 | 58.0 | 4.2 |
| S4-2 5-6cm | 22.11.08 | 18.9.09 | 0.0478 | 329-349 | 992 | 54 | 86233 | 181842 | 600 | 1.69 | 60.0 | 4.4 |
| S4-2 6-7cm | 22.11.08 | 17.9.09 | 0.0521 | 329-349 | 805 | 53 | 83748 | 179970 | 600 | 1.70 | 45.8 | 3.8 |
| S4-2 7-8cm | 22.11.08 | 21.9.09 | 0.0496 | 329-349 | 2288 | 91 | 251612 | 181801 | 600 | 1.69 | 45.1 | 2.8 |
| S4-2 8-9cm | 22.11.08 | 22.9.09 | 0.0477 | 329-349 | 750 | 52 | 87942 | 189620 | 600 | 1.67 | 43.1 | 3.7 |

***APPENDIX VI***

**Appendix VI Table A44: Data and results from Ra-226 measurements on core L1-1.**

| Sample | | Measuring sample | | | | | | | Results | | | | | | | |
|---|---|---|---|---|---|---|---|---|---|---|---|---|---|---|---|---|
| Sample identity | Sample weight, kg | Counting time, sec. | Net counts in 609 keV roi | s(net counts in 609 keV roi) | Net counts in 352 keV roi | s(net counts in 352 keV roi) | Net counts in 295 keV roi | s(net counts in 295 keV roi) | Activity in 609 keV roi, Bq/kg (d.w.) | uncer-tainty | Activity in 352 keV roi, Bq/kg (d.w.) | uncer-tainty | Activity in 352 keV roi, Bq/kg (d.w.) | uncer-tainty | Mean activity, Ra-226, Bq/kg (d.w.) | uncer-tainty |
| L1-1 0-1cm | 0.0346 | 245981 | 3680 | 115 | 5317 | 122 | 3236 | 114 | 26.0 | 2.1 | 27.3 | 1.8 | 27.6 | 2.3 | 27.0 | 3.6 |
| L1-1 1-2cm | 0.0367 | 258873 | 4222 | 122 | 6114 | 128 | 3532 | 119 | 27.2 | 2.1 | 28.5 | 1.8 | 27.1 | 2.2 | 27.6 | 3.5 |
| L1-1 2-3cm | 0.0344 | 74068 | 1145 | 66 | 1739 | 67 | 1020 | 63 | 27.2 | 2.7 | 30.2 | 2.2 | 29.3 | 2.9 | 28.9 | 4.5 |
| L1-1 3-4cm | 0.0356 | 74857 | 1217 | 65 | 1714 | 69 | 1029 | 65 | 28.0 | 2.6 | 28.4 | 2.1 | 28.2 | 2.9 | 28.2 | 4.4 |
| L1-1 4-5cm | 0.0381 | 348683 | 5926 | 143 | 8444 | 151 | 5069 | 140 | 27.5 | 2.0 | 28.3 | 1.7 | 28.1 | 2.1 | 28.0 | 3.4 |
| L1-1 5-6cm | 0.037 | 166805 | 2786 | 97 | 4052 | 104 | 2109 | 98 | 27.8 | 2.2 | 29.2 | 1.9 | 24.6 | 2.3 | 27.2 | 3.7 |
| L1-1 6-7cm | 0.0373 | 88688 | 1435 | 72 | 1981 | 75 | 1351 | 69 | 26.5 | 2.4 | 26.3 | 1.9 | 30.3 | 2.7 | 27.7 | 4.1 |
| L1-1 7-8cm | 0.0425 | 90242 | 1511 | 74 | 2455 | 76 | 1377 | 72 | 24.3 | 2.1 | 28.9 | 1.9 | 26.6 | 2.4 | 26.6 | 3.7 |
| L1-1 8-9cm | 0.0451 | 252171 | 4977 | 122 | 6666 | 134 | 4019 | 126 | 27.7 | 1.9 | 26.4 | 1.6 | 26.4 | 2.0 | 26.8 | 3.1 |
| L1-1 9-10cm | 0.0432 | 80979 | 1480 | 68 | 2172 | 74 | 1218 | 69 | 26.5 | 2.2 | 28.0 | 1.9 | 25.8 | 2.4 | 26.8 | 3.8 |
| L1-1 10-11cm | 0.0478 | 84026 | 1796 | 67 | 2378 | 77 | 1475 | 71 | 28.7 | 2.1 | 26.9 | 1.8 | 27.7 | 2.3 | 27.8 | 3.6 |
| L1-1 11-12cm | 0.0414 | 84250 | 1473 | 71 | 2081 | 74 | 1211 | 71 | 26.2 | 2.3 | 26.6 | 1.9 | 25.5 | 2.5 | 26.1 | 3.8 |

**Appendix VI Table A45: Data and results from Ra-226 measurements on core L1-2.**

| Sample | | Measuring sample | | | | | | | Results | | | | | | | |
|---|---|---|---|---|---|---|---|---|---|---|---|---|---|---|---|---|
| Sample identity | Sample weight, kg | Counting time, sec. | Net counts in 609 keV roi | s(net counts in 609 keV roi) | Net counts in 352 keV roi | s(net counts in 352 keV roi) | Net counts in 295 keV roi | s(net counts in 295 keV roi) | Activity in 609 keV roi, Bq/kg (d.w.) | uncer-tainty | Activity in 352 keV roi, Bq/kg (d.w.) | uncer-tainty | Activity in 352 keV roi, Bq/kg (d.w.) | uncer-tainty | Mean activity, Ra-226, Bq/kg (d.w.) | uncer-tainty |
| L1-2 0-1cm | 0.042 | 94248 | 1590 | 68 | 2450 | 76 | 1406 | 71 | 24.8 | 2.1 | 27.8 | 1.8 | 26.3 | 2.3 | 26.3 | 3.6 |
| L1-2 1-2cm | 0.0474 | 167791 | 3299 | 89 | 4364 | 104 | 2650 | 99 | 26.3 | 1.8 | 24.7 | 1.5 | 24.8 | 1.9 | 25.3 | 3.1 |
| L1-2 2-3cm | 0.0441 | 250732 | 4801 | 107 | 6230 | 125 | 3824 | 118 | 27.4 | 1.8 | 25.2 | 1.5 | 25.7 | 1.9 | 26.1 | 3.1 |
| L1-2 3-4cm | 0.043 | 101639 | 1597 | 70 | 2411 | 77 | 1269 | 78 | 22.2 | 1.9 | 24.5 | 1.7 | 20.9 | 2.2 | 22.5 | 3.3 |
| L1-2 4-5cm | 0.0449 | 81379 | 1488 | 61 | 2147 | 71 | 1152 | 71 | 25.5 | 2.0 | 26.5 | 1.8 | 23.1 | 2.3 | 25.0 | 3.5 |
| L1-2 5-6cm | 0.0428 | 86258 | 1585 | 62 | 2156 | 74 | 1288 | 72 | 26.9 | 2.1 | 26.1 | 1.8 | 25.8 | 2.4 | 26.3 | 3.7 |
| L1-2 6-7cm | 0.0454 | 83517 | 1421 | 64 | 2197 | 71 | 1318 | 67 | 23.1 | 2.0 | 26.1 | 1.7 | 25.9 | 2.3 | 25.0 | 3.5 |
| L1-2 7-8cm | 0.0457 | 65440 | 1233 | 53 | 1649 | 63 | 894 | 62 | 25.9 | 2.1 | 24.7 | 1.8 | 21.8 | 2.3 | 24.1 | 3.6 |
| L1-2 8-9cm | 0.0472 | 242163 | 4206 | 108 | 6085 | 124 | 3555 | 121 | 22.8 | 1.6 | 23.8 | 1.4 | 22.9 | 1.8 | 23.2 | 2.8 |
| L1-2 9-10cm | 0.0456 | 84918 | 1493 | 64 | 2000 | 72 | 1080 | 71 | 24.0 | 2.0 | 22.9 | 1.6 | 20.1 | 2.1 | 22.3 | 3.3 |
| L1-2 10-11cm | 0.0442 | 82517 | 1461 | 62 | 1866 | 71 | 1072 | 71 | 24.9 | 2.0 | 22.5 | 1.6 | 21.3 | 2.3 | 22.9 | 3.5 |
| L1-2 11-12cm | 0.0438 | 88001 | 1418 | 64 | 2031 | 74 | 1141 | 72 | 22.5 | 1.9 | 23.3 | 1.7 | 21.4 | 2.2 | 22.4 | 3.4 |
| L1-2 12-13cm | 0.0454 | 83986 | 1342 | 62 | 2041 | 72 | 1139 | 70 | 21.5 | 1.9 | 23.8 | 1.7 | 21.8 | 2.2 | 22.4 | 3.3 |
| L1-2 13-14cm | 0.0477 | 339097 | 5945 | 130 | 8324 | 145 | 4514 | 144 | 22.8 | 1.6 | 22.9 | 1.4 | 20.3 | 1.6 | 22.0 | 2.7 |
| L1-2 14-15cm | 0.048 | 84157 | 1391 | 65 | 2093 | 71 | 1201 | 69 | 21.1 | 1.8 | 23.1 | 1.6 | 21.9 | 2.1 | 22.0 | 3.2 |

**Appendix VI Table A46: Data and results from Ra-226 measurements on core L2-1.**

| Sample | | Measuring sample | | | | | | | Results | | | | | | | |
|---|---|---|---|---|---|---|---|---|---|---|---|---|---|---|---|---|
| Sample identity | Sample weight, kg | Counting time, sec. | Net counts in 609 keV roi | s(net counts in 609 keV roi) | Net counts in 352 keV roi | s(net counts in 352 keV roi) | Net counts in 295 keV roi | s(net counts in 295 keV roi) | Activity in 609 keV roi, Bq/kg (d.w.) | uncer-tainty | Activity in 352 keV roi, Bq/kg (d.w.) | uncer-tainty | Activity in 352 keV roi, Bq/kg (d.w.) | uncer-tainty | Mean activity, Ra-226, Bq/kg (d.w.) | uncer-tainty |
| L2-1 0-1cm | 0.0427 | 80659 | 1298 | 70 | 1927 | 71 | 1188 | 66 | 23.0 | 2.2 | 24.9 | 1.8 | 25.5 | 2.4 | 24.4 | 3.7 |
| L2-1 1-2cm | 0.0435 | 81857 | 1475 | 71 | 2137 | 73 | 1234 | 71 | 25.8 | 2.2 | 27.0 | 1.8 | 25.7 | 2.4 | 26.2 | 3.7 |
| L2-1 2-3cm | 0.0448 | 81671 | 1523 | 70 | 1965 | 76 | 1051 | 70 | 26.1 | 2.2 | 23.9 | 1.7 | 20.8 | 2.2 | 23.6 | 3.5 |
| L2-1 3-4cm | 0.0451 | 84126 | 1549 | 66 | 1967 | 78 | 1105 | 75 | 25.6 | 2.1 | 23.0 | 1.7 | 21.1 | 2.3 | 23.2 | 3.5 |
| L2-1 4-5cm | 0.0496 | 107251 | 2038 | 81 | 2872 | 88 | 1718 | 81 | 24.1 | 1.9 | 24.4 | 1.6 | 24.1 | 2.0 | 24.2 | 3.2 |
| L2-1 5-6cm | 0.0464 | 154974 | 2919 | 94 | 3947 | 104 | 2365 | 96 | 25.5 | 1.9 | 24.6 | 1.6 | 24.4 | 2.0 | 24.8 | 3.1 |
| L2-1 6-7cm | 0.0499 | 101024 | 1792 | 78 | 2436 | 81 | 1527 | 76 | 22.1 | 1.8 | 21.5 | 1.5 | 22.4 | 2.0 | 22.0 | 3.1 |
| L2-1 7-8cm | 0.0497 | 66798 | 1174 | 63 | 1664 | 68 | 996 | 62 | 22.0 | 2.0 | 22.4 | 1.6 | 22.2 | 2.2 | 22.2 | 3.4 |
| L2-1 8-9cm | 0.0491 | 86055 | 1509 | 73 | 2144 | 74 | 1238 | 70 | 22.2 | 1.9 | 22.7 | 1.6 | 21.6 | 2.0 | 22.1 | 3.2 |
| L2-1 9-10cm | 0.0491 | 84405 | 1519 | 69 | 1944 | 76 | 1034 | 72 | 22.9 | 1.9 | 20.7 | 1.5 | 17.9 | 2.0 | 20.5 | 3.1 |
| L2-1 10-11cm | 0.0516 | 256847 | 4583 | 124 | 6449 | 130 | 3579 | 124 | 21.5 | 1.5 | 21.8 | 1.3 | 19.8 | 1.6 | 21.0 | 2.6 |
| L2-1 11-12cm | 0.0528 | 83581 | 1414 | 67 | 1994 | 75 | 1024 | 69 | 19.8 | 1.7 | 20.1 | 1.4 | 16.6 | 1.8 | 18.8 | 2.9 |
| L2-1 12-13cm | 0.049 | 67315 | 1183 | 58 | 1558 | 66 | 891 | 62 | 22.3 | 1.9 | 20.9 | 1.6 | 19.6 | 2.1 | 20.9 | 3.3 |

**Appendix VI Table A47: Data and results from Ra-226 measurements on core L2-2.**

| Sample | | Measuring sample | | | | | | | Results | | | | | | | |
|---|---|---|---|---|---|---|---|---|---|---|---|---|---|---|---|---|
| Sample identity | Sample weight, kg | Counting time, sec. | Net counts in 609 keV roi | s(net counts in 609 keV roi) | Net counts in 352 keV roi | s(net counts in 352 keV roi) | Net counts in 295 keV roi | s(net counts in 295 keV roi) | Activity in 609 keV roi, Bq/kg (d.w.) | uncer-tainty | Activity in 352 keV roi, Bq/kg (d.w.) | uncer-tainty | Activity in 352 keV roi, Bq/kg (d.w.) | uncer-tainty | Mean activity, Ra-226, Bq/kg (d.w.) | uncer-tainty |
| L2-2 0-1cm | 0.0502 | 87572 | 1631 | 75 | 2513 | 76 | 1466 | 72 | 23.3 | 1.9 | 26.0 | 1.7 | 25.0 | 2.1 | 24.8 | 3.3 |
| L2-2 1-2cm | 0.0486 | 82279 | 1511 | 74 | 2187 | 74 | 1209 | 70 | 23.7 | 2.0 | 24.6 | 1.7 | 22.3 | 2.1 | 23.5 | 3.4 |
| L2-2 2-3cm | 0.0511 | 90314 | 1808 | 74 | 2389 | 82 | 1495 | 72 | 24.9 | 1.9 | 23.3 | 1.6 | 24.3 | 2.0 | 24.2 | 3.2 |
| L2-2 3-4cm | 0.0499 | 78798 | 1557 | 68 | 2077 | 75 | 1304 | 68 | 25.1 | 2.0 | 23.8 | 1.6 | 24.9 | 2.2 | 24.6 | 3.4 |
| L2-2 4-5cm | 0.0496 | 92445 | 1749 | 75 | 2437 | 82 | 1357 | 75 | 24.0 | 1.9 | 23.9 | 1.6 | 21.8 | 2.0 | 23.3 | 3.2 |
| L2-2 5-6cm | 0.0496 | 71836 | 1195 | 65 | 1796 | 69 | 1124 | 65 | 20.6 | 1.9 | 22.5 | 1.6 | 23.5 | 2.2 | 22.2 | 3.3 |
| L2-2 6-7cm | 0.0558 | 72587 | 1330 | 64 | 1974 | 72 | 1146 | 66 | 20.6 | 1.7 | 22.0 | 1.5 | 21.1 | 2.0 | 21.2 | 3.0 |
| L2-2 7-8cm | 0.0484 | 102055 | 1591 | 82 | 2537 | 81 | 1518 | 77 | 19.5 | 1.8 | 22.9 | 1.5 | 22.7 | 2.0 | 21.7 | 3.1 |
| L2-2 8-9cm | 0.0486 | 329124 | 5910 | 138 | 8327 | 149 | 4793 | 140 | 23.0 | 1.6 | 23.3 | 1.4 | 22.1 | 1.7 | 22.8 | 2.7 |
| L2-2 9-10cm | 0.0519 | 87760 | 1595 | 74 | 2253 | 78 | 1279 | 74 | 21.9 | 1.8 | 22.2 | 1.5 | 20.7 | 2.0 | 21.6 | 3.1 |

**Appendix VI Table A48: Data and results from Ra-226 measurements on core S1-1.**

| Sample | | Measuring sample | | | | | | | Results | | | | | | | |
|---|---|---|---|---|---|---|---|---|---|---|---|---|---|---|---|---|
| Sample identity | Sample weight, kg | Counting time, sec. | Net counts in 609 keV roi | s(net counts in 609 keV roi) | Net counts in 352 keV roi | s(net counts in 352 keV roi) | Net counts in 295 keV roi | s(net counts in 295 keV roi) | Activity in 609 keV roi, Bq/kg (d.w.) | uncer-tainty | Activity in 352 keV roi, Bq/kg (d.w.) | uncer-tainty | Activity in 352 keV roi, Bq/kg (d.w.) | uncer-tainty | Mean activity, Ra-226, Bq/kg (d.w.) | uncer-tainty |
| S1-1 0-1cm | 0.05 | 17416 | 364 | 34 | 506 | 35 | 279 | 35 | 26.7 | 3.3 | 26.5 | 2.5 | 23.9 | 3.7 | 25.7 | 5.6 |
| S1-1 1-2cm | 0.0423 | 12411 | 223 | 30 | 300 | 29 | 192 | 27 | 26.5 | 4.5 | 25.4 | 3.2 | 27.2 | 4.7 | 26.4 | 7.2 |
| S1-1 2-3cm | 0.0415 | 83800 | 1434 | 72 | 2171 | 75 | 1186 | 71 | 25.5 | 2.3 | 28.0 | 1.9 | 25.0 | 2.4 | 26.2 | 3.8 |
| S1-1 3-4cm | 0.045 | 80523 | 1589 | 69 | 2150 | 78 | 1296 | 69 | 27.8 | 2.2 | 26.8 | 1.8 | 26.7 | 2.4 | 27.1 | 3.7 |
| S1-1 4-5cm | 0.0423 | 88609 | 1741 | 72 | 2337 | 79 | 1249 | 76 | 29.4 | 2.3 | 28.1 | 1.9 | 24.4 | 2.4 | 27.3 | 3.8 |
| S1-1 5-6cm | 0.0396 | 93698 | 1650 | 74 | 2418 | 80 | 1337 | 77 | 27.6 | 2.3 | 29.3 | 2.0 | 26.5 | 2.5 | 27.8 | 4.0 |
| S1-1 6-7cm | 0.0418 | 90182 | 1680 | 75 | 2289 | 79 | 1282 | 75 | 28.0 | 2.3 | 27.2 | 1.9 | 25.0 | 2.4 | 26.7 | 3.8 |
| S1-1 7-8cm | 0.041 | 80859 | 1554 | 67 | 2113 | 74 | 1166 | 70 | 29.6 | 2.4 | 28.7 | 2.0 | 25.9 | 2.5 | 28.0 | 4.0 |
| S1-1 8-9cm | 0.0426 | 88118 | 1668 | 74 | 2373 | 78 | 1372 | 71 | 28.0 | 2.3 | 28.5 | 1.9 | 27.2 | 2.4 | 27.9 | 3.8 |
| S1-1 9-10cm | 0.045 | 74240 | 1245 | 71 | 1895 | 74 | 1235 | 68 | 22.9 | 2.2 | 25.4 | 1.8 | 27.7 | 2.5 | 25.4 | 3.8 |
| S1-1 10-11cm | 0.0472 | 674888 | 12969 | 207 | 18314 | 219 | 11130 | 202 | 25.7 | 1.7 | 26.0 | 1.5 | 26.2 | 1.8 | 25.9 | 2.8 |
| S1-1 11-12cm | 0.0482 | 81850 | 1680 | 72 | 2305 | 78 | 1348 | 71 | 27.1 | 2.1 | 26.5 | 1.8 | 25.6 | 2.2 | 26.4 | 3.6 |
| S1-1 12-13cm | 0.0486 | 71040 | 1486 | 65 | 1948 | 72 | 1145 | 69 | 27.5 | 2.2 | 25.5 | 1.8 | 24.8 | 2.3 | 25.9 | 3.6 |
| S1-1 13-14cm | 0.045 | 242765 | 5118 | 120 | 6936 | 131 | 4120 | 121 | 30.0 | 2.0 | 28.9 | 1.7 | 28.4 | 2.0 | 29.1 | 3.3 |
| S1-1 14-15cm | 0.049 | 83599 | 1668 | 73 | 2584 | 79 | 1429 | 73 | 25.8 | 2.1 | 28.9 | 1.8 | 26.2 | 2.2 | 27.0 | 3.6 |
| S1-1 15-16cm | 0.0468 | 246471 | 5527 | 124 | 7729 | 134 | 4482 | 125 | 30.9 | 2.0 | 30.8 | 1.8 | 29.4 | 2.0 | 30.4 | 3.3 |

**Appendix VI Table A49: Data and results from Ra-226 measurements on core S1-2.**

| Sample | | Measuring sample | | | | | | | Results | | | | | | | |
|---|---|---|---|---|---|---|---|---|---|---|---|---|---|---|---|---|
| Sample identity | Sample weight, kg | Counting time, sec. | Net counts in 609 keV roi | s(net counts in 609 keV roi) | Net counts in 352 keV roi | s(net counts in 352 keV roi) | Net counts in 295 keV roi | s(net counts in 295 keV roi) | Activity in 609 keV roi, Bq/kg (d.w.) | uncer-tainty | Activity in 352 keV roi, Bq/kg (d.w.) | uncer-tainty | Activity in 352 keV roi, Bq/kg (d.w.) | uncer-tainty | Mean activity, Ra-226, Bq/kg (d.w.) | uncer-tainty |
| S1-2 0-1cm | 0.0341 | 84760 | 1354 | 59 | 1845 | 69 | 1040 | 70 | 28.6 | 2.4 | 28.0 | 2.0 | 25.8 | 2.8 | 27.5 | 4.3 |
| S1-2 1-2cm | 0.0393 | 86103 | 1508 | 61 | 2065 | 71 | 1129 | 73 | 27.7 | 2.2 | 27.1 | 1.9 | 24.2 | 2.5 | 26.3 | 3.9 |
| S1-2 2-3cm | 0.0405 | 518931 | 9426 | 155 | 13035 | 184 | 7687 | 177 | 28.0 | 1.9 | 27.7 | 1.6 | 27.0 | 2.0 | 27.6 | 3.2 |
| S1-2 3-4cm | 0.0338 | 86543 | 1386 | 60 | 2008 | 72 | 1086 | 70 | 28.9 | 2.5 | 30.4 | 2.1 | 26.7 | 2.8 | 28.7 | 4.3 |
| S1-2 4-5cm | 0.0357 | 272311 | 4582 | 112 | 6685 | 128 | 3752 | 123 | 29.0 | 2.1 | 30.7 | 1.9 | 28.2 | 2.3 | 29.3 | 3.6 |
| S1-2 5-6cm | 0.0299 | 81232 | 1197 | 59 | 1671 | 68 | 1134 | 62 | 29.5 | 2.8 | 29.9 | 2.3 | 34.2 | 3.2 | 31.2 | 4.8 |
| S1-2 6-7cm | 0.0338 | 67770 | 1117 | 51 | 1578 | 60 | 936 | 61 | 29.9 | 2.6 | 30.5 | 2.2 | 29.9 | 3.1 | 30.1 | 4.6 |
| S1-2 7-8cm | 0.0348 | 89023 | 1538 | 61 | 2055 | 73 | 1184 | 71 | 30.7 | 2.5 | 29.3 | 2.1 | 27.8 | 2.8 | 29.3 | 4.3 |
| S1-2 8-9cm | 0.0362 | 73433 | 1295 | 55 | 1737 | 1737 | 954 | 65 | 30.3 | 2.5 | 29.0 | 33.2 | 26.0 | 2.8 | 28.4 | 33.4 |
| S1-2 9-10cm | 0.0372 | 255994 | 4344 | 108 | 6117 | 123 | 3656 | 121 | 28.2 | 2.0 | 28.5 | 1.8 | 28.2 | 2.2 | 28.3 | 3.5 |
| S1-2 10-11cm | 0.0363 | 90313 | 1508 | 65 | 1968 | 74 | 1384 | 71 | 28.3 | 2.4 | 26.3 | 1.9 | 31.3 | 2.8 | 28.6 | 4.1 |
| S1-2 11-12cm | 0.0411 | 84009 | 1515 | 61 | 2023 | 75 | 1246 | 69 | 27.4 | 2.2 | 26.1 | 1.8 | 26.7 | 2.5 | 26.7 | 3.8 |
| S1-2 12-13cm | 0.0395 | 86575 | 1574 | 66 | 2336 | 76 | 1447 | 72 | 28.8 | 2.3 | 30.8 | 2.0 | 31.8 | 2.7 | 30.5 | 4.1 |
| S1-2 13-14cm | 0.0395 | 85072 | 1510 | 63 | 2209 | 72 | 1285 | 70 | 28.0 | 2.3 | 29.5 | 2.0 | 28.3 | 2.6 | 28.6 | 4.0 |
| S1-2 14-15cm | 0.0413 | 272196 | 5377 | 115 | 7666 | 134 | 4151 | 131 | 30.3 | 2.0 | 31.0 | 1.8 | 27.4 | 2.1 | 29.5 | 3.4 |

**Appendix VI Table A50: Data and results from Ra-226 measurements on core S1-2.**

| Sample | | Measuring sample | | | | | | | Results | | | | | | | |
|---|---|---|---|---|---|---|---|---|---|---|---|---|---|---|---|---|
| Sample identity | Sample weight, kg | Counting time, sec. | Net counts in 609 keV roi | s(net counts in 609 keV roi) | Net counts in 352 keV roi | s(net counts in 352 keV roi) | Net counts in 295 keV roi | s(net counts in 295 keV roi) | Activity in 609 keV roi, Bq/kg (d.w.) | uncer-tainty | Activity in 352 keV roi, Bq/kg (d.w.) | uncer-tainty | Activity in 352 keV roi, Bq/kg (d.w.) | uncer-tainty | Mean activity, Ra-226, Bq/kg (d.w.) | uncer-tainty |
| S1-3 0-1cm | 0.0388 | 76302 | 1518 | 64 | 1999 | 73 | 1079 | 70 | 32.5 | 2.5 | 30.4 | 2.1 | 26.7 | 2.7 | 29.9 | 4.3 |
| S1-3 1-2cm | 0.0324 | 84489 | 1503 | 59 | 1878 | 72 | 1177 | 71 | 34.2 | 2.7 | 30.1 | 2.2 | 31.5 | 3.1 | 31.9 | 4.7 |
| S1-3 2-3cm | 0.0361 | 171372 | 2996 | 89 | 4352 | 105 | 2410 | 104 | 30.1 | 2.2 | 31.5 | 2.0 | 28.6 | 2.4 | 30.0 | 3.8 |
| S1-3 3-4cm | 0.0358 | 81151 | 1407 | 60 | 1905 | 72 | 1326 | 67 | 30.0 | 2.5 | 29.1 | 2.1 | 34.2 | 2.9 | 31.1 | 4.4 |
| S1-3 4-5cm | 0.0332 | 251380 | 4194 | 109 | 5743 | 124 | 3579 | 120 | 30.9 | 2.3 | 30.4 | 1.9 | 31.5 | 2.5 | 30.9 | 3.9 |
| S1-3 5-6cm | 0.0322 | 79277 | 1194 | 61 | 1726 | 67 | 1034 | 65 | 28.2 | 2.6 | 29.6 | 2.2 | 29.4 | 3.0 | 29.1 | 4.6 |
| S1-3 6-7cm | 0.0353 | 109959 | 1938 | 70 | 2808 | 82 | 1551 | 82 | 31.0 | 2.4 | 32.4 | 2.1 | 29.3 | 2.7 | 30.9 | 4.2 |
| S1-3 7-8cm | 0.0368 | 76907 | 1319 | 62 | 1945 | 69 | 1119 | 67 | 28.8 | 2.5 | 30.8 | 2.1 | 29.1 | 2.8 | 29.6 | 4.3 |
| S1-3 8-9cm | 0.0331 | 76207 | 1153 | 60 | 1788 | 65 | 1054 | 65 | 27.6 | 2.6 | 31.4 | 2.2 | 30.6 | 3.1 | 29.8 | 4.6 |
| S1-3 9-10cm | 0.0401 | 268255 | 4491 | 115 | 7223 | 130 | 4096 | 126 | 25.7 | 1.9 | 30.3 | 1.8 | 28.2 | 2.1 | 28.1 | 3.4 |
| S1-3 10-11cm | 0.0381 | 80850 | 1374 | 63 | 2018 | 69 | 1187 | 69 | 27.5 | 2.3 | 29.3 | 2.0 | 28.4 | 2.7 | 28.4 | 4.1 |
| S1-3 11-12cm | 0.0385 | 90468 | 1888 | 63 | 2440 | 76 | 1278 | 64 | 34.6 | 2.5 | 31.6 | 2.1 | 26.9 | 2.4 | 31.1 | 4.0 |
| S1-3 12-13cm | 0.035 | 85929 | 1552 | 57 | 2091 | 73 | 1244 | 71 | 32.2 | 2.5 | 31.0 | 2.1 | 30.5 | 2.9 | 31.2 | 4.4 |
| S1-3 13-14cm | 0.0339 | 69883 | 1181 | 55 | 1601 | 63 | 903 | 65 | 30.7 | 2.6 | 29.8 | 2.2 | 27.6 | 3.1 | 29.4 | 4.6 |

**Appendix VI Table A51: Data and results from Ra-226 measurements on core S2-1.**

| Sample | | Measuring sample | | | | | | | Results | | | | | | | |
|---|---|---|---|---|---|---|---|---|---|---|---|---|---|---|---|---|
| Sample identity | Sample weight, kg | Counting time, sec. | Net counts in 609 keV roi | s(net counts in 609 keV roi) | Net counts in 352 keV roi | s(net counts in 352 keV roi) | Net counts in 295 keV roi | s(net counts in 295 keV roi) | Activity in 609 keV roi, Bq/kg (d.w.) | uncer-tainty | Activity in 352 keV roi, Bq/kg (d.w.) | uncer-tainty | Activity in 352 keV roi, Bq/kg (d.w.) | uncer-tainty | Mean activity, Ra-226, Bq/kg (d.w.) | uncer-tainty |
| S2-1 0-1cm | 0.048 | 86226 | 1978 | 87 | 3200 | 93 | 1805 | 87 | 30.9 | 2.4 | 36.1 | 2.2 | 33.5 | 2.7 | 33.5 | 4.2 |
| S2-1 1-2cm | 0.042 | 17071 | 395 | 37 | 538 | 42 | 354 | 38 | 35.7 | 4.3 | 34.5 | 3.5 | 37.9 | 5.0 | 36.0 | 7.5 |
| S2-1 2-3cm | 0.0432 | 17000 | 354 | 39 | 560 | 42 | 368 | 38 | 30.8 | 4.3 | 35.2 | 3.5 | 38.6 | 4.9 | 34.9 | 7.4 |
| S2-1 3-4cm | 0.0443 | 94106 | 2533 | 91 | 3473 | 105 | 2218 | 94 | 40.1 | 2.8 | 38.9 | 2.4 | 41.3 | 3.0 | 40.1 | 4.8 |
| S2-1 4-5cm | 0.0456 | 23621 | 672 | 40 | 838 | 51 | 517 | 49 | 41.4 | 3.6 | 36.2 | 3.1 | 37.0 | 4.4 | 38.2 | 6.4 |
| S2-1 5-6cm | 0.0459 | 87110 | 2354 | 79 | 3411 | 95 | 1976 | 94 | 38.9 | 2.6 | 40.0 | 2.4 | 38.3 | 3.0 | 39.1 | 4.6 |
| S2-1 6-7cm | 0.0442 | 19367 | 450 | 38 | 656 | 44 | 473 | 40 | 34.1 | 3.8 | 35.5 | 3.2 | 43.0 | 4.6 | 37.5 | 6.8 |
| S2-1 7-8cm | 0.0489 | 15702 | 455 | 30 | 549 | 40 | 402 | 38 | 39.4 | 3.6 | 33.2 | 3.2 | 40.9 | 4.8 | 37.9 | 6.8 |
| S2-1 8-9cm | 0.0476 | 62537 | 1772 | 62 | 2525 | 74 | 1413 | 74 | 39.5 | 2.7 | 39.9 | 2.4 | 36.7 | 3.0 | 38.7 | 4.7 |
| S2-1 9-10cm | 0.0468 | 88289 | 2446 | 76 | 3480 | 88 | 2065 | 87 | 39.2 | 2.6 | 39.5 | 2.3 | 38.8 | 2.8 | 39.2 | 4.5 |
| S2-1 10-11cm | 0.0485 | 239405 | 6790 | 130 | 9478 | 149 | 5805 | 141 | 38.8 | 2.3 | 38.3 | 2.1 | 38.9 | 2.4 | 38.7 | 4.0 |
| S2-1 11-12cm | 0.049 | 63224 | 1779 | 70 | 2590 | 78 | 1512 | 73 | 38.1 | 2.7 | 39.4 | 2.4 | 38.0 | 2.9 | 38.5 | 4.6 |
| S2-1 12-13cm | 0.0475 | 71502 | 1901 | 71 | 2807 | 78 | 1682 | 77 | 36.9 | 2.6 | 38.8 | 2.3 | 38.5 | 2.9 | 38.1 | 4.5 |
| S2-1 13-14cm | 0.0483 | 14942 | 407 | 35 | 562 | 42 | 386 | 34 | 37.3 | 4.1 | 36.4 | 3.5 | 41.8 | 4.6 | 38.5 | 7.1 |
| S2-1 14-15cm | 0.047 | 242516 | 7129 | 145 | 9961 | 152 | 5580 | 141 | 41.7 | 2.5 | 41.2 | 2.2 | 38.0 | 2.4 | 40.3 | 4.1 |

**Appendix VI Table A52: Data and results from Ra-226 measurements on core S2-2.**

| Sample | | Measuring sample | | | | | | | Results | | | | | | | |
|---|---|---|---|---|---|---|---|---|---|---|---|---|---|---|---|---|
| Sample identity | Sample weight, kg | Counting time, sec. | Net counts in 609 keV roi | s(net counts in 609 keV roi) | Net counts in 352 keV roi | s(net counts in 352 keV roi) | Net counts in 295 keV roi | s(net counts in 295 keV roi) | Activity in 609 keV roi, Bq/kg (d.w.) | uncer-tainty | Activity in 352 keV roi, Bq/kg (d.w.) | uncer-tainty | Activity in 352 keV roi, Bq/kg (d.w.) | uncer-tainty | Mean activity, Ra-226, Bq/kg (d.w.) | uncer-tainty |
| S2-2 0-1cm | 0.0383 | 87994 | 2103 | 83 | 2890 | 95 | 1690 | 88 | 40.6 | 3.0 | 39.6 | 2.5 | 38.2 | 3.2 | 39.5 | 5.0 |
| S2-2 1-2cm | 0.0391 | 14502 | 296 | 37 | 403 | 39 | 285 | 35 | 33.2 | 5.2 | 32.2 | 3.9 | 38.4 | 5.7 | 34.6 | 8.6 |
| S2-2 2-3cm | 0.0408 | 14021 | 345 | 32 | 542 | 37 | 265 | 39 | 39.4 | 4.7 | 44.4 | 4.0 | 35.2 | 6.1 | 39.7 | 8.7 |
| S2-2 3-4cm | 0.0419 | 257725 | 7164 | 150 | 9898 | 171 | 5963 | 155 | 44.0 | 2.7 | 42.9 | 2.4 | 42.8 | 2.7 | 43.2 | 4.5 |
| S2-2 4-5cm | 0.0386 | 80479 | 1913 | 81 | 2982 | 89 | 1589 | 87 | 40.1 | 3.0 | 44.8 | 2.8 | 39.1 | 3.3 | 41.3 | 5.3 |
| S2-2 5-6cm | 0.0438 | 85883 | 2436 | 86 | 3285 | 97 | 1868 | 88 | 43.0 | 2.9 | 40.9 | 2.5 | 38.3 | 3.0 | 40.7 | 4.9 |
| S2-2 6-7cm | 0.0396 | 86406 | 2111 | 82 | 3145 | 89 | 1702 | 86 | 40.3 | 2.9 | 42.8 | 2.6 | 38.0 | 3.1 | 40.4 | 5.0 |
| S2-2 7-8cm | 0.0418 | 85360 | 2161 | 83 | 3206 | 88 | 1865 | 83 | 39.7 | 2.8 | 42.0 | 2.5 | 40.3 | 3.1 | 40.7 | 4.9 |
| S2-2 8-9cm | 0.0392 | 259157 | 6459 | 142 | 8799 | 154 | 5502 | 140 | 41.6 | 2.6 | 40.1 | 2.3 | 41.7 | 2.7 | 41.1 | 4.4 |
| S2-2 9-10cm | 0.0425 | 87889 | 2358 | 83 | 3252 | 89 | 1865 | 84 | 41.7 | 2.9 | 40.6 | 2.4 | 38.4 | 2.9 | 40.2 | 4.8 |
| S2-2 10-11cm | 0.0461 | 93160 | 2370 | 93 | 3700 | 95 | 2066 | 88 | 36.2 | 2.6 | 40.5 | 2.4 | 37.2 | 2.8 | 37.9 | 4.5 |
| S2-2 11-12cm | 0.0444 | 79272 | 2056 | 84 | 3048 | 87 | 1625 | 81 | 38.4 | 2.8 | 40.6 | 2.5 | 35.4 | 2.9 | 38.1 | 4.7 |
| S2-2 12-13cm | 0.0441 | 83127 | 2149 | 83 | 3081 | 89 | 1925 | 79 | 38.5 | 2.7 | 39.2 | 2.4 | 40.7 | 3.0 | 39.5 | 4.7 |
| S2-2 13-14cm | 0.0478 | 869884 | 24988 | 277 | 35172 | 294 | 21196 | 271 | 40.0 | 2.3 | 39.8 | 2.1 | 39.7 | 2.3 | 39.8 | 3.9 |
| S2-2 14-15cm | 0.0412 | 247286 | 6352 | 141 | 9347 | 150 | 5440 | 139 | 41.0 | 2.5 | 42.9 | 2.4 | 41.2 | 2.7 | 41.7 | 4.4 |
| S2-2 15-16cm | 0.0446 | 80053 | 2366 | 80 | 3231 | 86 | 1691 | 81 | 44.2 | 2.9 | 42.6 | 2.5 | 36.4 | 2.9 | 41.1 | 4.8 |

**Appendix VI Table A53: Data and results from Ra-226 measurements on core S3-1.**

| Sample | | Measuring sample | | | | | | | Results | | | | | | | |
|---|---|---|---|---|---|---|---|---|---|---|---|---|---|---|---|---|
| Sample identity | Sample weight, kg | Counting time, sec. | Net counts in 609 keV roi | s(net counts in 609 keV roi) | Net counts in 352 keV roi | s(net counts in 352 keV roi) | Net counts in 295 keV roi | s(net counts in 295 keV roi) | Activity in 609 keV roi, Bq/kg (d.w.) | uncer-tainty | Activity in 352 keV roi, Bq/kg (d.w.) | uncer-tainty | Activity in 352 keV roi, Bq/kg (d.w.) | uncer-tainty | Mean activity, Ra-226, Bq/kg (d.w.) | uncer-tainty |
| S3-1 0-1cm | 0.0492 | 75750 | 1797 | 71 | 2491 | 81 | 1483 | 1483 | 31.4 | 2.3 | 30.9 | 2.0 | 30.4 | 33.5 | 30.9 | 33.7 |
| S3-1 1-2cm | 0.0301 | 259065 | 4400 | 120 | 6130 | 131 | 3772 | 120 | 34.8 | 2.6 | 34.9 | 2.2 | 35.7 | 2.8 | 35.1 | 4.3 |
| S3-1 2-3cm | 0.0452 | 81223 | 1717 | 72 | 2327 | 78 | 1451 | 70 | 29.9 | 2.3 | 28.8 | 1.9 | 29.9 | 2.5 | 29.6 | 3.9 |
| S3-1 3-4cm | 0.0451 | 75149 | 1704 | 67 | 2140 | 74 | 1292 | 69 | 32.5 | 2.4 | 28.7 | 1.9 | 28.7 | 2.5 | 30.0 | 4.0 |
| S3-1 4-5cm | 0.0448 | 99750 | 2030 | 81 | 2818 | 90 | 1582 | 81 | 28.9 | 2.2 | 28.6 | 1.9 | 26.4 | 2.3 | 28.0 | 3.7 |
| S3-1 5-6cm | 0.0493 | 85075 | 1762 | 74 | 2609 | 82 | 1631 | 72 | 26.8 | 2.1 | 28.5 | 1.8 | 29.6 | 2.3 | 28.3 | 3.6 |
| S3-1 6-7cm | 0.0404 | 81661 | 1640 | 71 | 2188 | 76 | 1397 | 70 | 31.6 | 2.5 | 29.9 | 2.0 | 31.9 | 2.7 | 31.1 | 4.2 |

**Appendix VI Table A54: Data and results from Ra-226 measurements on core S4-1 (0-1cm) and S4-2 (1-6cm).**

| Sample | | Measuring sample | | | | | | | Results | | | | | | | |
|---|---|---|---|---|---|---|---|---|---|---|---|---|---|---|---|---|
| Sample identity | Sample weight, kg | Counting time, sec. | Net counts in 609 keV roi | s(net counts in 609 keV roi) | Net counts in 352 keV roi | s(net counts in 352 keV roi) | Net counts in 295 keV roi | s(net counts in 295 keV roi) | Activity in 609 keV roi, Bq/kg (d.w.) | uncer-tainty | Activity in 352 keV roi, Bq/kg (d.w.) | uncer-tainty | Activity in 352 keV roi, Bq/kg (d.w.) | uncer-tainty | Mean activity, Ra-226, Bq/kg (d.w.) | uncer-tainty |
| S4-1 0-1cm | 0.0444 | 98658 | 2499 | 88 | 3439 | 104 | 2139 | 96 | 37.4 | 2.6 | 36.4 | 2.3 | 37.7 | 2.9 | 37.2 | 4.5 |
| S4-2 1-2cm | 0.0467 | 73411 | 2013 | 82 | 2999 | 93 | 1637 | 85 | 30.8 | 2.5 | 41.2 | 2.5 | 46.1 | 3.3 | 39.4 | 4.9 |
| S4-2 2-3cm | 0.0466 | 529315 | 15328 | 216 | 22220 | 241 | 12912 | 221 | 34.2 | 2.1 | 42.5 | 2.2 | 49.0 | 2.8 | 41.9 | 4.1 |
| S4-2 3-4cm | 0.044 | 74904 | 1882 | 81 | 2833 | 85 | 1529 | 79 | 29.5 | 2.5 | 40.2 | 2.5 | 44.6 | 3.2 | 38.1 | 4.8 |
| S4-2 4-5cm | 0.0483 | 88768 | 2490 | 86 | 3672 | 94 | 2121 | 86 | 32.2 | 2.4 | 40.4 | 2.4 | 45.7 | 3.0 | 39.4 | 4.5 |
| S4-2 5-6cm | 0.0478 | 86233 | 2475 | 87 | 3452 | 90 | 2146 | 84 | 34.1 | 2.5 | 39.4 | 2.3 | 47.3 | 3.1 | 40.3 | 4.6 |
| S4-2 6-7cm | 0.0521 | 83748 | 2518 | 84 | 3482 | 94 | 2029 | 86 | 30.3 | 2.2 | 37.6 | 2.2 | 45.6 | 3.0 | 37.9 | 4.3 |
| S4-2 7-8cm | 0.0496 | 251612 | 7171 | 151 | 10441 | 160 | 6366 | 146 | 33.4 | 2.1 | 39.4 | 2.1 | 45.3 | 2.7 | 39.4 | 4.0 |
| S4-2 8-9cm | 0.0477 | 87942 | 2502 | 86 | 3431 | 96 | 2020 | 87 | 31.2 | 2.4 | 38.4 | 2.3 | 47.0 | 3.1 | 38.8 | 4.5 |